St Mary the Virgin Blanchland

HISTORY, ARCHITECTURE, ACOUSTICS

REPORT 2025

Made possible with Heritage Fund

Newcastle University / Centre for Landscape

Dr Gianluca Foschi

Visiting Researcher, Newcastle University
School of History, Classics & Archaeology
Newcastle upon Tyne, UK
ORCID: 0000-0002-8827-3569

gianluca.foschi@newcastle.ac.uk

Table of Contents

Table of Figures

List of Tables

1. Introduction

The Grade I-listed Premonstratensian Abbey of Blanchland (*Historic England*, 1017683)[1] (**Figure 1**) in Northumberland[2] was the subject of a detailed analysis of its architecture and acoustics within the 6As of Blanchland Project (Blanchland Community Development Organisation Ltd, 2022).[3] This document reports on the most significant results of this extensive investigation, which leveraged terrestrial laser scanning, 3D digital modelling and acoustic simulations to advance understanding of the abbey and its historic background.

Figure 1. St Mary the Virgin, Blanchland, on 11 February 2023 (left) and 21 January 2023 (right).

This research includes the most detailed and accurate survey of the abbey to date. Potential design principles used by the architects during the construction of the abbey have been consistently identified. An innovative AI approach built on robust metrological theory has also provided insights into possible units of measurement used to design the abbey in the Middle Ages. An understanding of the current building's acoustics has been achieved, alongside a large dataset for further analysis. Additionally, this study has enabled clarification of the chronology and context of the first medieval documents concerning the abbey.

[1] Blanchland Premonstratensian Abbey, Blanchland - 1017683 | Historic England
[2] National Grid Reference: NGR NZ 095 515.
[3] 6As of Blanchland | The National Lottery Heritage Fund

2. Aims, Objectives, Outputs

The research and analysis described in this document had four main aims:

Aim 1. Clarify the historical circumstances in which Blanchland Abbey was founded.

Aim 2. Meet the recommendation set out by Peter Ryder's Archaeological Assessment (Ryder, 2017) about the high desirability of a modern survey of the church, including external and internal elevations.

Aim 3. Advance knowledge on the architectural design of the twelfth/thirteenth-century abbey.

Aim 4. Provide a general interpretation of the building's acoustics along with detailed data from acoustic surveys and room acoustic simulations.

The objectives to fulfil each aim were set as follows:

For Aim 1.:

- **Objective 1.1.** Detailed analysis of selected written sources.

For Aim 2.:

- **Objective 2.1.** Laser scanning survey of the interior and exterior of the abbey.

For Aim 3.:

- **Objective 3.1.** Analysis of salient features of the medieval building conducted on data from terrestrial laser scanning.

For Aim 4.:

- **Objective 4.1.** On-site acoustic survey of Blanchland Abbey.
- **Objective 4.2.** Room acoustic simulations on the 3D digital model of the building designed based on data from terrestrial laser scanning.

The following outputs have been produced:

For Objective 1.1: **Section 2.2** and **Appendix I**.

For Objective 2.1: data in **Appendix II**, **Appendix III**.

For Objective 3.1: **Section 2.2**, data in **Appendix IV**, **Appendix V** and **Appendix VI**.

For Objective 4.1: data in **Appendix VII**.

For Objective 4.2: **Section 2.4**, data in **Appendix VIII** and **Appendix IX**.

2.1. Methodology

2.1.1. Critical Analysis of Written Sources (Objective 1.1)

Information about the foundation of the abbey was researched and verified based on the critical edition of relevant written sources, in comparison with scientific literature on the topic.

2.1.2. Terrestrial Laser Scanning (Objective 2.1)

The terrestrial laser scanning (TLS) structural survey of the abbey was conducted on 14 January and 21 January 2023 by Dr Gianluca Foschi, and on 11 February 2023 by Dr Gianluca Foschi and Dr Vicky Manolopoulou. TLS was performed using a FARO Focus3D X 330 laser scanner from Newcastle University's McCord Centre for Landscape.

Over three days, a total of 55 laser scans were obtained (40 full colour + 15 greyscale), covering the interior, exterior and immediate surroundings of the abbey. The only part of the building that was not recorded by TLS was the staircase inside the tower at the north end of the transept, given its secondary relevance for architectural and acoustic analysis and the time constraints involved. Additionally, the remains of the abbey incorporated into the Lord Crewe Arms' masonry were scanned only from a distance, being partially obscured by vegetation. The coverage and resolution of the survey were designed to facilitate the integration of any past or future data into the existing point cloud.

The laser scans were processed and registered into a unified point cloud by Dr Gianluca Foschi using Newcastle University's FARO Scene v. 6.2.

The final point cloud comprises a total of 612,899,515 points, with an average accuracy of 0.0029 m. A full report on the point cloud registration is included as **Appendix I**.

2.1.3. Architectural Analysis (Objective 3.1)

The dataset from terrestrial laser scanning enabled an unprecedentedly accurate investigation of the design of the medieval building.

To conduct the analysis, the project point cloud of the site was exported from FARO Scene in .rcp format and imported into Autodesk AutoCAD. Since the exported point cloud retains real dimensions, it was possible to measure and analyse in detail every recorded feature of the building directly in AutoCAD.

Measurements were taken from the point cloud and recorded in a spreadsheet for spatial analysis. Hypothetical design procedures were assessed directly on the point cloud.

The identification of possible division methods for the design of the medieval lancet windows allowed for the creation of reverse engineering algorithms to explore the possible use of specific units of measurement during the construction of the abbey.

The theoretical basis for the algorithms was elaborated within doctoral research conducted at Newcastle University (Foschi, 2022).

Artificial intelligence – in particular Claude Opus 4 – was used to facilitate the calculations, which were then manually assessed.

2.1.4. Acoustic Survey and Data Processing (Objective 4.1)

Figure 2. Acoustic test setup and FARO Focus3D X 330 laser scanner. Blanchland, 14 January 2023.

The acoustic survey of the abbey was conducted on 14 January 2023 by Rebecca Romeo Pitone and Dr Gianluca Foschi. ODEON Room Acoustics software – installed on a laptop from the McCord Centre for Landscape – was used to perform the survey, in combination with equipment from Apex Acoustics Ltd comprising a dodecahedron loudspeaker Norsonic 283, a power amplifier Norsonic 280, a class 1 precision microphone NTi M2230, and an audio interface Focusrite Scarlett 2i2 3rd Gen.

Prior to the acoustic survey, calibration of the equipment was performed in compliance with ODEON Room Acoustic Software guidelines (ODEON Room Acoustics Software, 2020). Subsequently, the acoustics of the abbey were excited using a 1,000 ms sweep signal spanning frequencies from 63 to 8,000 Hz. The loudspeaker (sound source) reproducing the signal was positioned at two key locations for historic acoustic performance in the abbey: the area in front of the altar, on the axis of the main nave, and the pulpit, in the south-central area of the main nave. Twelve microphone positions were tested for each of the two sound source locations, resulting in a total of twenty-four sweep signals being recorded, processed and stored by the ODEON software.

The acoustic survey covered the entire main nave of the abbey. It was performed in accordance with international acoustic standards (ISO 3382-1, 2009; ISO 3382-2, 2008) and speech intelligibility standards (IEC 60268-16, 2020; ISO 9921, 2003), following guidelines for acoustic surveys in churches (Cirillo & Martellotta, 2006; Martellotta et al., 2009).

2.1.5. 3D Digital Modelling and Room Acoustic Simulations (Objective 4.2)

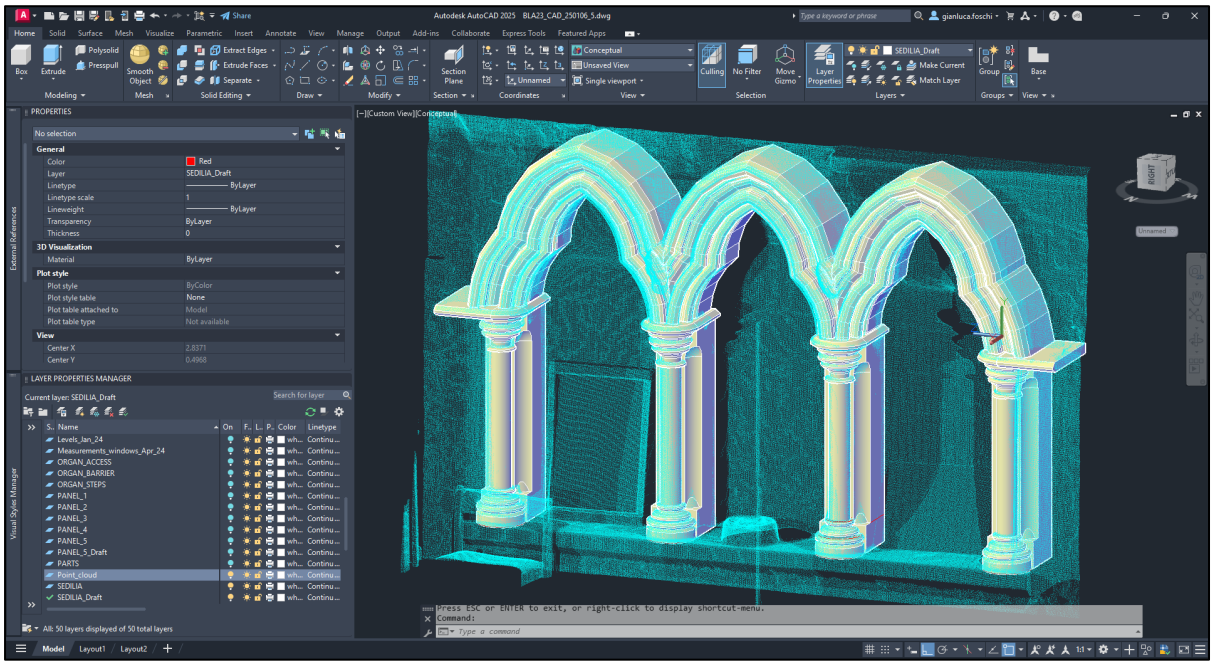

Figure 3. Digital modelling (grey) of the sedilia *in the nave's south wall using AutoCAD based on the TLS point cloud (cyan).*

A three-dimensional digital model of the current building's interior was manually designed using AutoCAD 2025. Solid geometry was modelled in the software based with the building's point cloud obtained from terrestrial laser scanning and exported as .rcp from FARO Scene. The solids were combined into a single object, which was then subtracted from a larger solid. This operation created two nested solids, the smaller of which represented the interior of the building. Once the outer solid was removed, the inner one was converted into an unsmoothed mesh and subsequently exploded, producing an accurate watertight model of the building's interior.

The model retained the colours of the solid's surfaces, which were differentiated according to the material they represent. This allowed the polygons to be separated into different layers using a colour-based quick selection in AutoCAD.

The digital model was imported into ODEON Room Acoustics software, v. 16.10, where different sound absorption coefficients and scattering coefficients were assigned to each layer. In modern acoustics, sound absorption and scattering coefficients define the extent to which a surface absorbs sound (therefore reducing sound reflection and

reverberation) and scatters sound in the space, respectively. The coefficients for the model of Blanchland Abbey were taken from scientific literature and the ODEON built-in library (**Table 1**). Environmental conditions of 4°C and 77% relative humidity – required by ODEON software for the acoustic simulation – are estimated based on weather data for Blanchland on 14 January 2023 at approximately noon (*Time and Date*).[4]

Within the software, the on-site surveys were digitally reproduced. At this stage, the coefficients assigned to the materials could be optimised until the measured results of the acoustic survey matched the simulated parameters reproduced in ODEON. For this purpose, the software's Genetic Algorithm was run on the model for approximately 168 hours (**Figure 34**).

Layer	Material	Scatter	Transp	Type	63 Hz	125 Hz	250 Hz	500 Hz	1000 Hz	2000 Hz	4000 Hz	8000 Hz	Total Surfaces	Total Area
DIBOND	Steel door	0.01	0	Normal	0.036	0.09	0.055	0.05	0.146	0.097	0.007	0.054	1	0.24
FABRIC_ALTAR_TABLECLOTH_HANGING	Curtains	0.2	0	Normal	0.059	0.048	0.068	0.12	0.675	0.743	0.736	0.794	3	3.74
FABRIC_ALTAR_TABLECLOTH_ON_WOOD	Curtains	0.2	0	Normal	0.059	0.048	0.068	0.12	0.675	0.743	0.736	0.794	4	2.11
FABRIC_CARPETS	Carpet heavy, on concrete (Harris, 1991)	0.1	0	Normal	0.028	0.032	0.074	0.14	0.192	0.801	0.833	0.75	26	54.04
FABRIC_CHAIRS_CUSHIONS	Pillow / Quilt	0.05	0	Normal	0.241	0.176	0.192	0.37	0.541	0.873	0.963	0.99	260	9.1
FABRIC_CURTAINS	Curtains	0.2	0	Fractional	0.059	0.048	0.068	0.12	0.675	0.743	0.736	0.794	89	4.8
FABRIC_CUSHIONS	Pillow / Quilt	0.05	0	Normal	0.241	0.176	0.192	0.37	0.541	0.873	0.963	0.99	739	23.98
FABRIC_KNEELER	Pillow / Quilt	0.05	0	Normal	0.241	0.176	0.192	0.37	0.541	0.873	0.963	0.99	4	1.04
FABRIC_PULPIT	Curtains	0.2	0	Normal	0.059	0.048	0.068	0.12	0.675	0.743	0.736	0.794	1	0.31
FLOWERS	Flowers	0.6	0.8	Normal	0.047	0.129	0.131	0.186	0.308	0.274	0.477	0.755	82	1.4
FOAMEX	Steel door	0.01	0	Normal	0.036	0.09	0.055	0.05	0.146	0.097	0.007	0.054	6	0.9
GLASS_FRAMES	Single pane of glass (Ref. Multiconsult, Norway)	0.01	0	Normal	0.199	0.153	0.043	0.049	0.046	0.015	0.015	0.047	1	0.3
GLASS_FURNITURE	Single pane of glass (Ref. Multiconsult, Norway)	0.01	0	Normal	0.199	0.153	0.043	0.049	0.046	0.015	0.015	0.047	1	0.45
GLASS_STAINED	Glass, ordinary window glass (Harris, 1991)	0.1	0	Normal	0.106	0.497	0.426	0.26	0.129	0.077	0.03	0.019	54	72.25
MARBLE_EPIGRAPH	Marble or glazed tile (Harris, 1991)	0.05	0	Normal	0.023	0.044	0.049	0.021	0.021	0.039	0.031	0.054	6	1.08
MARBLE_GRAVESTONES	Marble or glazed tile (Harris, 1991)	0.05	0	Normal	0.023	0.044	0.049	0.021	0.021	0.039	0.031	0.054	41	14.48
MARBLE_VASE	Marble or glazed tile (Harris, 1991)	0.05	0	Normal	0.023	0.044	0.049	0.021	0.021	0.039	0.031	0.054	623	1.37
METAL_ALTAR_FURNITURE	Metal, organ pipes and furniture	0.01	0	Normal	0.279	0.321	0.389	0.363	0.276	0.41	0.189	0.291	1108	0.31
METAL_FRAMES	Steel door	0.01	0	Normal	0.036	0.09	0.055	0.05	0.146	0.097	0.007	0.054	1	0.18
METAL_ORGAN	Metal, organ pipes and furniture	0.01	0	Normal	0.279	0.321	0.389	0.363	0.276	0.41	0.189	0.291	675	19.71
METAL_POSTERS	Metal, organ pipes and furniture	0.01	0	Normal	0.279	0.321	0.389	0.363	0.276	0.41	0.189	0.291	26	0.34
PAINT_FRAMES	Solid wooden door (Bobran, 1973)	0.05	0	Normal	0.299	0.079	0.029	0.078	0.119	0.132	0.209	0.089	4	4.51
PAPER_BOOK	Plaster with wallpaper on backing paper (Bobran, 1973)	0.05	0	Normal	0.035	0.024	0.059	0.052	0.109	0.076	0.072	0.106	6	0.1
PLASTERBOARD_CEILING	Plasterboard (12mm(1/2") in suspended ceiling grid)	0.01	0	Normal	0.112	0.107	0.074	0.056	0.095	0.068	0.115	0.066	416	65.36
PLASTIC_POSTERS	Linoleum or vinyl stuck to concrete (Petersen, 1983)	0.01	0	Normal	0.026	0.041	0.018	0.041	0.057	0.101	0.06	0.043	2	3.26
PLATFORMS	Hollow wooden podium (Ref. Dalenbck, CATT)	0.05	0	Normal	0.435	0.285	0.432	0.246	0.203	0.193	0.068	0.055	6	63.93
STONE_CURVE	Sandstone	0.05	0	Fractional	0.045	0.074	0.073	0.093	0.104	0.089	0.053	0.035	6295	103.75
STONE_FLAT	Sandstone	0.05	0	Normal	0.045	0.074	0.073	0.093	0.104	0.089	0.053	0.035	6297	780
STONE_FLOOR	Sandstone	0.05	0	Normal	0.045	0.074	0.073	0.093	0.104	0.089	0.053	0.035	77	275.42
STONE_FONT	Sandstone	0.05	0	Normal	0.045	0.074	0.073	0.093	0.104	0.089	0.053	0.035	67	3.83
TRANSPARENT_SOUND_SOURCES	Transparent	0.01	0	Normal	0	0	0	0	0	0	0	0	144	0.48
WAX_ALTAR_FURNITURE	Linoleum or vinyl stuck to concrete (Petersen, 1983)	0.01	0	Normal	0.026	0.041	0.018	0.041	0.057	0.101	0.06	0.043	20	0
WOOD_BEAMS_CEILING	Coffered ceiling	0.05	0	Normal	0.712	0.289	0.282	0.223	0.183	0.152	0.227	0.184	1008	27.47
WOOD_CHAIRS	Solid wooden door (Bobran, 1973)	0.05	0	Normal	0.299	0.079	0.029	0.078	0.119	0.132	0.209	0.089	3326	30.38
WOOD_CHANCEL_CURVE	Solid wooden door (Bobran, 1973)	0.05	0	Fractional	0.299	0.079	0.029	0.078	0.119	0.132	0.209	0.089	54	2
WOOD_CHANCEL_FLAT	Solid wooden door (Bobran, 1973)	0.05	0	Normal	0.299	0.079	0.029	0.078	0.119	0.132	0.209	0.089	22368	52.57
WOOD_CHOIR	Solid wooden door (Bobran, 1973)	0.05	0	Normal	0.299	0.079	0.029	0.078	0.119	0.132	0.209	0.089	2068	39.65
WOOD_CHOIR_PANELS_CURVE	Plywood paneling, 1 cm thick (Harris, 1991)	0.05	0	Fractional	0.423	0.233	0.118	0.088	0.084	0.128	0.166	0.164	15	0.84
WOOD_CHOIR_PANELS_FLAT	Plywood paneling, 1 cm thick (Harris, 1991)	0.05	0	Normal	0.423	0.233	0.118	0.088	0.084	0.128	0.166	0.164	9124	100.12
WOOD_COFFERED_CEILING	Coffered ceiling	0.05	0	Normal	0.712	0.289	0.282	0.223	0.183	0.152	0.227	0.184	20860	212.04
WOOD_DOORS	Solid wooden door (Bobran, 1973)	0.05	0	Normal	0.299	0.079	0.029	0.078	0.119	0.132	0.209	0.089	134	13.6
WOOD_FONT	Solid wooden door (Bobran, 1973)	0.05	0	Normal	0.299	0.079	0.029	0.078	0.119	0.132	0.209	0.089	45	1.22
WOOD_FRAMES	Solid wooden door (Bobran, 1973)	0.05	0	Normal	0.299	0.079	0.029	0.078	0.119	0.132	0.209	0.089	441	12.27
WOOD_FRAMEWORK_CURVE	Solid wooden door (Bobran, 1973)	0.05	0	Fractional	0.299	0.079	0.029	0.078	0.119	0.132	0.209	0.089	71	0.81
WOOD_FRAMEWORK_FLAT	Solid wooden door (Bobran, 1973)	0.05	0	Normal	0.299	0.079	0.029	0.078	0.119	0.132	0.209	0.089	3540	34.73
WOOD_FURNITURE	Solid wooden door (Bobran, 1973)	0.05	0	Normal	0.299	0.079	0.029	0.078	0.119	0.132	0.209	0.089	535	9.95
WOOD_KNEELERS	Solid wooden door (Bobran, 1973)	0.05	0	Normal	0.299	0.079	0.029	0.078	0.119	0.132	0.209	0.089	856	7.03
WOOD_ORGAN	Solid wooden door (Bobran, 1973)	0.05	0	Normal	0.299	0.079	0.029	0.078	0.119	0.132	0.209	0.089	225	58.79
WOOD_ORGAN_ACCESS	Solid wooden door (Bobran, 1973)	0.05	0	Normal	0.299	0.079	0.029	0.078	0.119	0.132	0.209	0.089	40	4.51
WOOD_PANEL_CEILING	Coffered ceiling	0.05	0	Normal	0.712	0.289	0.282	0.223	0.183	0.152	0.227	0.184	52	28.57
WOOD_PEWS	Solid wooden door (Bobran, 1973)	0.05	0	Normal	0.299	0.079	0.029	0.078	0.119	0.132	0.209	0.089	2216	150.19
WOOD_PLATFORMS	Hollow wooden podium (Ref. Dalenbck, CATT)	0.05	0	Normal	0.435	0.285	0.432	0.246	0.203	0.193	0.068	0.055	71	93.32
WOOD_PULPIT_STAND	Solid wooden door (Bobran, 1973)	0.05	0	Normal	0.299	0.079	0.029	0.078	0.119	0.132	0.209	0.089	82	0.1
WOOD_TABLES	Solid wooden door (Bobran, 1973)	0.05	0	Normal	0.299	0.079	0.029	0.078	0.119	0.132	0.209	0.089	2504	22.38
WOOD_TRUSSES_CEILING	Solid wooden door (Bobran, 1973)	0.05	0	Normal	0.299	0.079	0.029	0.078	0.119	0.132	0.209	0.089	163	66.18

Table 1. Material layers and acoustic coefficients for the digital model of Blanchland Abbey.

The main sound parameters considered for the acoustic analysis of the building are listed in **Table 2**. Just Noticeable Difference (JND) values are also included in the table. These values represent the variation for each parameter that is likely to produce a noticeable change in perception. For instance, if EDT (early decay time) increases by less than 5% – i.e. the JND for this parameter – the listener will not perceive any change. Conversely, if EDT increases by 6% or more, the space will likely be perceived as more

[4] https://www.timeanddate.com/weather/@2655379/historic?month=1&year=2023

reverberant. JNDs are crucial in acoustic analysis, as enable identification of changes in auditory perception that are likely to be noticed.

The digital model produced for room acoustic simulation is meets all the requirements for a thorough acoustic investigation. Once imported into ODEON, the model includes 86,883 surfaces and is far more detailed than required by the software. Although the high number of surfaces makes acoustic calculations slower, it does not affect their reliability. Its adherence to the TLS point cloud of the building guarantees that the inclination of walls and presence of furniture – which may affect results dramatically (e.g.: ODEON Room Acoustics Software, 2020, p. 26) – are exceptionally close to reality. Additionally, the model is designed to be subsequently improved and rendered, for the production of an annotated virtual tour of the building as it was in 2023.[5]

Five versions of Blanchland Abbey have been analysed acoustically. While each scenario is generally discussed in the main text, the detailed results are available in the dataset (**0**). The first simulation reproduces the building in the same conditions as it was when surveyed in January 2024. This calibration exercise aimed to align the digital model with real acoustic conditions and develop general understanding of how sound behaves in the space. The second scenario involved removing the wooden choir to explore how it affects sound perception in the nave. The third investigation examined the acoustics with all the furniture removed, determining how furnishings influence the perception of sound within the building. The fourth scenario explored the effect of a plastered nave ceiling, assessing how the absence of timber transforms the acoustics of the church. The fifth test positioned a sound source in the west area of the nave with the audience distributed in the transept and tower, investigating auditory experience across the northern wing of the building compared to the nave.

[5] Similarly, for instance, to the virtual tour of Building A from Thirlings reconstructed at Jarrow Hall: https://skfb.ly/oSO8K

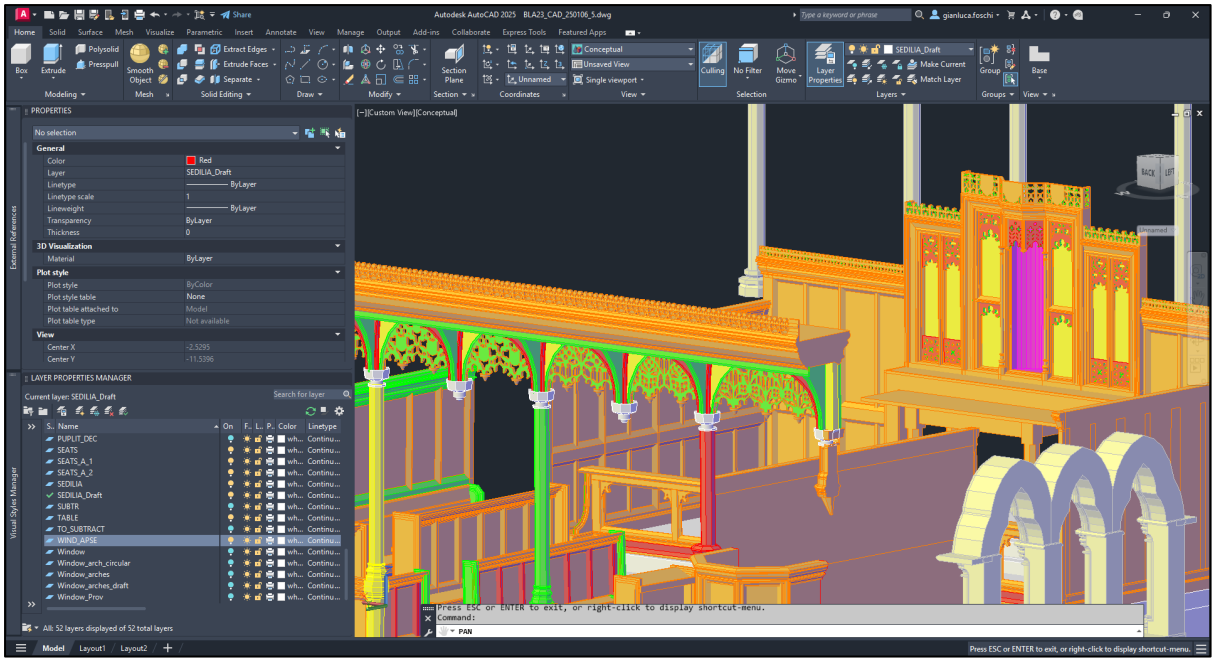

Figure 4. 3D digital modelling of the wooden furniture in the chancel using AutoCAD based on the TLS point cloud.

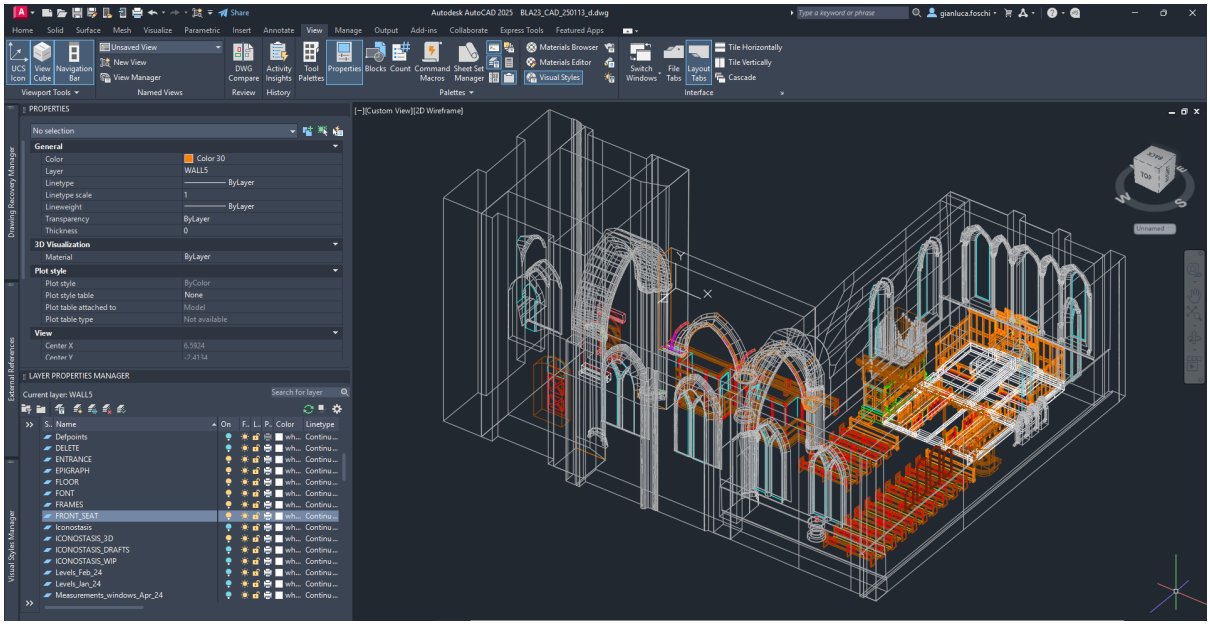

Figure 5. 3D digital modelling of the interior of Blanchland abbey using AutoCAD based on the TLS point cloud.

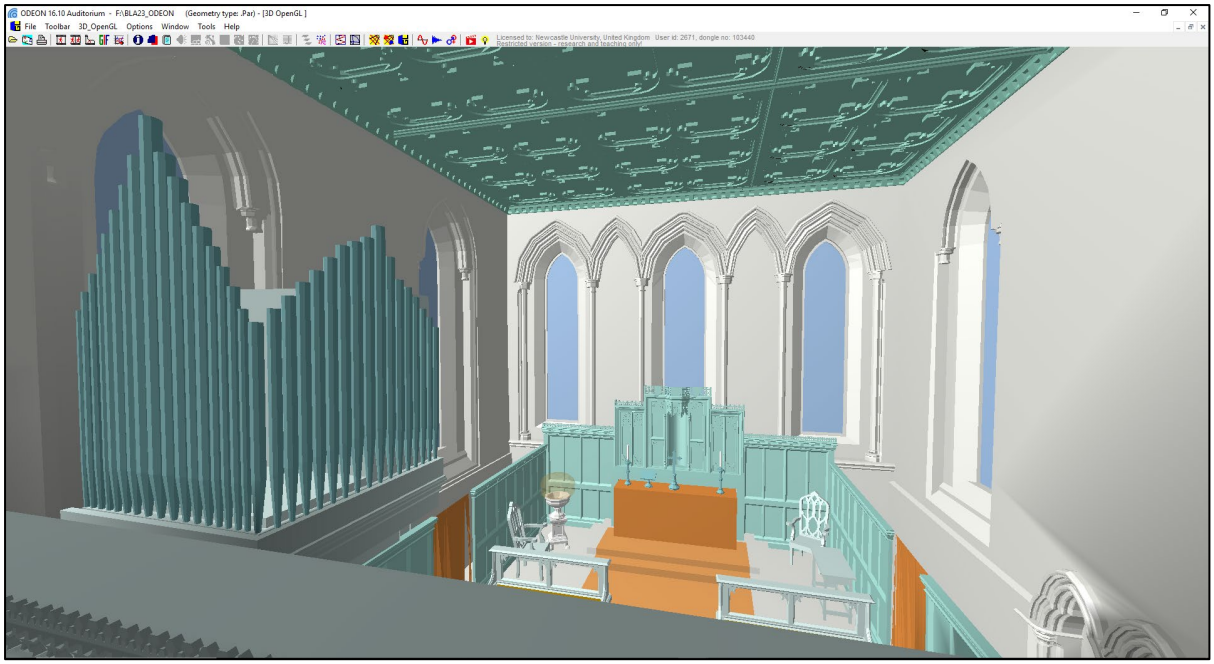

Figure 6. View of the chancel of Blanchland abbey from the 3D model of the building opened in ODEON Auditorium.

Sound parameters				
Parameter	**Unit**	**Range of averaged values (Hz)**	**JND**	**Subjective description**
EDT	S	500-1K	5%	Perceived reverberation
T_{30}	S	500-1K	5%	Reverberation
Ts	Ms	500-1K	10	Balance between reverberation and clarity
SPL	dB	500-1K	1	Strength
D_{50}		500-1K	0.05	Clarity
C_{80}	dB	500-2K	1	Clarity
LF_{80}		125-1K	0.05	Apparent source width (early lateral fraction)
Echo		500-2K	0.05	Unpleasant perception of echo
STI		/	0.03	Speech intelligibility

Table 2. Sound parameters investigated on the model of Blanchland Abbey.

2.2. Historical Context of the Foundation

Documentary evidence for the foundation of a Premonstratensian site at Blanchland indicates that Walterus II de Bolebec granted land for constructing the abbey in 1165, at a critical juncture in his personal and political life. Walterus's father was Baron Walterus I de Bolebec and his mother was Helwisa. His brother Hugo had died that same year, leaving behind a young heir. Walterus assumed wardship of the boy, along with Hugo's possessions. Let us now examine the evidence to resolve some confusion in scientific literature.

There are five known medieval documents relating to the foundation of the Premonstratensian abbey at Blanchland. Four of these appear in the Charter Rolls of Henry III (Cart. 54 m. 13: Great Britain. Public Record Office, 1906, p. 134), confirmed in Westminster on 12 February 1270. They are all undated and were published in the *Monasticon Anglicanum* (Dugdale et al., 1830, p. 886), with the exception of the second document. The fifth is the Chronicle of Melrose abbey, which will be discussed later.

The first document from Henry III's records is the foundation grant by Walterus de Bolebek, written in the presence of the Bishop of Durham Hugone, G. the prior and the monastic community of Durham, William the archdeacon, Simone the chamberlain, Adam of St. Egidius, Walkelino the dean, Ricardo of Colinham (Collingham?) and Willielmo of Hovedone (Hoveton?). This charter confirms that Walterus, with the consent of his bishop and heirs, has granted and given land to God, St Mary the Virgin and the community of twelve canons of the Premonstratensian order for establishing the abbey ('*ad faciendam abbaciam*'). Following the custom of medieval grants, the boundaries of the land are carefully described, leaving no doubt about the identification of the abbey with the one in Blanchland on the River Derwent (Hodgson, 1902, p. 313).[6] The charter also grants the churches of Herla (Harelaw) and Bywell to the canons, together with other possessions

The second document – not published in the *Monasticon Anglicanum* – is a grant by another Walterus the Bolebec, the son of his namesake in the foundation charter. He confirms to the canons all that was granted by his father. The witnesses are: "Robert son of Roger, Henry son of Hervi, Walter son of Gilbert, Gilbert de la Vale, Bernard Dareyns, William de Kinebel" (Great Britain. Public Record Office, 1906, p. 134). This document is extremely important being the key to understanding that the Walterus of Bolebek of the third charter is not the founder of Blanchland but his son. Important works such as the *Monasticon Anglicanum* and Hodgson's *History of Northumberland* miss this

[6] As discussed below in the text, Hodgson mistakenly identifies the founder of Blanchland abbey with his homonymous son, based on an omission in the *Monasticon Anglicarum*.

information, and identify father and son as the same person (Dugdale et al., 1830, p. 886; Hodgson, 1902, pp. 222, 224).

The third document is another charter by the same Walterus de Bolebek. He bestows upon God and the church of St Mary of Blanchland, and to the canons there serving God ('*Deo et ecclesiae S. Mariae de Blancalanda, et canonicis ibidem Deo servientibus*'), every right and patronage he and his ancestors had in the church of St Andrew of Hedon, with its appurtenances. Walterus's concession is made for the soul of his father Walterus, and for the souls of his other ancestors ('*pro anima patris mei Walteri, et pro animabus aliorum antecessorum meorum*'). The statement is followed by the customary list of witnesses, which comprises: his lady and mother Sibilla, his brother Hugone of Bolebek, the parish priest of Stiford Wicardo, Hugone of Crawdene, Reginaldo of Krenebel, Thurstano the son of Ricardo, Ranulfo of Grey, Rogero of Cogners, the cleric Eustachio, Gilberto de la Vale, and others unnamed.

In the fourth document recorded in Henry III's Charter Rolls, Hugo de Bolebek confirms the grant of his predecessors' land to God, Saint Mary, his abbey of Blanchland and the canons and fraters there serving God ('*Deo e St Mariae et abbatiae meae de Blancalanda, et canonicis et fratribus ibidem Deo servientibus*'). The text continues by specifying how Hugo and his family will be able to build towns, manors, warrens and cattle stations on the specified land, and which rights the canons and brothers have in using the land. The witnesses are: Roberto son of Rogero, Eustachio of Vesey, Ricardo of Umfrevil, Rogero de Merley, Rogero Bertram., Gilberto de la Val, Otewero of Insula, Roberto de la Vale, Johane of Tirtelingtone, Willielmo the son of Reginaldo, Rugero of Slaueleye, Willielmo of Kinebele, and many unnamed others.

Before proceeding, it is necessary to consider the *Liber vitae* of Durham (Stevenson, 1841, p. 101), where these members of the Bolebec family (cf. Hodgson, 1902) are registered as follows:

> '*Walterus de Bolebech* [this is Walterus II, the founder of Blanchland's abbey]
>
> *Sibilla uxor ejus* [his wife Sibilla, mentioned in the second charter]
>
> *Walterus de Bolebech pater ejus* [Walterus I, the father of the founder]
>
> *Helvwis mater ejus* [Helvwis, the mother of the founder]
>
> *Hugo de Boleb' frater ejus* [Hugo, the brother of the founder, who had died in 1165, as we shall see]
>
> *Walt' et Hugo fil' ejus* [these are the two sons of the founder, the Walter of the second and third charters and probably the Hugo of the fourth charter]".

Let us now turn to the fifth documentary evidence, which provides an anchor to date the establishment of the Premonstratensian order in Blanchland. It comes from the Chronicle of Melrose Abbey, the well-known manuscript written between the 12th and 13th centuries now in the British Library (Cotton MS Faustina IX). The Chronicle briefly records that the Premonstratensian order came to 'Blanchelande' in 1165: '*Ordo Praemonstratensis venit ad Blanchelande*' (Stevenson, 1835). Editors of the manuscript have interpreted this record as a reference to the Premonstratensian abbey of Blanchelande in Normandy (Stevenson, 1835, p. 80, note m). The Norman house was founded in 1154-1155 following a vow made during the Crusade by Richard de la Haye, seneschal to King Henry I, and by Mathilde de Vernon, Richard's wife (Bondéelle-Souchier, 2000, pp. 83-84). Given the focus of the Chronicle on northern Britain, the absence of any precise reference to Normandy and the chronological discrepancy – 1165 instead of 1154-1155 – there is little doubt that the Chronicle of Melrose refers to Blanchland on the River Derwent. The year 1165 corresponds with the lengthy episcopate of Hugone in Durham (i.e. Hugh de Puiset, bishop 1153-1195), who is mentioned in the foundation charter of Walterus de Bolebek. On this basis, the foundation of the Premonstratensian community on the River Derwent can be dated to 1165, in close connection with Blanchelande Abbey in Normandy, which had been founded approximately ten years earlier.[7]

Finally, it is worth considering the evidence from the Pipe Rolls and the Red Book of the Exchequer (cf. Round, 1913, p. xxxix ff.) (see **Appendix I**). These documents show that Walterus de Bolebec – the same person who granted land to the Premonstratensian canons for the foundation of Blanchland Abbey – had lost his elder brother Hugo by 1165. Hugo's son and heir – also named Walterus – was still a minor at the time and his uncle Walterus began paying to obtain wardship of the boy from the King, together with Hugo's lands (Hall, 1896, pp. 316-317; The Pipe Roll Society, 1887, pp. 22-23).
This means that Walterus founded Blanchland immediately after his responsibility and power in the Bolebec family had reached a peak. By 1165, he had become the only living son of his father, and was managing the extensive estate of his deceased brother. Both Blanchland's foundation charter and the *Liber vitae* of Durham – where his family is mentioned in reference to him – testify to the strong ties that Walterus had established with the bishopric of Durham. Walterus was probably acting to consolidate his authority, and the foundation of Blanchland may be understood within this context. The extent to which Walterus' investment in the establishment of the Premonstratensian

[7] Note the existence of two homonymous abbeys in Guernsey and Whitland: see p. 312 of Hodgson, J. C. (1902). *A History of Northumberland. Issued under the Direction of The Northumberland County History Committee* (Vol. 6, The Parish of Bywell St, Peter; The Parish of Bywell St Andrew; With Blanchland; The Chapelry or Parish of Slaley). Andrew Reid & Company, Limited.

community related to the wardship of his nephew and Hugo's lands is difficult to assess based on the available evidence. The question certainly warrants further investigation.

In 1166, Walterus made the final payment to the King, and his account was declared closed (Hall, 1896, pp. 316-317; The Pipe Roll Society, 1889, p. 105), meaning that securing the wardship of his nephew and Hugo's lands was settled. Just one year later, the wardship was assigned to Reginald de Courtenay, who was paying the scutage to the King and managing the estates of Walterus de Bolebec (The Pipe Roll Society, 1890, pp. 10-11).

2.3. Architectural Analysis

2.3.1. Comparison with Other Premonstratensian Abbeys

Previous structural analysis established that the Abbey of St Mary the Virgin in Blanchland underwent major alterations that significantly reduced its size and completely transformed its appearance (Knowles, 1902; Ryder, 2017). To understand the original outline and visual impact of the abbey immediately following its construction, we must examine the site's archaeological record alongside documented examples of Premonstratensian abbeys (Clapham, 1923).[8] The dimensions of what remains of the original phase of the building closely match those of abbeys such as Bayham and Titchfield (**Figure 8**).

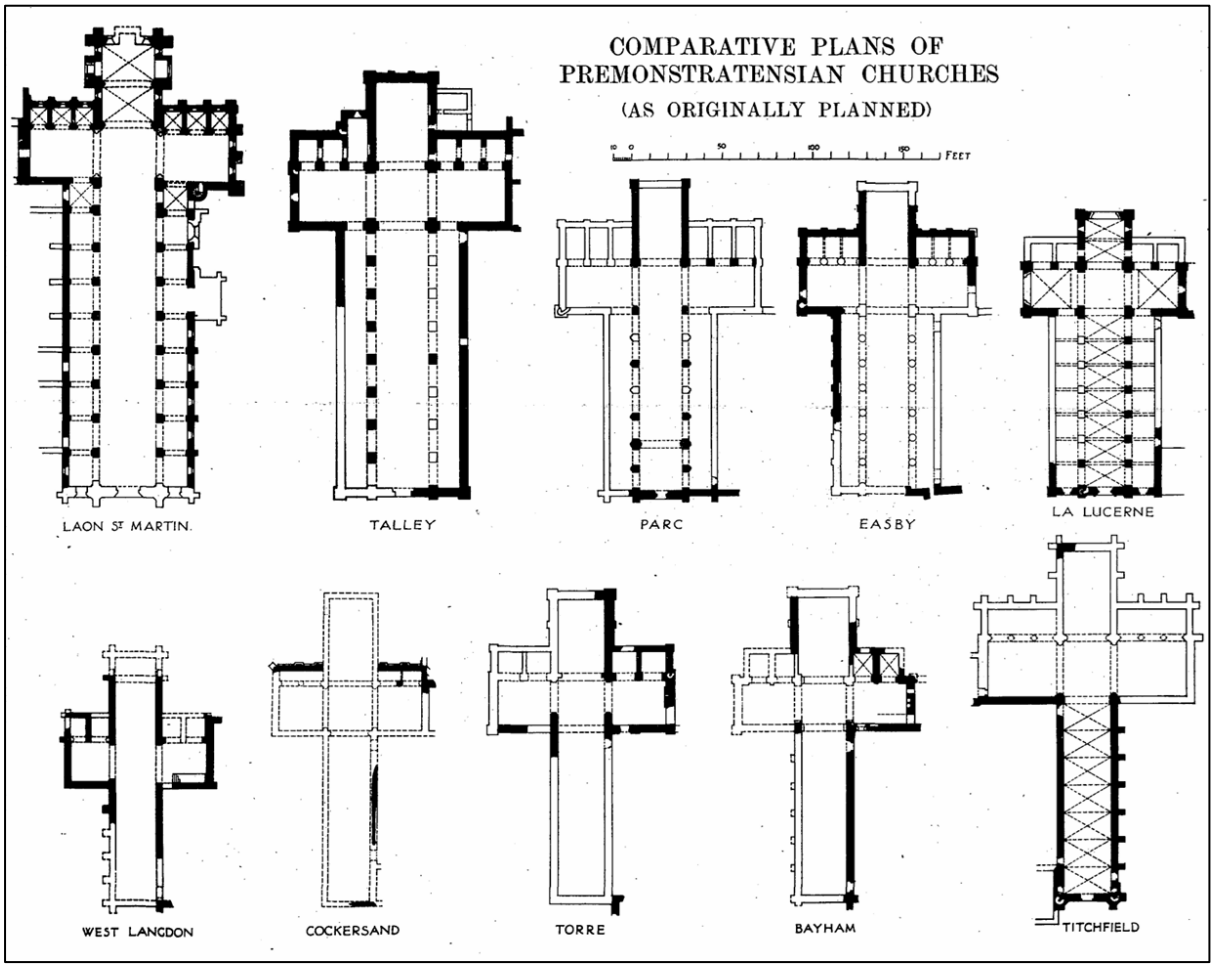

Figure 7. Plans of nine Premonstratensian abbeys, from Clapham 1923: Plate XX.

[8] These include Alnwick (no longer standing), Coverham, Easby, Egglestone, and Beauchief.

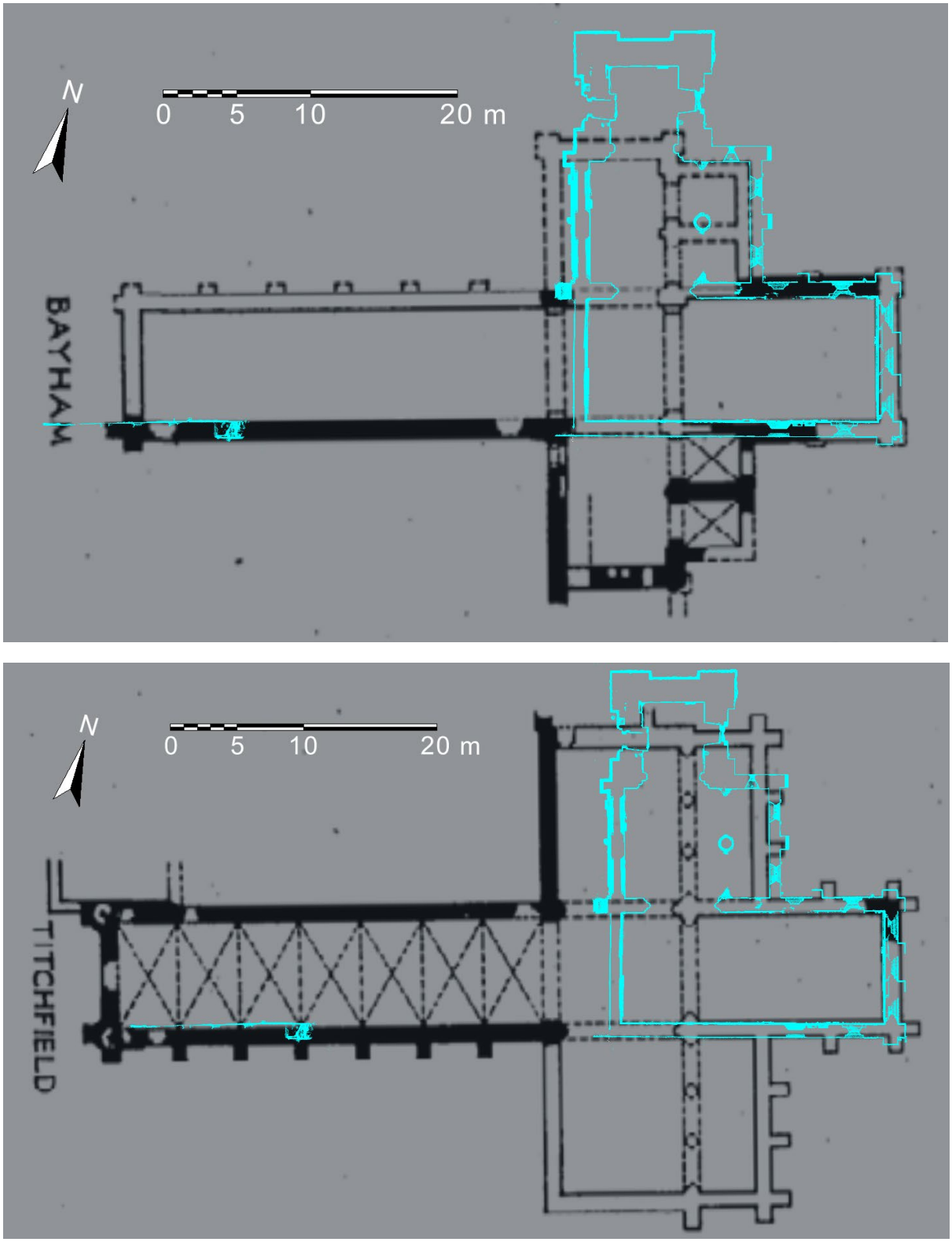

Figure 8. a and b. Scale comparison of the TLS point cloud of Blanchland abbey (cyan) and the original plans of the Premonstratensian abbeys of Bayham (above) and Titchfield (below) according to Clapham 1923: Plate XX.

Establishing the precise length of the medieval abbey requires further investigation of the masonry adjacent to the Lord Crewe Arms, which includes a blocked lancet window, possible remains of a piscina, and traces of additional openings. Laser scanning data show that the lancet window is at a considerably higher level than the chancel windows, which is reasonable considering that monastic structures probably abutted the lowest portion of the nave's south wall. A 6:1 ratio for the length and width of the medieval abbey appears likely, but it is not possible to confirms this hypothesis without further structural analysis. An accurate laser scanning survey of the masonry around the lancet window integrated with the point cloud described in this analysis may enable us to narrow down the location of the abbey's western façade. It is noteworthy that the anonymous 1950s plan of the abbey records the foundations of a large tower in the façade area (Young et al., 2023, p. 19, fig. 6).[9] Unfortunately, the source of this information is currently unknown. The presence of a tower and exact location of the façade can be verified only through new archaeological investigation, in the area between the western portion of the abbey's graveyard and the Post Office, including the B6306 pavement and carriageway.

[9] 'SUBSTANTIAL FOUNDS / INDICATING LARGE / WEST TOWER'

2.3.2. Structural Deformation

The new survey reveals that the twelfth-century side walls of the nave suffered noticeable deformation before the building was restored. In particular, measurements show outward tilts of approximately 0.9° for the south wall and 1.3° for the north wall (**Figure 9**, **Figure 10**).[10]

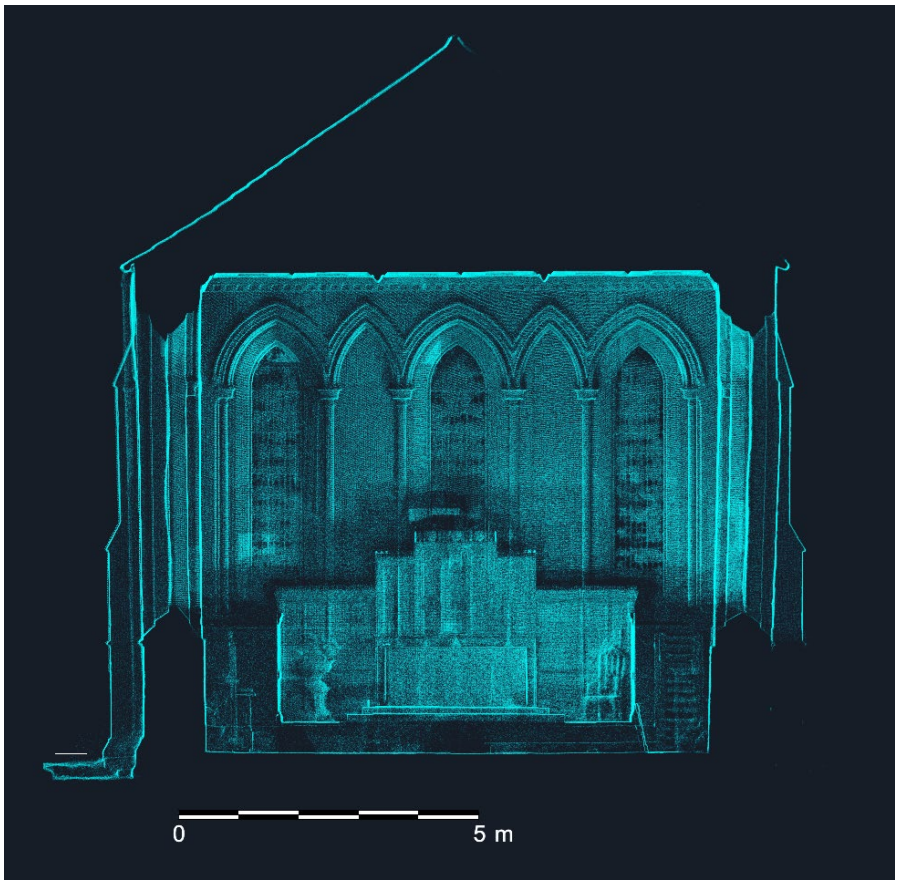

Figure 9. Section of the TLS point cloud of the abbey showing the eastern end of the chancel and the outward leaning of the medieval side walls.

[10] For the chronology of the building's restorations cf. especially Ryder, P. F. (2017). *St Mary the Virgin: Blanchland. An Archaeological Assessment. March 2017.* , Young, R., Newton, A. C., & Severn Newton, S. (2023). *Historical and Archaeological Research at Blanchland Abbey*.

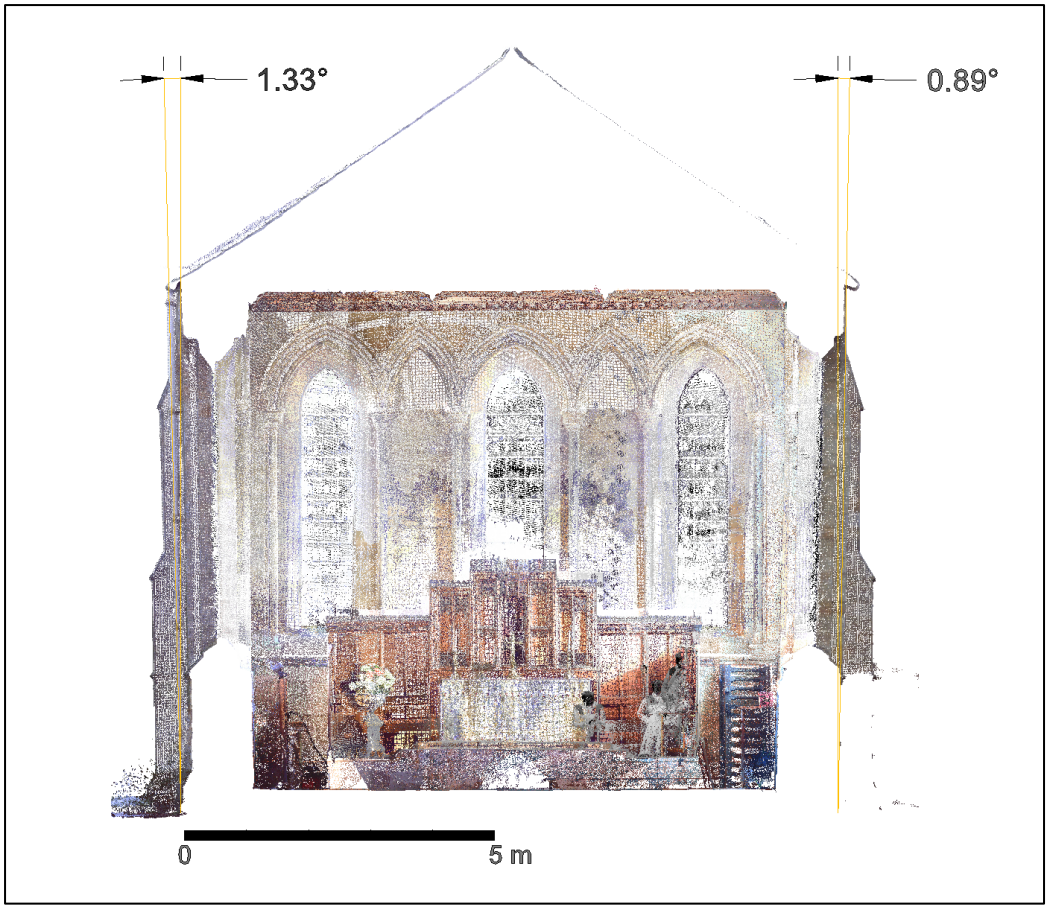

Figure 10. Section of the TLS point cloud of the chancel viewed from the west showing the inclination of the medieval side walls.

2.3.3. Roof Tabling in the Tower's South Wall

The projecting roof tabling in the south wall of the tower provides a reliable indication of the roof system when the tower was built. Indeed, the tabling is not an insertion, but was carved directly into the sandstone blocks of the tower's masonry. The TLS point cloud enabled analysis for the first of the metrics of the tower's south surface and visualisation of the relation between its external and internal portions (**Figure 11**). Measured on the point cloud, the projecting roof tabling has a pitch of 56°. This is consistent with other eleventh to thirteenth-century examples of churches in Britain (Reed, p. 1, fig. 2: 55° in Barton-upon-Humber; cf. Reed, 2020).

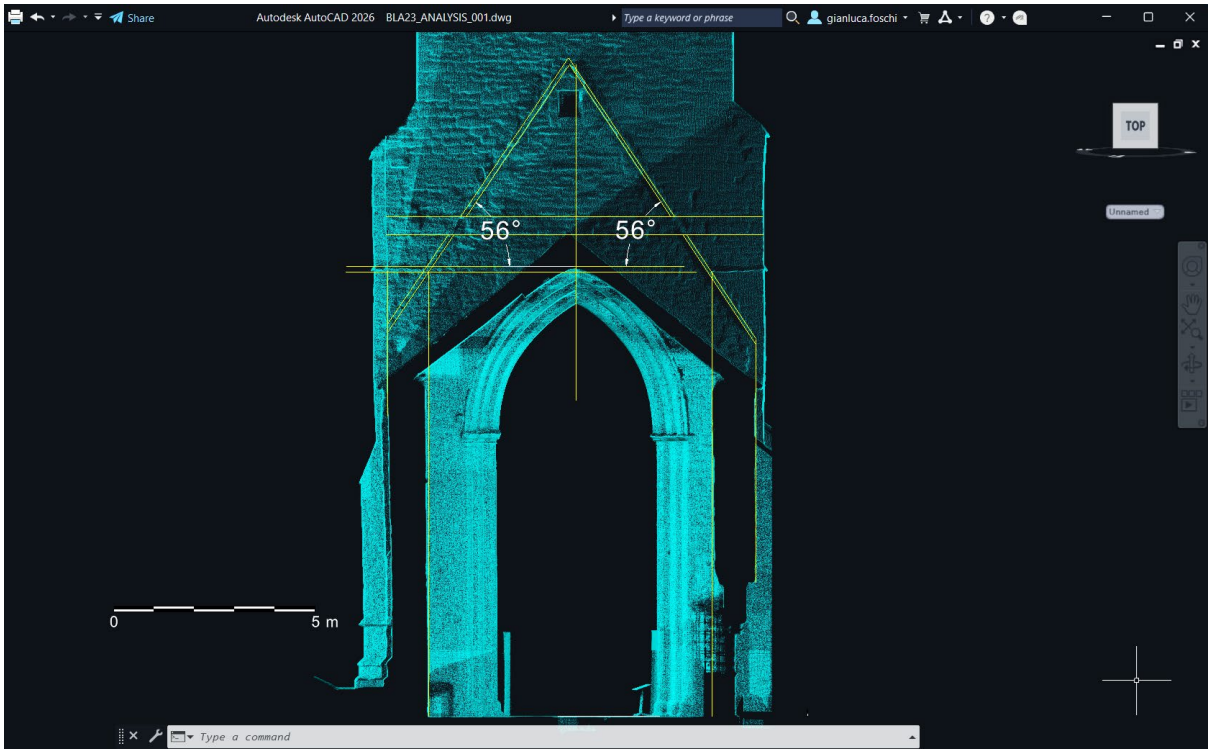

Figure 11. Analysis of the projecting roof tabling in the south side of the tower, performed on the TLS point cloud.

The two points where the projecting roof tabling intersects the horizontal moulding of the tower clearly define the internal width of the transept (**Figure 11**). The line connecting these two points is at the same height as the apex of the northern arch of the transept. This line is approximately 11.04 m above the datum in **Figure 16**. No horizontal structure of the roof system could have been present below this level, otherwise it would have obstructed the open span of the transept's northern arch. This means that no tiebeam could be placed at the level of the eaves, which could not have been higher than 9.24 m above the datum in **Figure 16**, as indicated by the eastern lower limit of the roof tabling. Since stone vaulting must be excluded due to the absence of substantial buttresses and abutments in the perimeter walls, the transept must have been covered with a wooden roof without a tiebeam at its base. This information is of considerable interest as it suggests that, when the tower was constructed, the transept may have had a roof similar to rare vernacular examples documented in County Durham around the mid-thirteenth century (Roberts, 2008, p. 29, fig. 2).

Significantly, the higher moulding of the transept's southern arch appears to have reached a maximum height of approximately 8.24 m above the datum in **Figure 16**, corresponding to a level 1 m lower than the eaves of the transept. Unlike the northern arch of the transept, the southern arch would therefore have allowed for a timber truss roof system with a tiebeam at its base. This reinforces the hypothesis that the transept and tower may not have been built simultaneously. The tower may have been added

later, with the original roof of the transept being replaced by a more sophisticated truss structure. However, as will be seen in the analysis of the windows, the medieval builders of the nave, transept and tower appear to have followed similar design methods.

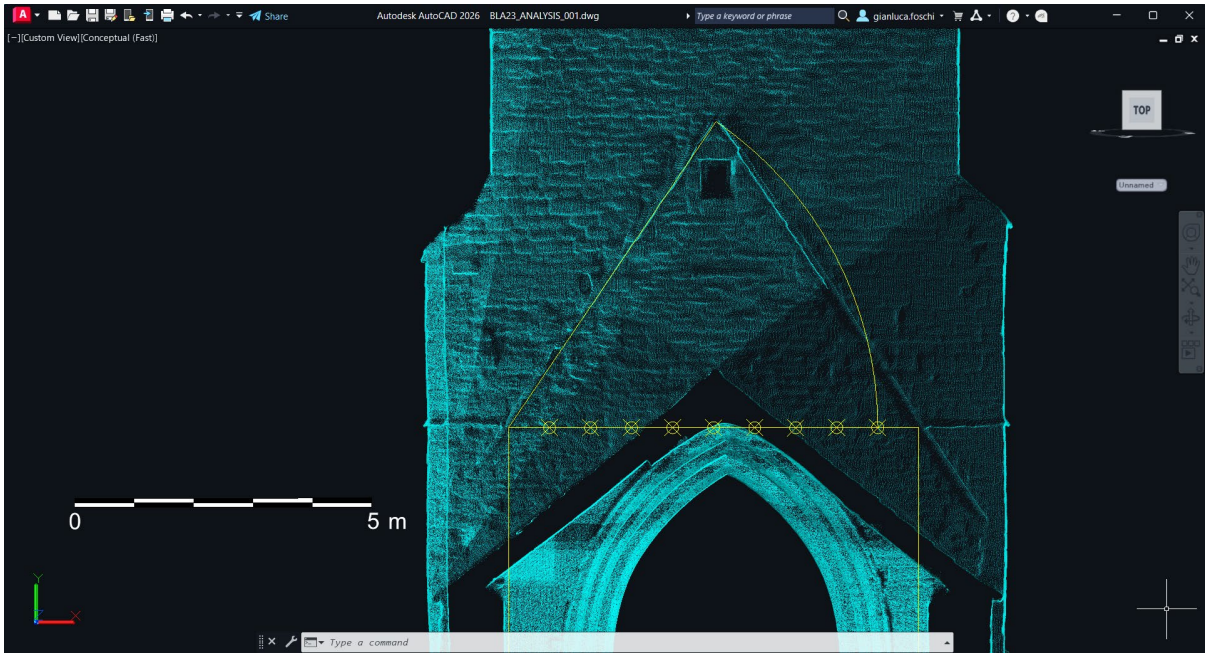

Figure 12. South side of the tower viewed from south on the TLS point cloud. Subdivision of the internal width of the apse into 10 segments to trace the apex of the 56° roof defined by the projecting tabling.

The ridge beam at the apex of the transept's roof contemporary with the tower was probably accommodated near the small vertical opening on the tower's south wall. This opening measures approximately 0.648 x 0.508 m, its height and width being in a 4:3 ratio.

Regarding the design method of the roof, analysis of the point cloud {**Figure 12**) shows that determining the roof pitch was not based solely on subdividing of the tiebeam's width – eaves included – into 16 segments (cf. Reed, 2020). The apex of the roof tabling on the south wall of the tower can be accurately determined by dividing the internal width of the transept – approximately **6.90 m** - into 10 segments of **0.69 m** each. This dimension will be examined further when investigating the possible unit of measurement used in the building's design (see **2.3.5.12**).

2.3.4. Structure East of the Tower

Projecting roof tabling carved directly into the sandstone blocks of the tower's east wall shows that a building once existed in that area. Unfortunately, its remains could not be identified during the most recent excavations (Young et al., 2023, p. 19). The outline of the building appears in an anonymous plan produced around 1950. The document seems to suggest that the foundations and north-east corner of the building were

identified, but it is currently impossible to verify the extent to which such information is reliable. The fact that the roof tabling appears to be part of the masonry rather than a later insertion confirms that the structure must have been built contemporarily with the tower. Low wall remains extending outwards from the northern portion of the tower may be related directly to this building. These traces appear to form a wall approximately 0.93 m wide. Most walls found during the excavations of 2012-2014 in the south range of the monastery and chapter house share a similar thickness (Carlton & Ryder, 2020, pp. 92-93). It is also intriguing that the position and hypothetical size of the building seem symmetrical with the chapter house, mirrored on the central axis of the abbey's nave (**Figure 14**). Only further investigation may clarify the chronology and function of this structure.

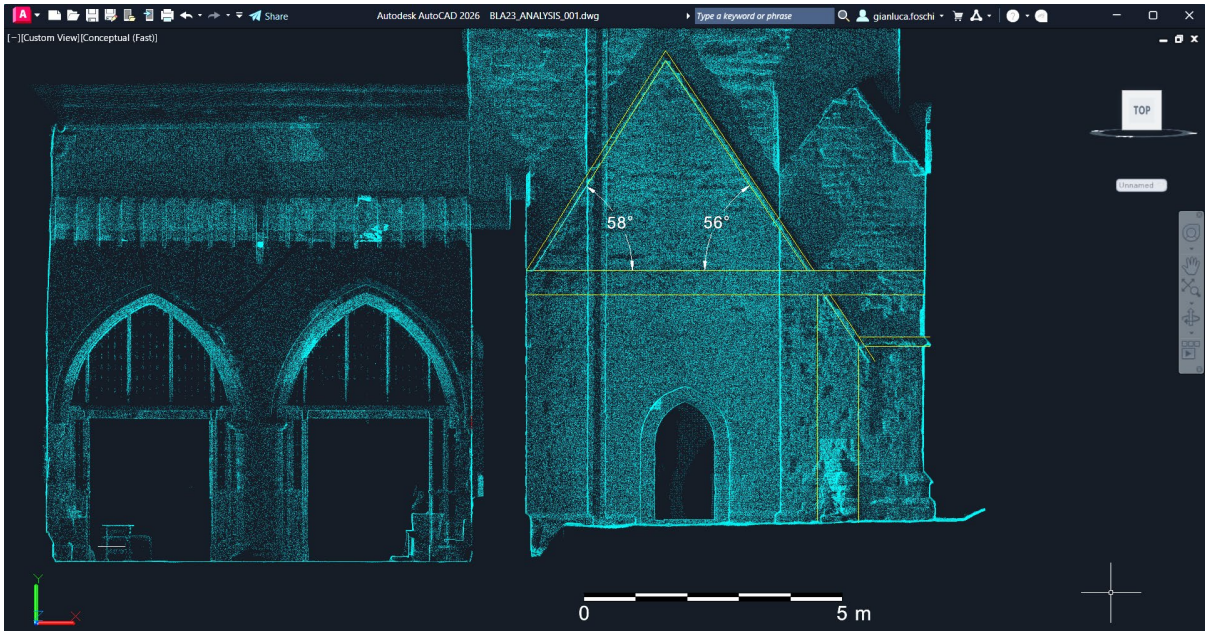

Figure 13. East side of the tower viewed from east on the TLS point cloud. The projecting roof tabling defines a 56-58° pitch. The remains of a wall possibly contemporary to the tower are visible to the north of the tower's doorway near ground level.

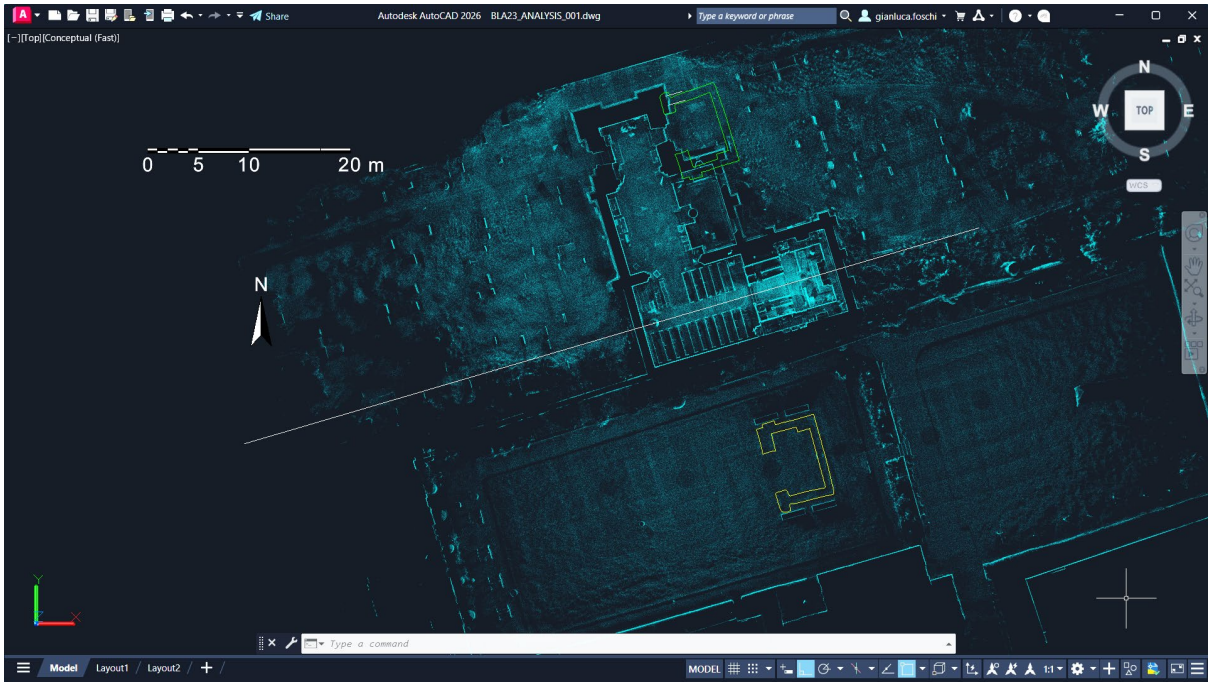

Figure 14. The outline of the chapter house (yellow) of the abbey excavated in 2012-2014 (Carlton & Ryder, 2020), mirrored (green) to the south of the building using the axe (white) of the abbey's nave as mirroring line.

2.3.5. Metrological Analysis

Precise terrestrial laser scanning data has enabled fresh insight into how this abbey was designed during the medieval period. Analysis of the TLS data suggests that the mouldings in the external masonry of the medieval abbey were fundamental to the measurement control system used during construction.

Most notably, the pointed arches throughout the building clearly follow a simple and consistent procedure. The curves of each opening are defined by circles centred on two points, determined by dividing an imaginary line between the springing point of the hood mouldings into equal parts. The specific centring methods found in the abbey's openings are discussed below.

This method – based on the hood mouldings – can be identified not only in the side windows of the main nave, but also throughout the opening of the transept and tower, which previous analysis suggest post-date the nave (Carlton & Ryder, 2020; Ryder, 2017). The consistent design of openings according to metrics defined by the mouldings is of some importance. This demonstrates that the mouldings served not merely as practical weather protection for the openings, but played an active role in controlling measurements during the building's design and construction. This finding contributes to our broader understanding of Gothic architectural design, showing that builders worked to standardised procedures throughout the full building process. If the nave, transept and tower are not contemporary with one another, this suggests design procedures that remained consistent over time, spanning at least several decades.

2.3.5.1. *Overall Dimensions*

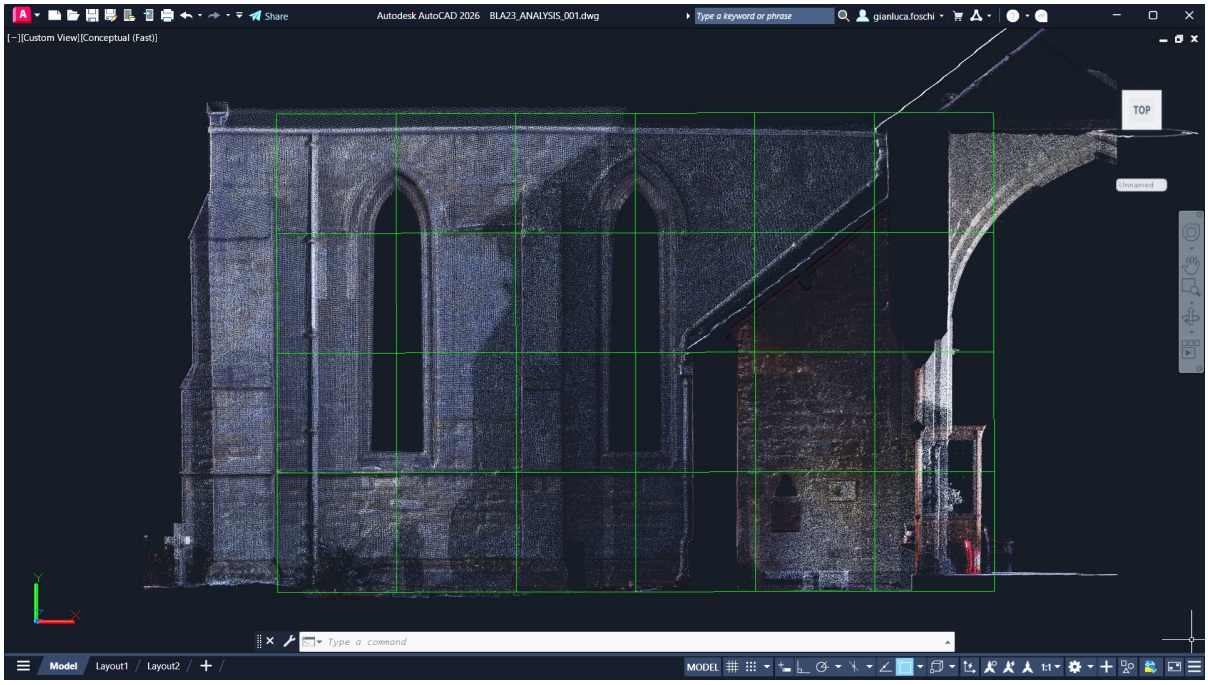

Figure 15. Grid of squares measuring 2.185 m superimposed on the external face of the north wall of the chancel. The grid aligns with the rhythm of the windows, the mouldings and the inner eastern end of the chancel.

The analysis of the building based on TLS data has revealed clear dimensional relationships between mouldings and windows in the external masonry of the chancel. The horizontal distance between the axes of the lancet windows in the north wall – equal to **4.369 m** – corresponds accurately to the vertical distance between the mouldings on the external face of the same wall (**Figure 15**). To illustrate this finding, a grid of squares measuring half this distance has been superimposed on the TLS point cloud of the elevation. This reveals other correspondences: the lower limit of the grid is at the same level as the floor of the chapel north of the transept, while the east limit of the grid aligns closely with the east inner end of the chancel.

The upper limit of the grid suggests a possible height for the eaves of the medieval nave, approximately **8.416 m** above the upper surface of the central slab grave cover in the transept, which serves as the datum (reference level) for the present analysis (**Figure 16**). The floor of the chapel north of the transept – 0.289 m below the datum in **Figure 16 –** is similar to that of the trench immediately outside the north wall of the chancel (**Figure 15**) and may approximate a medieval level. The lower limit of the grid in **Figure 15** is at -0.3222 m below the datum, just 0.033 m below the floor in the northern chapel of the transept. It is worth noting that the archaeological investigations in 2023 exposed flooring (Figure 17) in the western end of the nave at a level of -0.464 below the datum in **Figure 16** (Young et al., 2023). This floor surface, of difficult chronology (Young et al., 2023, p. 117), is 0.175 m below the floor of the chapel north of the transept.

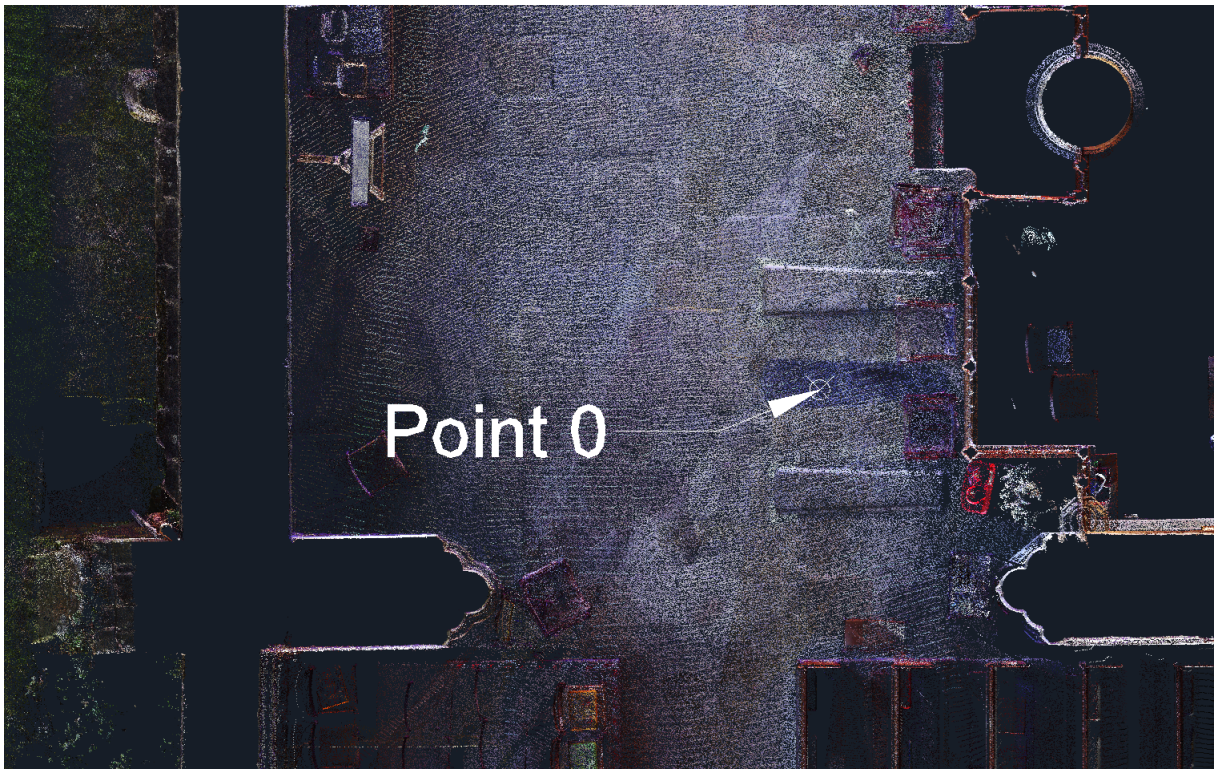

Figure 16. Reference point on the central slab grave cover in the transept, serving as the datum (level 0) for height measurement in this analysis.

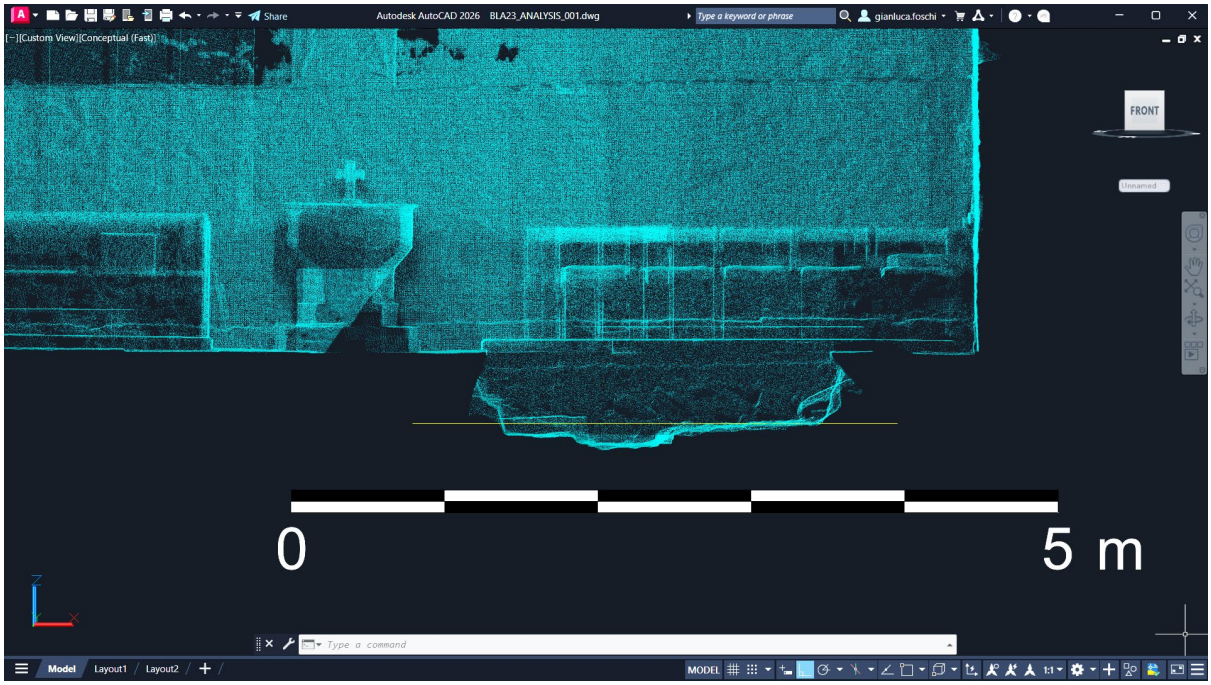

Figure 17. TLS point cloud of the excavation at the west end of the abbey's nave on 11 of February 2023. The yellow line marks the floor level exposed during excavation, situated 0.464 below the datum shown in Figure 16. See (Young et al., 2023, p. 112, context 411).

2.3.5.2. *Chancel, Windows in the North Wall*

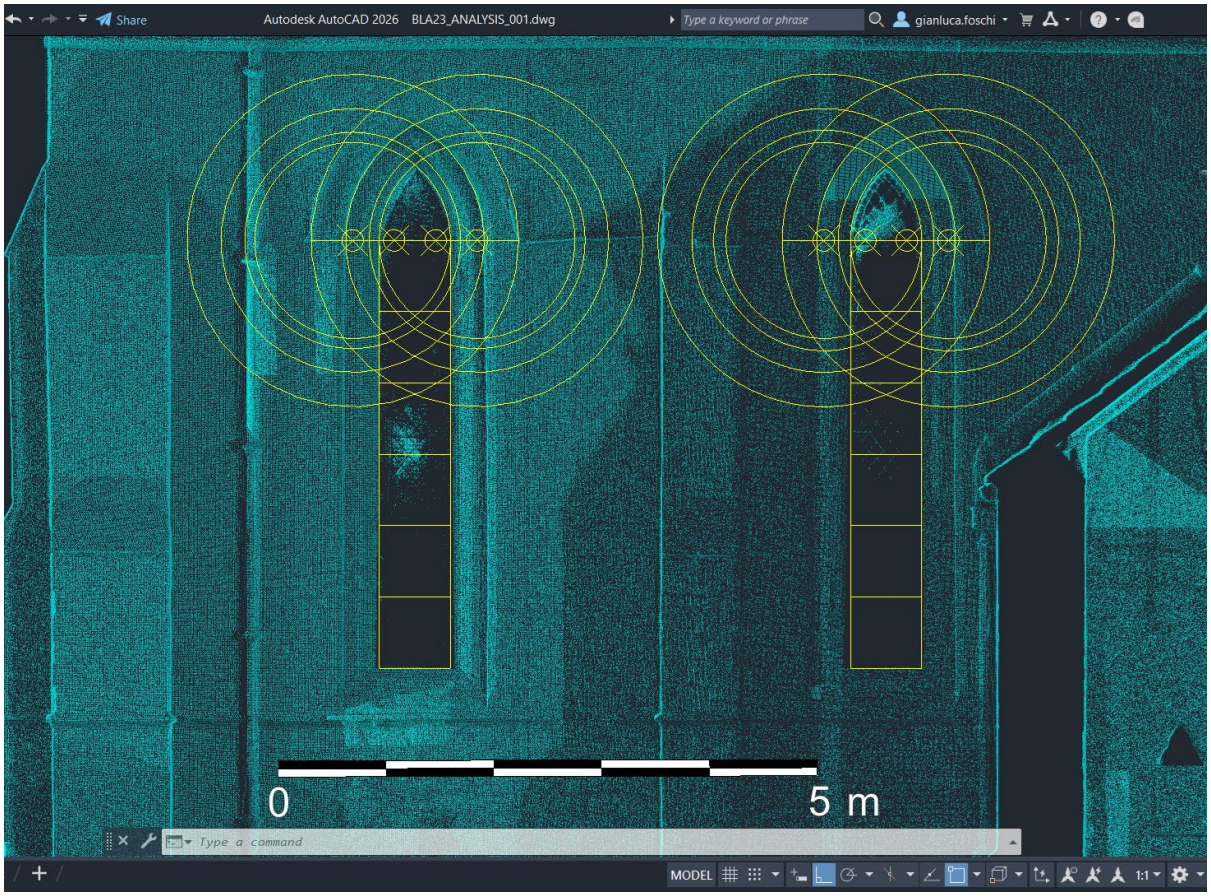

Figure 18. Design of the windows in the north wall of the chancel (viewed from the north) overlaid on the TLS point cloud.

The lancet windows of the chancel's north side wall were dated to the oldest surviving phase of the abbey's structure (Ryder, 2017, p. 11). Their design is based on a line drawn between the springing points of the hood moulding and divided into five equal parts. The circles defining the window arch curves are then centred on the first division from each end of the line (**Figure 18**). Direct measurement from the point cloud data gave a line length of **1.926 m**, making each of the five divisions **0.385 m**. The window opening below the arch spring measures approximately 3.961 x 0.66 m, giving a ratio of 6:1. Both windows were found to be virtually identical in size and design.

2.3.5.3. *Chancel, Windows in the South Wall*

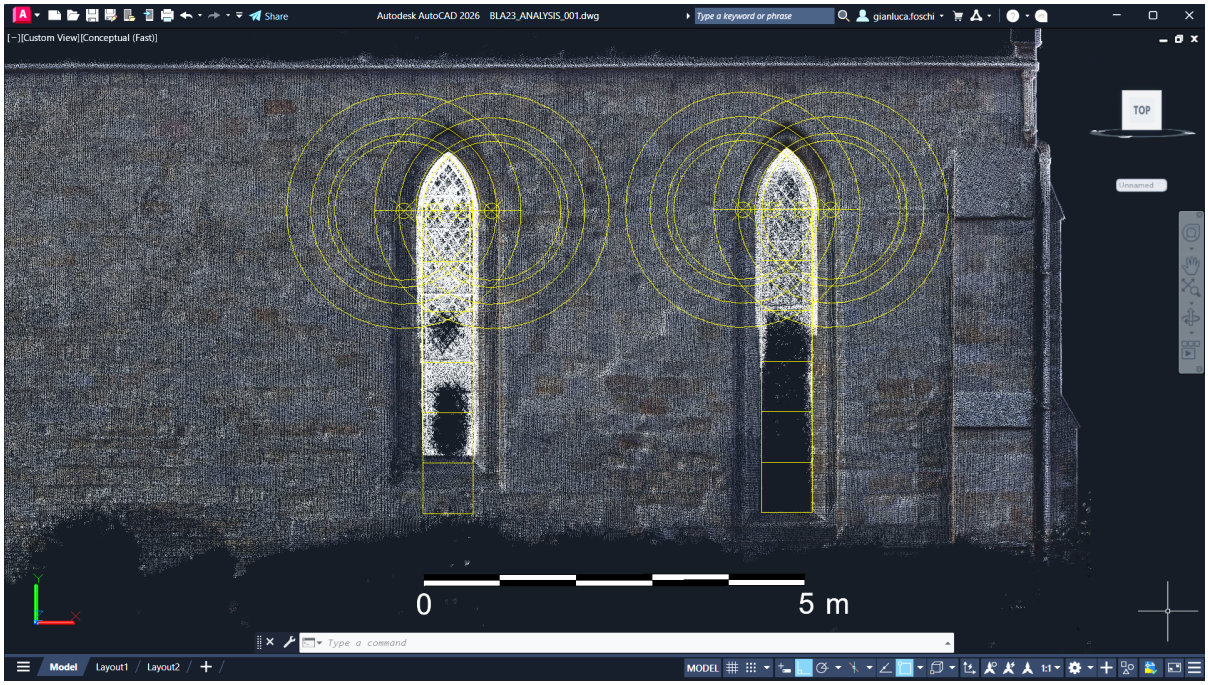

Figure 19. North wall window design (yellow) overlaid on the TLS point cloud of the south wall windows, viewed from the south.

Of the two windows in the south wall of the chancel (**Figure 19**), only the eastern one appears to retain original elements, including part of the hood moulding on its eastern side (Ryder, 2017).[11] The outline and dimensions of this opening are almost identical to those of the medieval windows in the north wall of the chancel. The western window was clearly rebuilt with care to reproduce the dimensions of the medieval originals. Consequently, its general outline and dimensions closely match those of the other three original chancel windows. One notable difference is that its sill is positioned considerably higher, making the opening shorter.

[11] The point cloud show irregularities in the masonry surface between the two windows (see **Figure 19**), which may correspond to the junction between the original medieval abbey wall to the east and later restoration work to the west.

2.3.5.4. *Transept, North Arch*

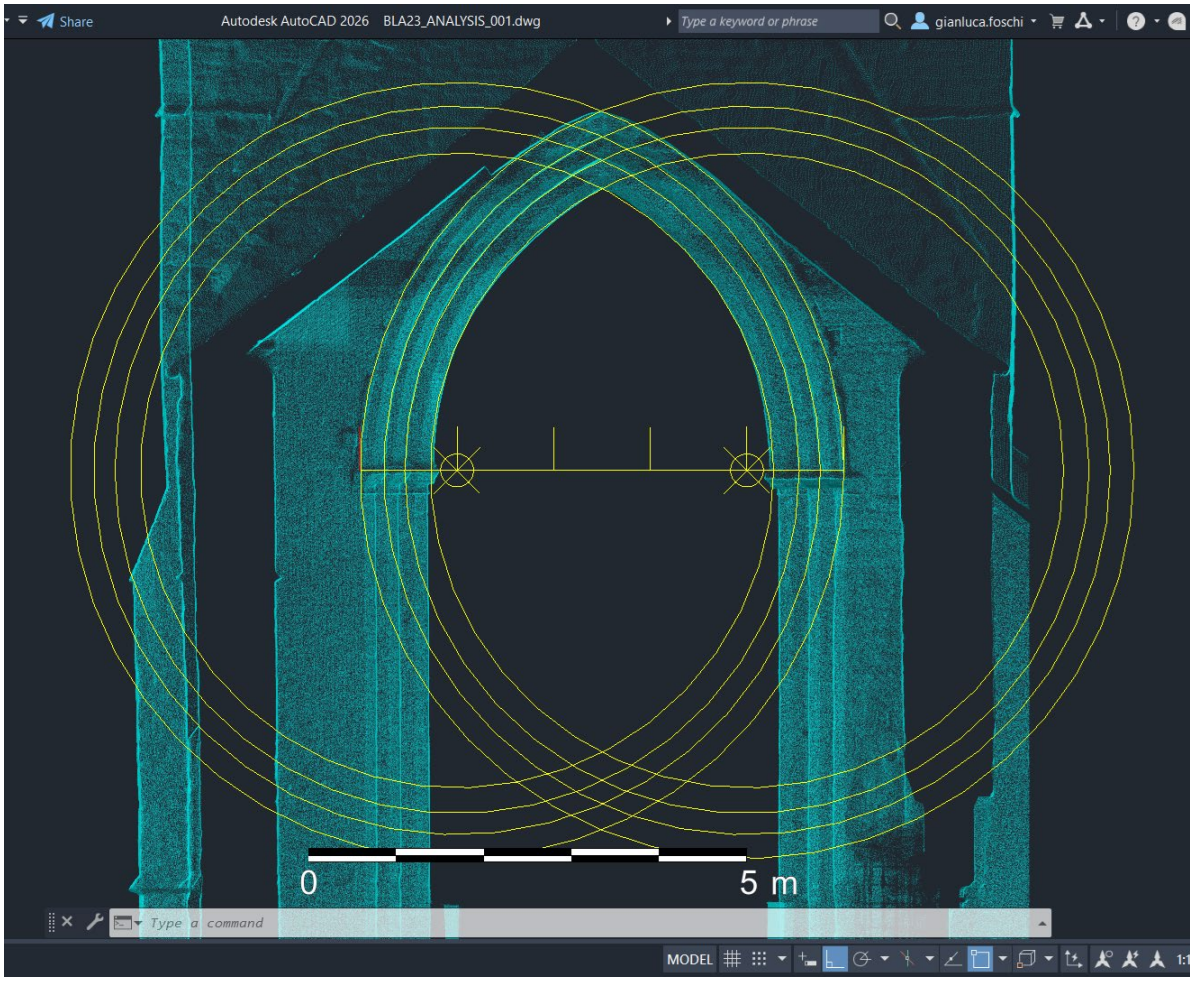

Figure 20. Conceptual design of the transept's north arch (seen from the south) drawn directly from the TLS point cloud.

The transept's north arch forms part of the north tower's masonry and has been dated to the mid-13th century (Ryder, 2017). The design of the arch is based on an imaginary line drawn between the springing points of the hood moulding and divided into five equal sections. The curves that define the three arch chamfers are all centred on the two outermost division points (**Figure 20**). The line measures **5.51 m**, making each division **1.102 m**.

2.3.5.5. *Transept, South Arch*

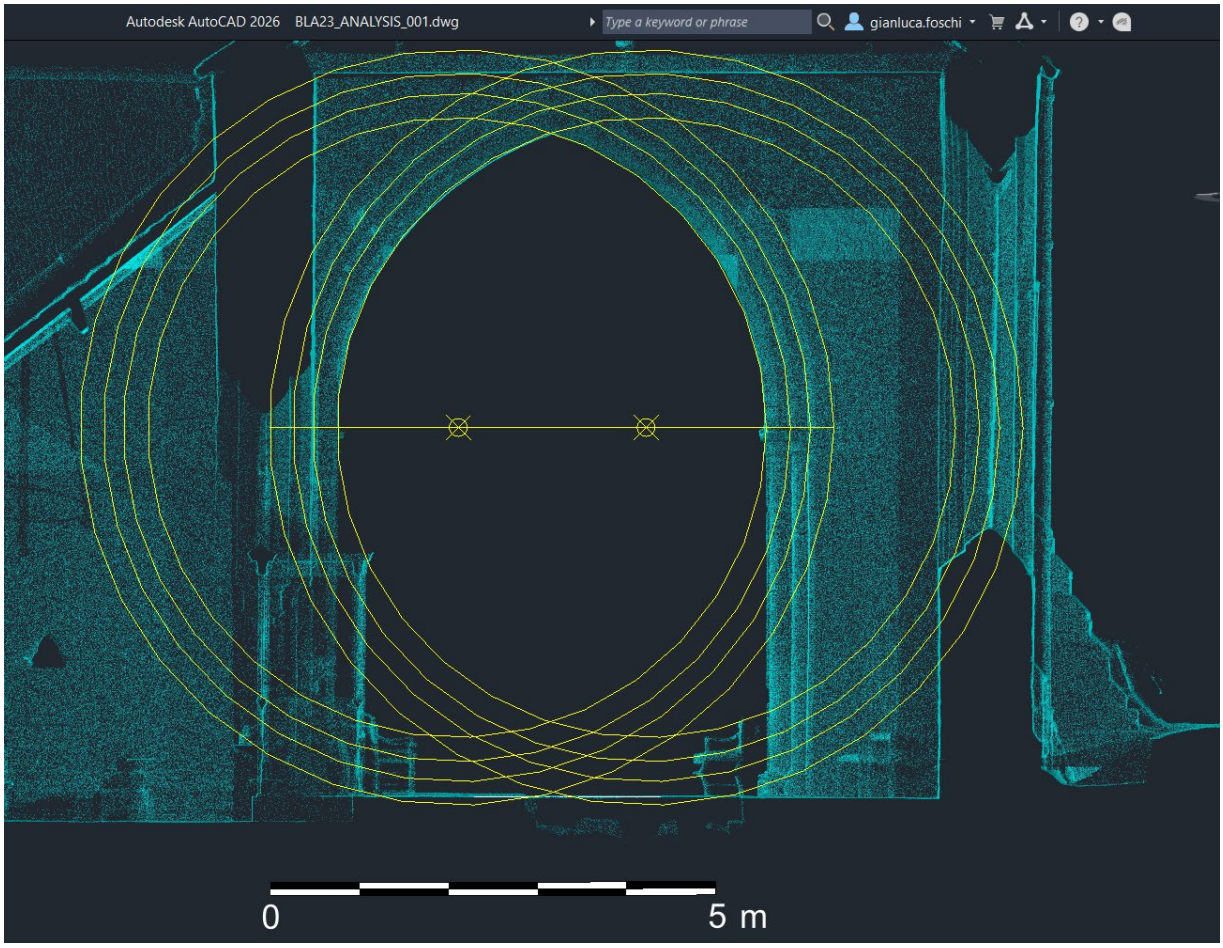

Figure 21. Conceptual design of the arch (viewed from the north) connecting the nave and the transept of the abbey, traced directly on the TLS point cloud.

Although its upper portions were partially rebuilt along with sections of the nave's north wall (Ryder, 2017, p. 9), the general outline of the arch connecting the transept and the nave appears to remain virtually unaltered. All the curves of the chamfers are centred on the two division points that split the line between the springing of the deteriorated moulding hood into three equal parts (**Figure 21**). The length of the line is **6.333** m, making each division **2.111** m.

2.3.5.6. *Transept, East Arches*

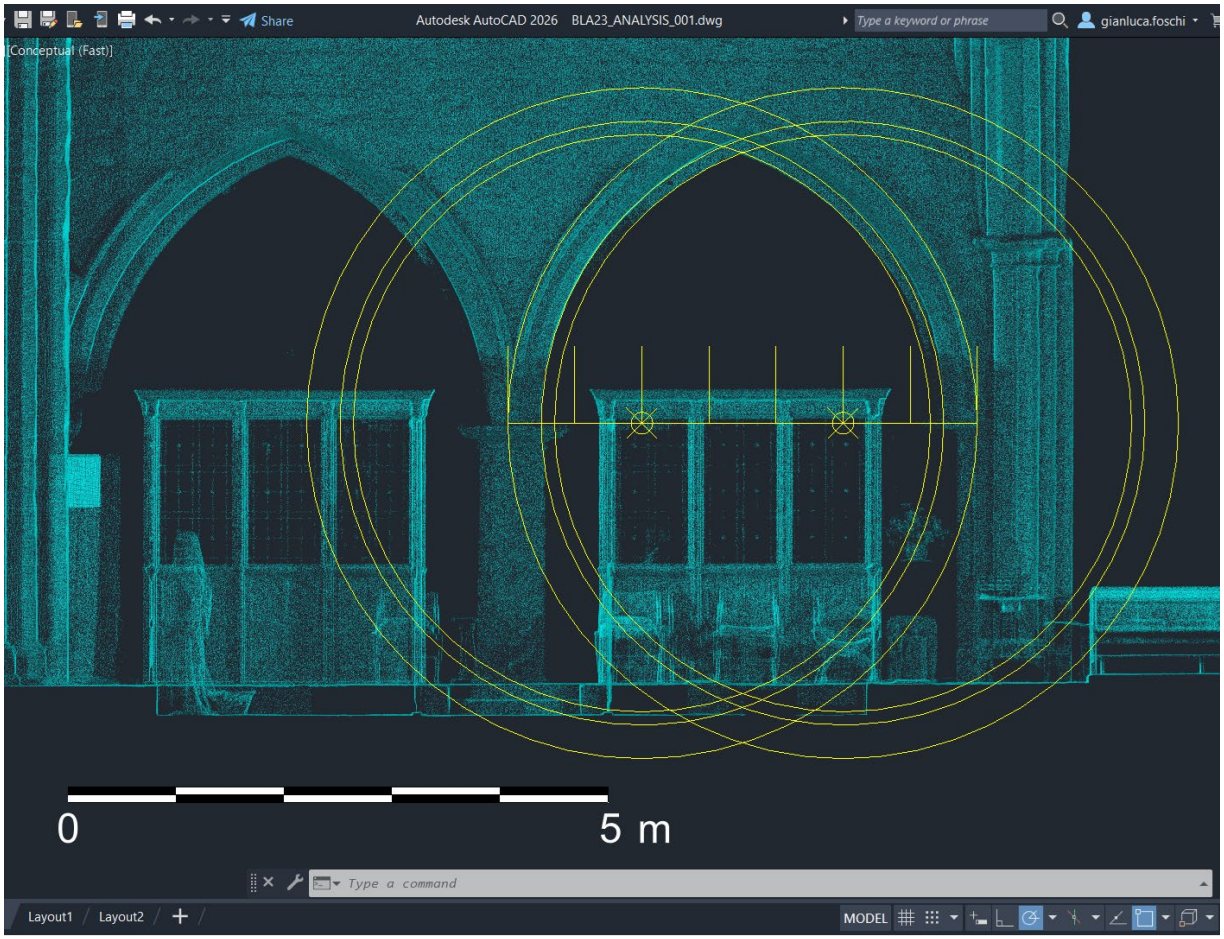

Figure 22. Hypothetical design of the southernmost of the two virtually identical arches in the east side of the transept, viewed from the west, traced on the TLS point cloud.

The chamfer curves of the two arches on the east side of the transept appear to be centred on the third division points from each end of a line drawn between the springing points of the hood mouldings and divided into seven equal parts. The line measures approximately **4.343 m**, making each part **0.62 m**. The line's length is almost identical to the distance between the axe of the windows on the north wall of the nave (4.369 m).

2.3.5.7. *Transept, West Windows*

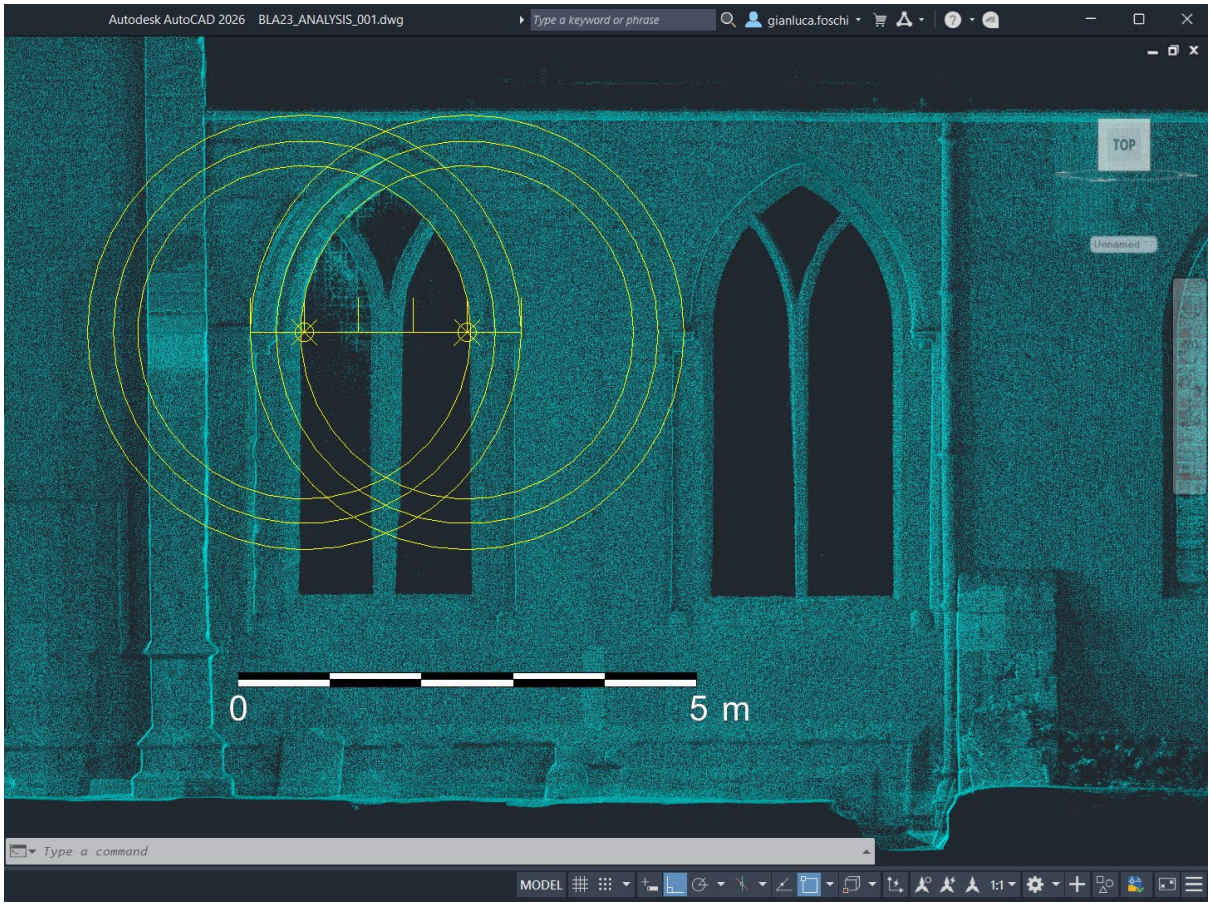

Figure 23. Design of the northernmost of the two virtually identical windows on the west side of the transept, viewed from the west. The design is overlaid directly on the TLS point cloud.

Of the two windows on the west side of the transept, only the northern one retains a portion of hood moulding on its northern side. Although much of the upper masonry to the south appears to be later restoration work, the window's outline seems to be preserved. The chamfers of its arch are centred on the first divisions from each end of a line drawn between the arch springers of the hood moulding and split into five equal parts (**Figure 23**). The line is **2.957 m** long, making each division **0.591 m**.

2.3.5.8. *Tower, North Window*

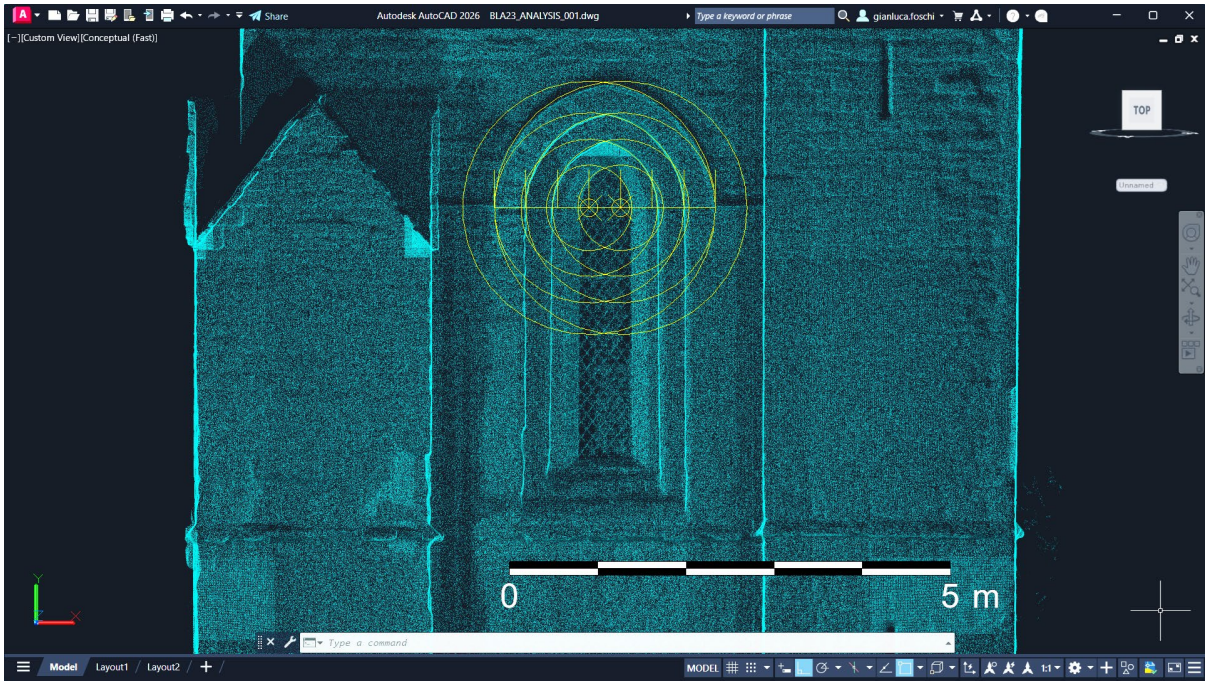

Figure 24. Design of the tower's north window, viewed from the north. The design is drafter directly on the TLS point cloud.

The design of the arches in the tower's north window is defined by the central divisions of a line drawn between the springing of the hood mouldings and divided into seven segments. The line is **2.507 m** long and gives segments of **0.358 m**.

2.3.5.9. *Tower, East Doorway*

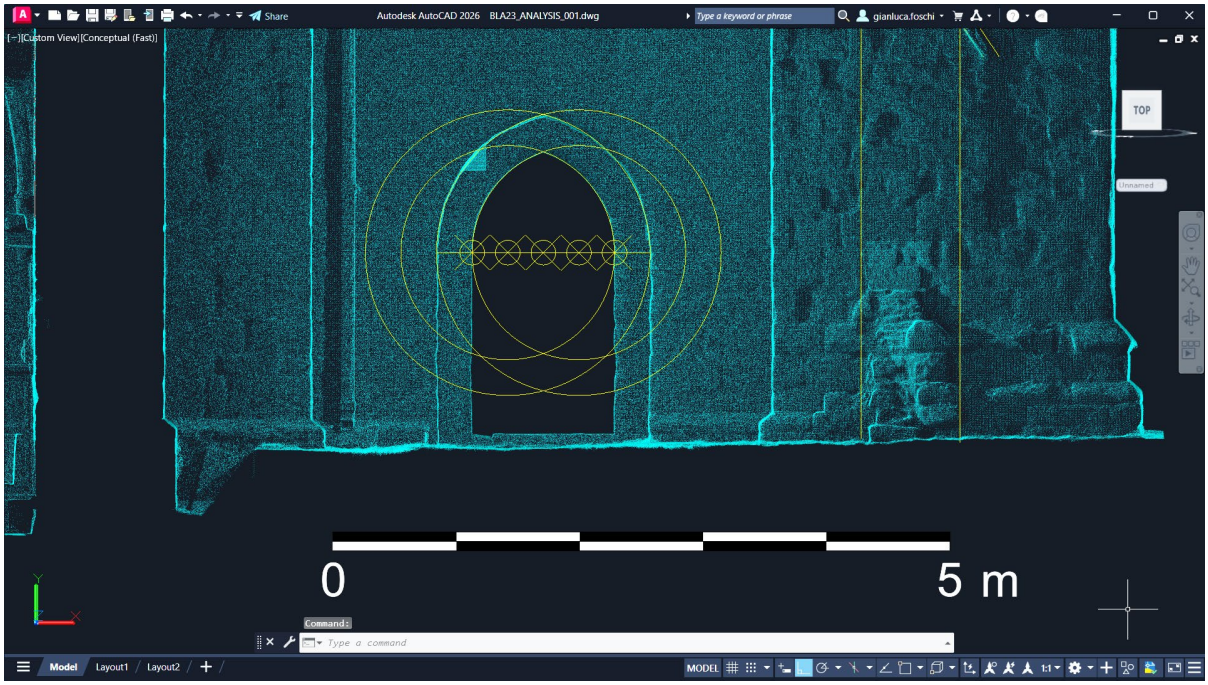

Figure 25. Design of the east doorway of the tower, seen from the east, traced directly on the TLS point cloud.

Among the analysed openings, only the east doorway of the tower lacks a hood moulding that defines its design. However, its outline and dimensions are identical to those of the west doorway of the tower, where the hood moulding is present and perfectly matches the established design system. The east doorway comprises two arches, both centred on the second division from each end of a line split into 6 parts and drawn between the jambs of the innermost doorway opening (**Figure 25**). The first division from each end defines the width of the external opening. The line measures **1.729 m**, making each division **0.288 m**.

2.3.5.10. Tower, West Doorway

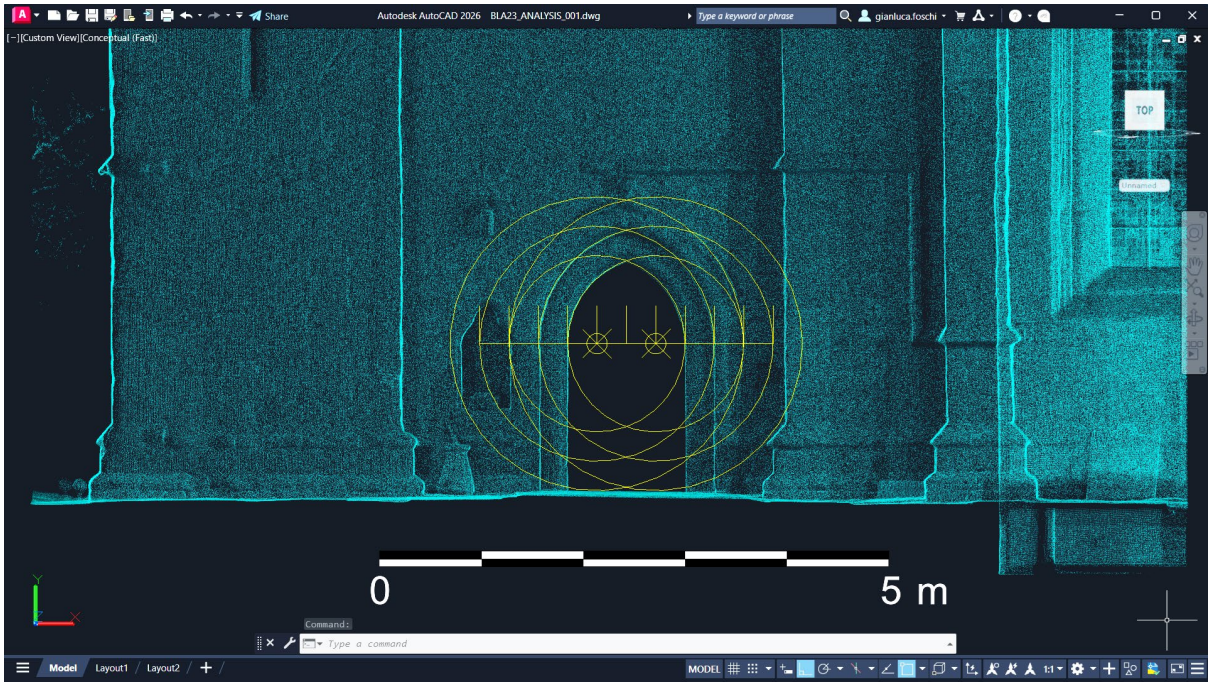

Figure 26. Design of the doorway on the west side of the tower, viewed from the west. The design is traced directly on the TLS point cloud.

The doorway on the west side of the tower is almost identical in outline and dimensions to the one on the east wall. The only difference is that the line defining the curves of the arches has two more segments at each end, accommodating the circles that define the hood moulding. The line is divided into ten segments, and the circles are centred on the fifth division points from each extremity (**Figure 26**). It measures **2.882 m**, giving segments of **0.288 m**.

2.3.5.11. *Tower, West Window*

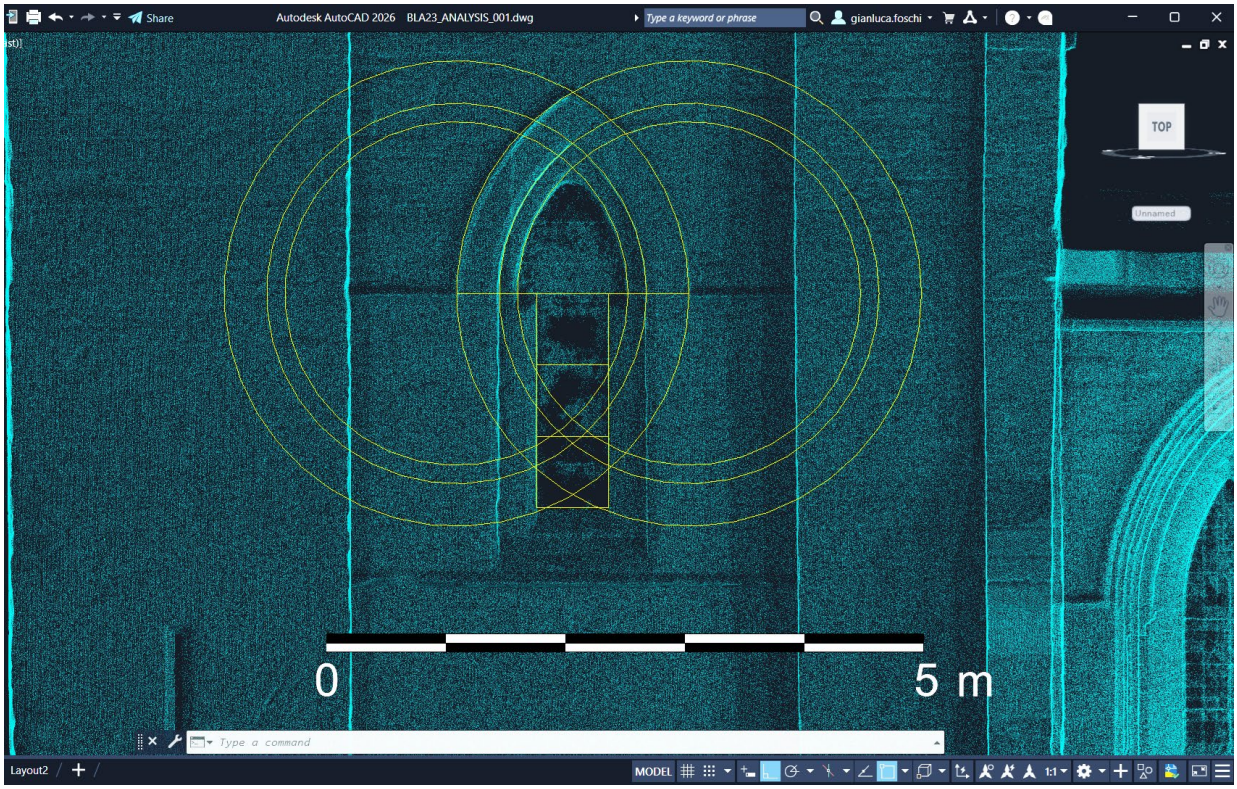

Figure 27. Design of the west window of the tower, seen from the west. The design is traced directly on the TLS point cloud.

The design of the west window of the tower is based on a line drawn between the springing points of the hood moulding. All the curves are defined by circles centred on either end of this line. It measures 1.945 m and its ratio to the overall width of the window frame – measuring approximately 1.238 m – appears to be 11:7. The innermost opening is approximately 1.792 x 0.597 m, giving a ratio of 3:1. Its width is 4/13 times the length of the line that defines the design of the window arches.

2.3.5.12. *Unit of Measurement*

The conceptual design of the windows analysed in the previous sections requires a considerable number of accurate divisions into segments of equal length. This situation raises the question of the unit of measurement. Did the builders use a uniform unit of measurement during the construction of the building?

The problem is complex and lacks straightforward solutions. Testing units of measurement and their submultiples on a dataset, however accurate (such as one acquired using TLS), opens up so many possibilities that narrowing the analysis to a single unit of measurement usually results in obscure conclusions that are biased and extremely difficult to challenge (Fernie, 1978, 1985, 1990). This premise highlights the provisional character of the results of this analysis regarding the possible units of measurement used during the construction of the building.

The abbey of St Mary in Blanchland presents a fortunate case: it has been possible to identify lengths that had to be divided into equal parts to centre the curves of the arches, and therefore measured using some sort of unit. Knowing into how many parts a measurable length had to be divided constrains the possibilities: the unit of measurement would have probably been such as to allow these divisions to produce whole numbers of sub-units.

Therefore, an algorithm was developed based on the following assumptions:

- The unit may have been a foot within the 0.25-0.35 m range[12]
- Each unit was probably subdivided into sub-units (inches) of 1/12 its value[13]
- The unit and its sub-units had to satisfy the following conditions, based on data from the design of the windows and the grid superimposed on the external north elevation of the chancel:
    - 4.369 m can be divided by 2 (chancel's north wall, windows: see **2.3.5.2**)
    - 3.961 m can be divided by 6 (chancel's north wall, windows: see **2.3.5.2**)
    - 1.926 m can be divided by 5 (chancel's north wall, windows: see **2.3.5.2**)
    - 5.510 m can be divided by 5 (transept, north arch: see **2.3.5.4**)
    - 6.333 m can be divided by 3 (transept, south arch: see **2.3.5.5**)
    - 4.343 m can be divided by 7 (transept, east arches: see **2.3.5.6**)
    - 2.957 m can be divided by 5 (transept, west window: see **2.3.5.7**)
    - 1.729 m can be divided by 6 (tower, east doorway: see **2.3.5.9**)
    - 1.945 m can be divided by 11 (tower, west window: see **2.3.5.11**)
    - 1.238 m can be divided by 7 (tower, west window: see **2.3.5.11**)
    - 0.597 m can be divided by 4 (tower, west window: see **2.3.5.11**)
    - 0.648 m can be divided by 4 (tower, south opening: see **2.3.3**)
    - 0.508 m can be divided by 3 (tower, south opening: see **2.3.3**)

[12] The historical values of ancient and medieval foot units in the Mediterranean and Northern Europe are consistently attested within this range. Cf. Fernie, E. (1978). Historical Metrology and Architectural History. *Art History*, *1*, 383-399. , Fernie, E. (1981). The Greek Metrological Relief in Oxford. *The Antiquaries Journal*, *61*, 255-263. , Fernie, E. (1985). Anglo-Saxon Lengths: The 'Northern' System, the Perch and the Foot. *Archaeological Journal*, *142*(1), 246-254. https://doi.org/10.1080/00665983.1985.11021064 , Fernie, E. (1990). A Beginner's Guide to the Study of Architectural Proportions and Systems of Length. In E. Fernie & P. Crossley (Eds.), *Medieval Architecture and its Intellectual Context. Studies in Honour of Peter Kidson* (pp. 229-237). The Hambledon Press. , Schilbach, E. (1970). *Byzantinische Metrologie*. C.H. Beck.

[13] The foot was usually subdivided into 12 inches or 16 digits.

- 6.901 m can be divided by 10 (transept, roof span: see **2.3.3**)

Artificial intelligence[14] was used to facilitate the calculation and avoid biased targeting of specific units. A detailed mathematical analysis of the calculation is provided in **Appendix V** and **Appendix VI**. All results were carefully verified manually.

The specified criteria are met by different potential unit of measurements, which may vary dramatically as soon as new data are added to the input. The automated approach makes it clear the great extent to which it is difficult – most times impossible – to recognise a single value that stands out based solely on dimensional data from buildings. What is evident – and of extreme importance – is that unit subdivisions would have made it possible for the builders to calculate virtually any needed measurement. This is why so many units fit building dimensions, while any practical application of building methods result in the quasi-impossibility to design complex structures in unit whole numbers without recurring to subunits and fractions. It was certainly the measurement system that was bended to the necessities of building practice, not the other way around.

Yet, the results of the algorithm tested in our analysis may be of some historic interest. The metric values that were recognised as the best fit for the set requirements and candidate for a foot unit used in Blanchland are: a) **0.265 m**; b) **0.266 m**; c) **0.264 m**; d) **0.308** m, e) **0.267m**. The value 0.308 M is of significant interest, being significantly close to the English foot of 0.3048 m. Although the unit ranks fourth based on the total absolute error, it is in second place when maximum error is considered (= 0.043 m). If the use of such unit in the early phases of the abbey Blanchland could be confirmed, this would contribute significantly to the debate about the diffusion of standardised units in Britain during the 12th century (Fernie, 1985, 1991).[15]

[14] Claude Opus 4.

[15] Cf. the well-known passage about King Henry I (1100-1135) by William of Malmensbury: '*Mercatorum falsam unlam castigavit; brachii sui mensura adhibita, omnibusque per Angliam proposita*'; 'He corrected the merchants' false ell – having applied the measure of his own arm – and set it before all throughout England.' *Gesta Regum Anglorum*, V, 41; p. 641 in: Hardy, T. D. (Ed.). (1840). *Willelmi Malmesbiriensis monachi Gesta Regum Anglorum atque Historia novella* (Vol. 2). Sumptibus Societatis. For research on historic foot values in Britain see also: Bettess, F. (1991). The Anglo-Saxon Foot: a Computerized Assessment. *Medieval Archaeology*, *35*(1), 44-50. https://doi.org/https://doi.org/10.5284/1071792 , Huggins, P. J. Ibid.Anglo-Saxon Timber Building Measurements: Recent Results. 6-28. https://doi.org/https://doi.org/10.1080/00766097.1991.11735536

Metric Dimension (m)	Original as Units + 12ths	Total 12ths	Divisible by	Exact Division?	Target Value (m)	Result as Units + 12ths	Calculated Value (m)	Error (m)	Unit Used (m)
4.369	14 + 2/12	170	2	✓ (85)	4.3633	7 + 1/12	2.182	-0.006	0.308
3.961	13 + 0/12	156	6	✓ (26)	4.0040	2 + 2/12	0.667	0.043	0.308
1.926	6 + 3/12	75	5	✓ (15)	1.9250	1 + 3/12	0.385	-0.001	0.308
5.510	17 + 11/12	215	5	✓ (43)	5.5183	3 + 7/12	1.104	0.008	0.308
6.333	20 + 6/12	246	3	✓ (82)	6.3140	6 + 10/12	2.105	-0.019	0.308
4.343	14 + 0/12	168	7	✓ (24)	4.3120	2 + 0/12	0.616	-0.031	0.308
2.957	9 + 7/12	115	5	✓ (23)	2.9517	1 + 11/12	0.590	-0.005	0.308
1.729	5 + 6/12	66	6	✓ (11)	1.6940	0 + 11/12	0.282	-0.035	0.308
1.945	6 + 5/12	77	11	✓ (7)	1.9763	0 + 7/12	0.180	0.031	0.308
1.238	4 + 1/12	49	7	✓ (7)	1.2577	0 + 7/12	0.180	0.020	0.308
0.597	2 + 0/12	24	4	✓ (6)	0.6160	0 + 6/12	0.154	0.019	0.308
0.648	2 + 0/12	24	4	✓ (6)	0.6160	0 + 6/12	0.154	-0.032	0.308
0.508	1 + 9/12	21	3	✓ (7)	0.5390	0 + 7/12	0.180	0.031	0.308
6.901	22 + 6/12	270	10	✓ (27)	6.9300	2 + 3/12	0.693	0.029	0.308

*Table 3. (from **Appendix VIII**) Constraints derived from the architectural analysis of the building translated into a unit of 0.308 m.*

2.4. Acoustics

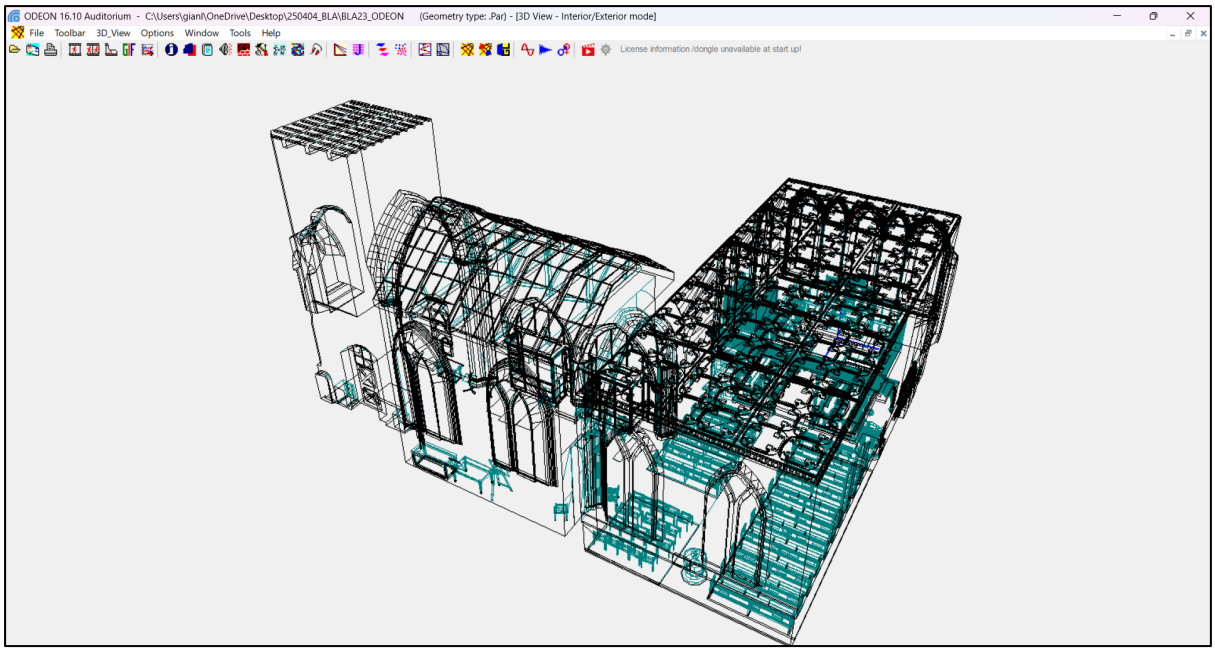

Figure 28. Acoustic model of St Mary the Virgin in Blanchland viewed in ODEON Auditorium software.

The acoustic tests performed in the nave shows that the abbey provides a space that favours musical warmth and vocal performances, while remaining highly suitable for speech. The building was tested without a congregation, and speech intelligibility is likely to improve significantly when the pews are fully occupied.

Sound parameters				Fully furnished	No chancel	Difference
Parameter	**Unit**	**Range (Hz)**	**JND**	**Source A (altar) Receivers 1 to 12**	**Source A (altar) Receivers 1 to 12**	
EDT	s	500-1K	5%	1.47	1.65	12.29 %
T_{30}	s	500-1K	5%	1.63	1.88	15.38
Ts	ms	500-1K	10	98	112	14
G	dB	500-1K	1	13.4	13.7	0.3
D_{50}		500-1K	0.05	0.46	0.42	-0.05
C_{80}	dB	500-2K	1	2.4	1.4	-1.0
LF_{80}		125-1K	0.05	0.23	0.23	-0.001
Echo		500-2K	0.05	0.47	0.48	0.01
STI min		/	0.03	0.55	0.51	-0.04
STI max		/	0.03	0.74	0.67	-0.07
STI aver		/	0.03	0.6	0.57	-0.03

Table 4. Parameters from the digital simulation of Blanchland abbey: fully furnished church vs church without the wooden chancel. The green rows indicate changes that are likely to be perceived by the human hear.

Sound parameters				Wooden ceiling, no furniture	Plaster ceiling, no furniture.	Difference
Parameter	Unit	Range (Hz)	JND	Source A (altar) Receivers 1 to 12	Source A (altar) Receivers 1 to 12	
EDT	s	500-1K	5%	1.94	2.75	41.75 %
T_{30}	s	500-1K	5%	2.15	2.89	34.42 %
Ts	ms	500-1K	10	129	186	58
G	dB	500-1K	1	14.6	15.9	1.3
D_{50}		500-1K	0.05	0.40	0.31	-0.09
C_{80}	dB	500-2K	1	0.5	-1.1	-1.7
LF_{80}		125-1K	0.05	0.22	0.22	0.000
Echo		500-2K	0.05	0.48	0.49	0.01
STI min		/	0.03	0.5	0.43	-0.07
STI max		/	0.03	0.6	0.53	-0.07
STI aver		/	0.03	0.54	0.47	-0.07

Table 5. Parameters from the digital simulation of Blanchland abbey: wooden ceiling vs plaster ceiling in the unfurnished church. The green rows indicate changes that are likely to be perceived by the human hear.

This immersive, yet not excessively reverberant character is primarily attributed to the wooden surfaces in the nave, particularly the choir and ceiling. These surfaces absorb sound at lower frequencies and reduce reverberation in the space, making sound more brilliant and enhancing speech clarity.

Digitally simulations of sound emitted from a source positioned in front of the altar (**Table 6**: source A), with part of the furniture removed, demonstrate the extent to which the absence of the chancel affects the nave's acoustics (**Table 4**, **Table 6**: receivers 1 to 12). Average EDT rises from 1.47 to 1.65 seconds, indicating significantly increased reverberation. This results in the average STI dropping from 0.60 to 0.57, which indicates that speech intelligibility declines from good to just above fair according to international standards (IEC 60268-16, 2020; ISO 9921, 2003). In simple terms, more effort is required to understand speech. The effect is even more dramatic when the abbey is simulated as if it were emptied of all furniture (**Figure 33**), with EDT increasing to 1.94 and STI dropping to 0.54.

When a plaster ceiling is simulated in the empty building instead of a wooden ceiling (**Table 5**), EDT jumps to 2.75 s and STI drops to 0.47, meaning that speech intelligibility is degraded to poor (IEC 60268-16, 2020; ISO 9921, 2003). To illustrate the wooden ceiling's impact on the church's acoustics: EDT increases by 41.75%, well beyond the 5% Just Noticeable Difference threshold.

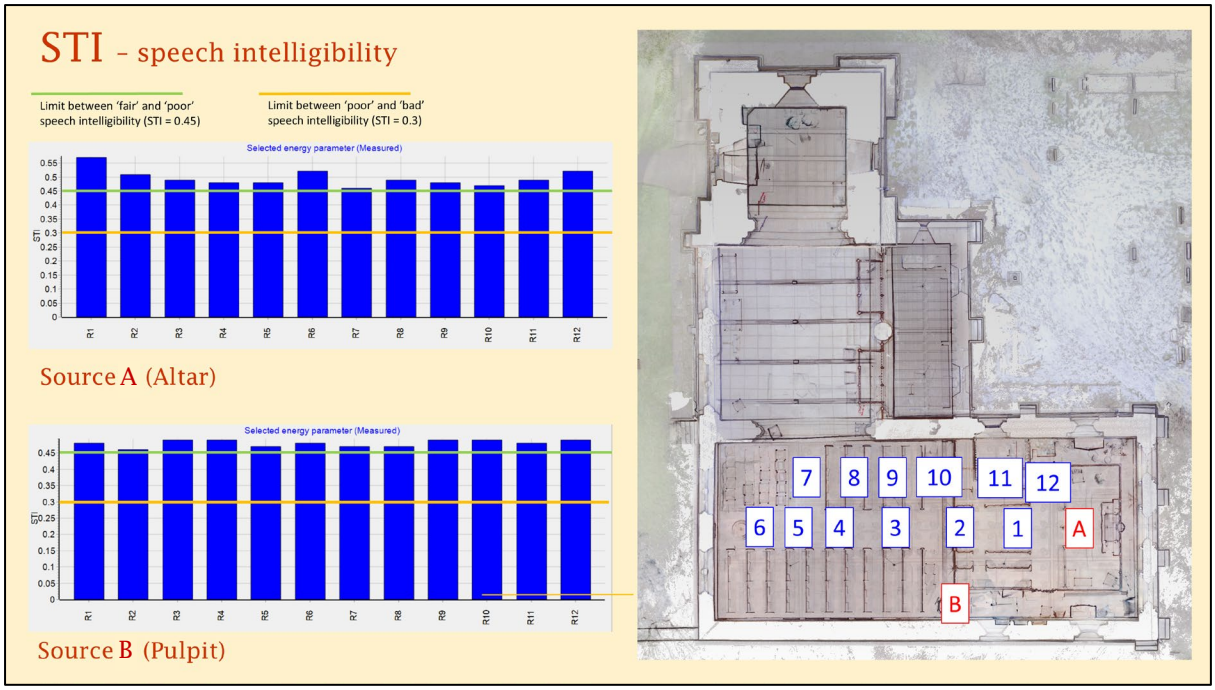

Table 6. Chart showing the difference in STI (speech transmission index) across listener positions in the nave with a sound source near the altar (above) and on the pulpit (below).

Sound parameters				Nave, fully furnished	Transept, fully furnished	Difference
Parameter	**Unit**	**Range (Hz)**	**JND**	**Source A (altar) Receivers 1 to 12**	**Source C (nave) Receivers 1 to 19**	
EDT	s	500-1K	5%	1.47	2.07	40.96 %
T_{30}	s	500-1K	5%	1.63	1.88	15.69 %
Ts	ms	500-1K	10	98	144	46
G	dB	500-1K	1	13.4	11.4	-2.1
D_{50}		500-1K	0.05	0.46	0.32	-0.15
C_{80}	dB	500-2K	1	2.4	-0.7	-3.1
LF_{80}		125-1K	0.05	0.23	0.33	0.096
Echo		500-2K	0.05	0.47	0.52	0.05
STI min		/	0.03	0.55	0.44	-0.11
STI max		/	0.03	0.74	0.56	-0.18
STI aver		/	0.03	0.6	0.49	-0.11

Table 7. Parameters from the digital simulation of Blanchland abbey: perception of sound from the altar received in the nave vs perception of sound from the western section of the nave received the transept, fully furnished church. The green rows indicate changes that are likely to be perceived by the human hear.

When the sound source is moved from the altar to the pulpit in the fully furnished church (**Table 6**: source B, receivers 1 to12), speech intelligibility becomes more homogeneous across the nave (**Table 6**), although overall acoustic changes are unlikely to be noticeable.

The transept and tower emerge as the most acoustically disadvantaged section of the church. This is due to its more enclosed position and different ceiling construction. Comparing acoustic parameters for sound from the altar received in the nave with those for sound from the western section of the nave received in the transept and tower (**Table 7**, **Figure 29**: source C, receivers 1 to 6 and 13 to 19) reveals significant differences. In the transept, EDT is more than 40% higher than in the nave while STI drops from 0.6 to 0.49. Under such conditions, the acoustics of the transept are comparable to those of the unfurnished church with a plaster ceiling in the nave (compare **Table 5** and **Table 7**).

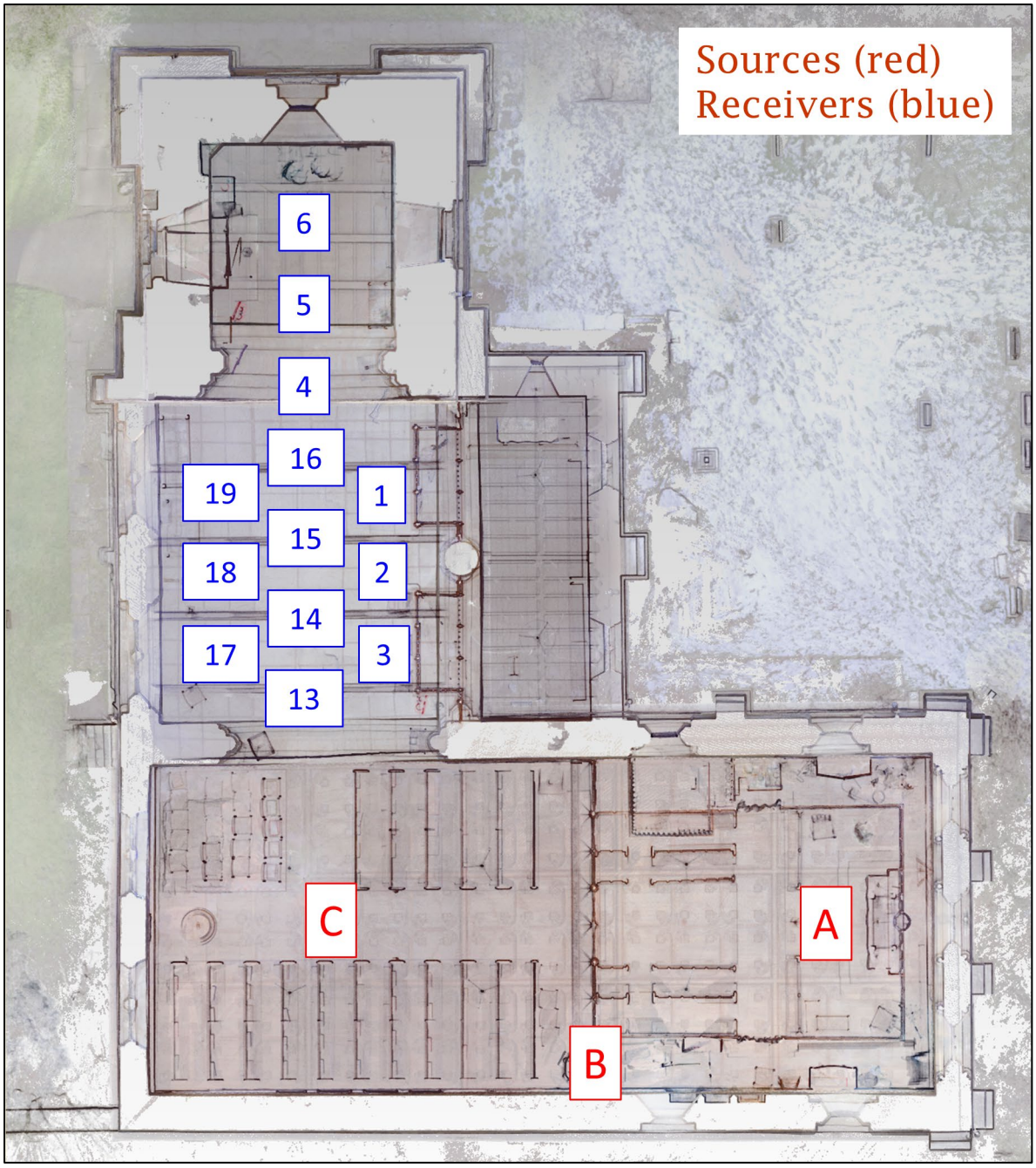

Figure 29. Position of sources (red) and receivers (blue) for the digital test of the transept's acoustics.

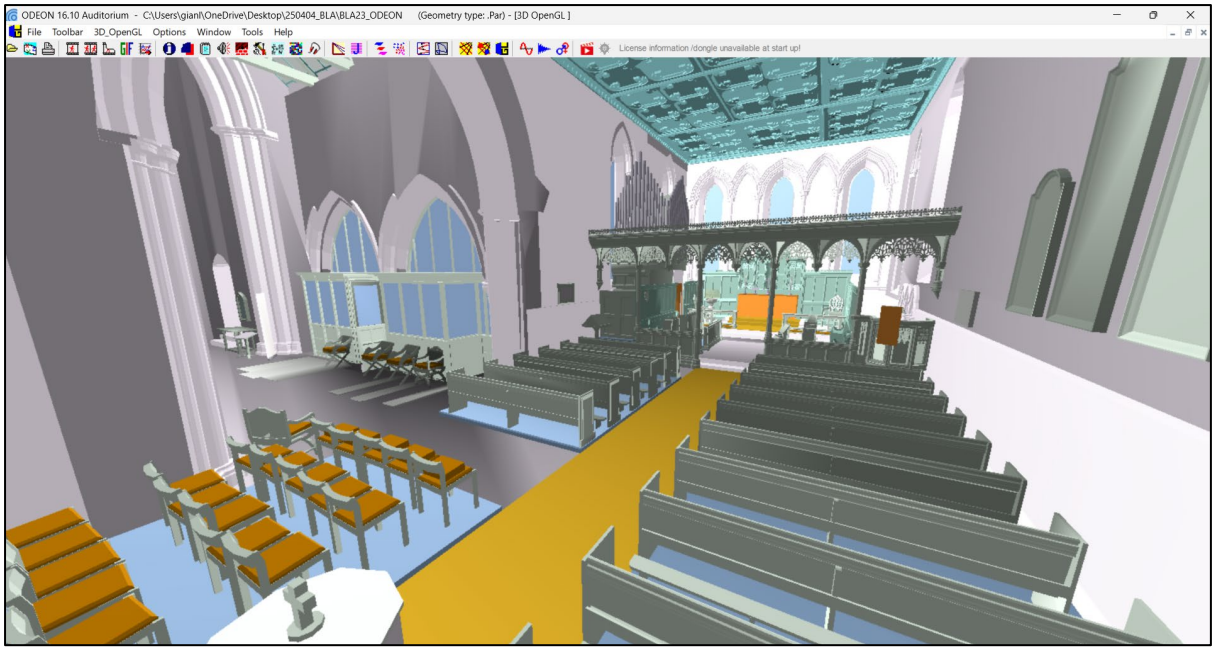

Figure 30. Acoustic model of the church: nave and transept.

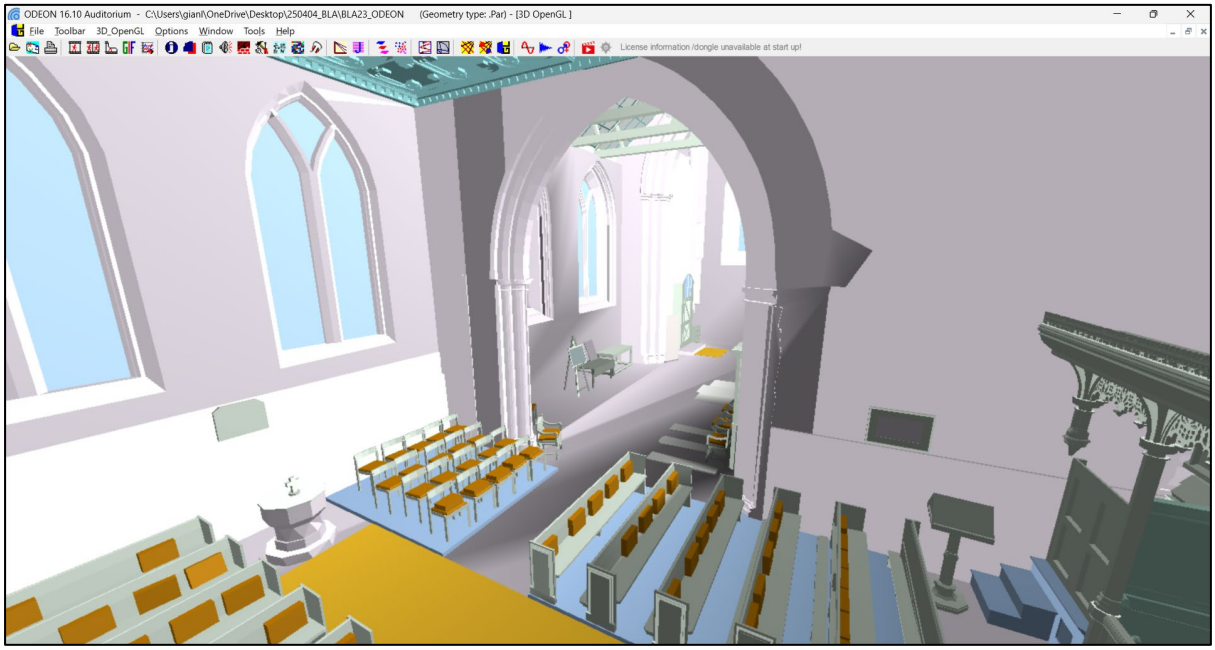

Figure 31. Acoustic model of the church: nave and transept.

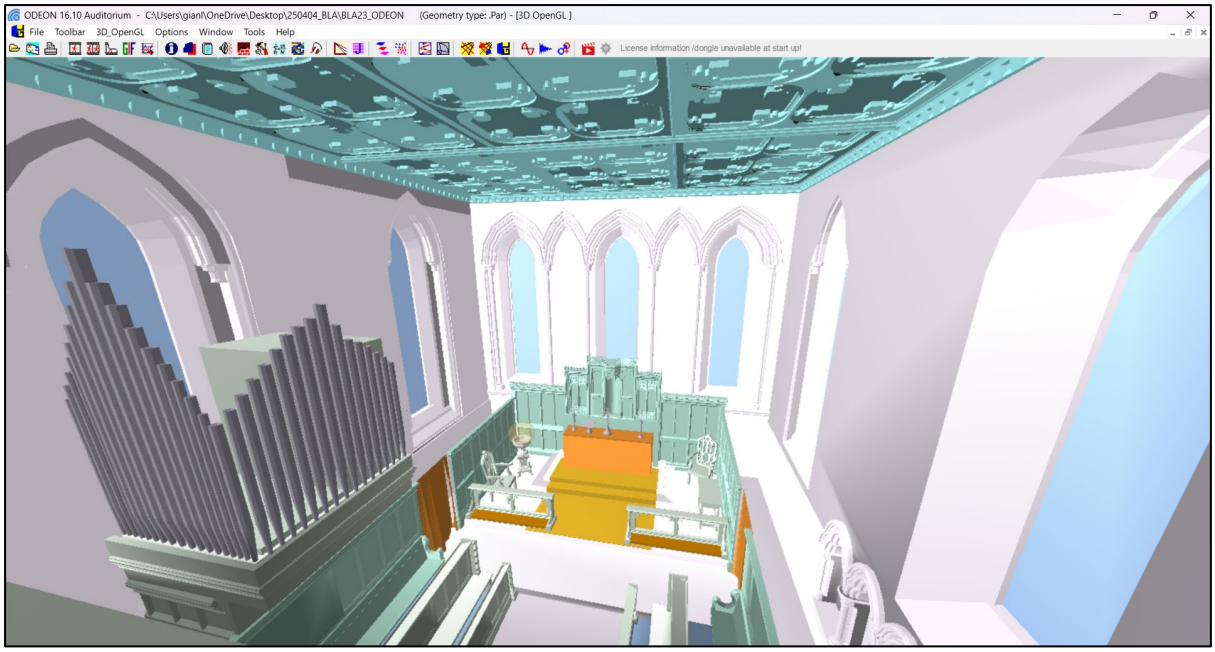

Figure 32. Acoustic model of the church: the chancel.

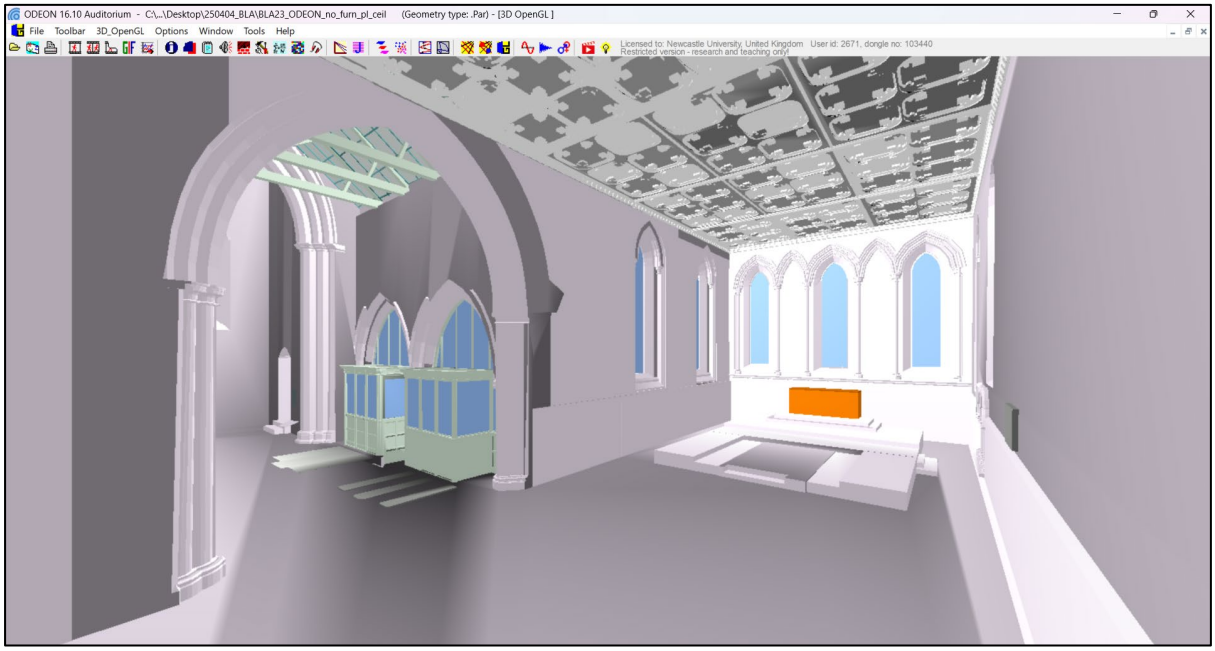

Figure 33. The model used for acoustic simulations in empty conditions.

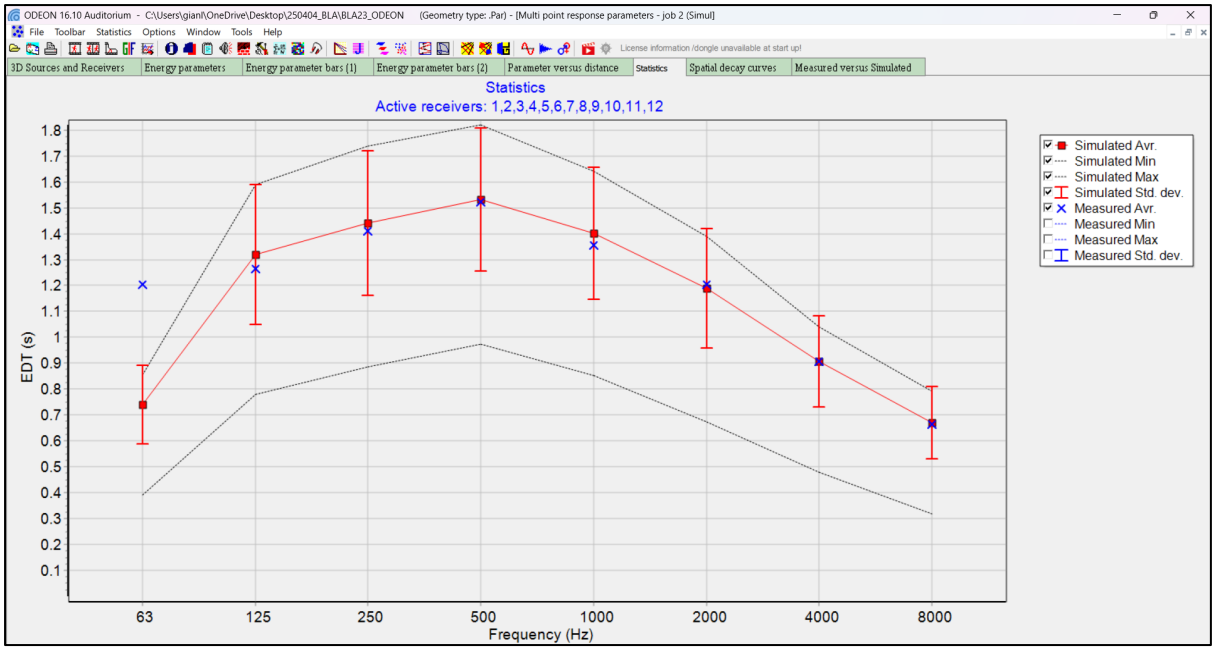

Figure 34. Average EDT (Early Decay Time, indicating reverberation) values from acoustic testing in Blanchland with a sound source positioned in front of the altar. Red squares represent digital simulation; blue triangles show values measured on-site.

2.5. Summary of Results

Aim 1. Clarify the historical circumstances in which Blanchland Abbey was founded.

This analysis has established that the abbey was founded by Walters de Bolebec, husband of Sibilla. Walterus founded the abbey immediately after his brother Hugo died, when he had taken wardship of his son and lands. The subsequent documents related to Blanchland were issued by Walterus's sons – Walterus and Hugo – around the late 12th century / first half of the 13th century.

Aim 2. Meet the recommendation set out by Peter Ryder's Archaeological Assessment (Ryder, 2017) about the high desirability of a modern survey of the church, including external and internal elevations.

The 3D full-colour laser scanning of Blanchland Abbey provides the most accurate and comprehensive survey of the building to date.

Aim 3. Advance knowledge on the architectural design of the twelfth/thirteenth-century abbey.

The analysis suggests that the arches of the abbey's medieval openings are all defined by two circles centred on a simple subdivision of the distance between the hood moulding's spring points. This indicates a consistent design method applied in the chancel, transept and tower across the late 12th and 13th centuries. AI-assisted reverse engineering based on metrological theory shows that a foot of 0.308 m subdivided into 12 inches is one of the possible units of measurement that allows calculation of the said divisions, the other being all values around 0.265 m. Further investigation is needed to ascertain whether Blanchland Abbey demonstrates the use of the standardised English foot of 0.3048 m as early as the 12th century. Analysis has also established that when the tower was built, the adjacent transept must have been covered by a truss roof without a tiebeam at its base, possibly similar to thirteenth-century vernacular examples in County Durham. The overall outline and dimensions of the abbey seem consistent with other single-nave Premonstratensian examples, especially Bayham and Titchfield. Only further investigation targeting the location of the western façade can clarify whether, as seems likely, the length and width of the abbey were in a 6:1 ratio and whether a tower abutted the western façade, as suggested by an anonymous survey from the 1950s.

Aim 4. Provide a general interpretation of the building's acoustics along with detailed data from acoustic surveys and room acoustic simulations.

The acoustic analysis of the abbey shows that the space is aurally warm and immersive, but not to the point of compromising speech intelligibility even when empty. Sound simulations suggest that the wooden surfaces of the chancel and nave's ceiling play a

significant role in improving speech intelligibility by absorbing low frequencies and containing excessive reverberation. The transept is acoustically the least favourable space for speech perception, and might need improvement based on specialist acoustic consultancy, which can build upon the robust acoustic dataset collected within this research.

2.6. Recommendations

A comprehensive terrestrial laser scanning survey of the remains of the abbey incorporated in the Lord Crewe Arms' masonry and the adjacent area in the graveyard may advance understanding of the medieval outline and dimensions of the building when integrated with the dataset produced for this analysis.

Archaeological excavations in the abbey's graveyard area adjacent to the Lord Crewe Arms and beneath the B6306 pavement and carriageway are highly desirable, as they may clarify the exact position of the medieval façade and the potential presence of a tower in front of it. Such information is relevant both to the history of the local community and to the broader question of the unusual outline of single-nave Premonstratensian abbeys like Blanchland's. The absence of substructures where the north-west corner of the medieval nave once stood makes this area particularly suitable for investigating the medieval outline of the building. At the same time, understanding the stratigraphic relationship between any buried structural remains, the elevation of the Lord Crewe Arms, the graveyard's boundary wall and the Post Office would enable us to refine the chronology of the village's core.

Acoustic consultancy to optimise sound perception according to the intended function of the transept in the future is recommended.

2.7. Acknowledgements

I would like to express my sincere gratitude to the Blanchland Community for their generous support and engagement throughout the course of this research. I am especially grateful to Yvonne Conchie, whose patience, commitment and enthusiasm have been a constant source of encouragement at every stage of the process.

I am indebted to many individuals, and in particular wish to thank Helen Savage, Tristan Spicer, Rob Young and Sheila and Andrew Newton for their invaluable advice and contributions.

It has been a privilege to work alongside such esteemed colleagues as Rebecca Romeo Pitone, Vicky Manolopoulou and Sam Turner. The support of Apex Acoustics, Durham University and Newcastle University's McCord Centre for Landscape was fundamental to the work.

This research was generously funded by the National Lottery Fund, whose support is gratefully acknowledged.

2.8. References

Bettess, F. (1991). The Anglo-Saxon Foot: a Computerized Assessment. *Medieval Archaeology*, *35*(1), 44-50. https://doi.org/https://doi.org/10.5284/1071792

Blanchland Community Development Organisation Ltd. (2022). *6As of Blanchland - National Lottery Grants for Heritage* [Grant]. South Tynedale. https://www.heritagefund.org.uk/projects/6as-blanchland

Bondéelle-Souchier, A. (2000). *Bibliothèque de l'ordre de Prémontré dans la France de l'Ancien Régime. I. Répertoire des abbayes*. Institut de Recherche et d'Histoire des Textes (IRHT). https://www.persee.fr/doc/dirht_0073-8212_2000_cat_58_1

Carlton, R. J., & Ryder, P. F. (2020). Archaeological Investigations at Blanchland Abbey 2012-14. *Durham Archaeological Journal*, *22*, 67-124.

Cirillo, E., & Martellotta, F. (2006). *Worship, Acoustics, and Architecture*. Multi-Science Publishing.

Clapham, A. W. (1923). IV. - The Architecture of the Premonstratensians, with Special Reference to their Buildings in England. *Archaeologia*, *73*, 117-146. https://doi.org/10.1017/S0261340900010316

Dugdale, W., Caley, J., Ellis, H., & Bandinel, B. (Eds.). (1830). *Monasticon Anglicanum: a History of the Abbies and Other Monasteries, Hospitals, Frieries, and Cathedral and Collegiate Churches, with their Dependencies, in England and Wales; also of all such Scotch, Irish, and French Monasteries as Were in any Manner Connected with Religious Houses in England. Together with a Particular Account of their Respective Foundations, Grants, and Donations, and a Full Statement of their Possessions, as well Temporal as Spiritual* (Vol. 6, 2). Harding and Lepard, Longman, Rees, Orme, Brown, and Green.

Fernie, E. (1978). Historical Metrology and Architectural History. *Art History*, *1*, 383-399.

Fernie, E. (1981). The Greek Metrological Relief in Oxford. *The Antiquaries Journal*, *61*, 255-263.

Fernie, E. (1985). Anglo-Saxon Lengths: The 'Northern' System, the Perch and the Foot. *Archaeological Journal*, *142*(1), 246-254. https://doi.org/10.1080/00665983.1985.11021064

Fernie, E. (1990). A Beginner's Guide to the Study of Architectural Proportions and Systems of Length. In E. Fernie & P. Crossley (Eds.), *Medieval Architecture and its Intellectual Context. Studies in Honour of Peter Kidson* (pp. 229-237). The Hambledon Press.

Fernie, E. (1991). Anglo-Saxon Lengths and the Evidence of the Buildings. *Medieval Archaeology*, *35*(1), 1-5. https://doi.org/https://doi.org/10.5284/1071789

Foschi, G. (2022). *The Role of Musical Proportions in Early Churches* Newcastle University].

Great Britain. Public Record Office (Ed.). (1906). *Calendar of the Charter Rolls Preserved in the Public Record Office. Vol II. Prepared Under the Superitendence of the Deputy Keeper of the Records. Henry III-Edward I. A.D. 1257-1300. Published by the Authority of his Majesty's Principal Secretary of State for the Home Department*. Mackie and Co. Ld.

Hall, H. (Ed.). (1896). *The Red Book of the Exchequer, Part I*. Eyre and Spottiswoode.

Hardy, T. D. (Ed.). (1840). *Willelmi Malmesbiriensis monachi Gesta Regum Anglorum atque Historia novella* (Vol. 2). Sumptibus Societatis.

Historic England. Retrieved 2 January 2025 from https://historicengland.org.uk/

Hodgson, J. C. (1902). *A History of Northumberland. Issued under the Direction of The Northumberland County History Committee* (Vol. 6, The Parish of Bywell St, Peter; The Parish of Bywell St Andrew; With Blanchland; The Chapelry or Parish of Slaley). Andrew Reid & Company, Limited.

Huggins, P. J. (1991). Anglo-Saxon Timber Building Measurements: Recent Results. *Medieval Archaeology*, *35*(1), 6-28. https://doi.org/https://doi.org/10.1080/00766097.1991.11735536

IEC 60268-16. (2020). *Sound System Equipment - Part 16: Objective Rating of Speech Intelligibility by Speech Transmission Index*.

ISO 3382-1. (2009). *Acoustics - Measurement of Room Acoustic Parameters - Part 1: Performance Spaces*.

ISO 3382-2. (2008). *Acoustics - Measurement of Room Acoustic Parameters - Part 2: Reverberation Time in Ordinary Rooms*.

ISO 9921. (2003). *Ergonomics — Assessment of speech communication*.

Knowles, W. H. (1902). The Premonstratensian Abbey of St. Mary, Blanchland, Northumberland. *The Archaeological Journal*, *59, 1*, 328-341.

Martellotta, F., Cirillo, E., Carbonari, A., & Ricciardi, P. (2009). Guidelines for Acoustical Measurements in Churches. *Applied Acoustics*, *70*, 378-388.

ODEON Room Acoustics Software. (2020). *User's Manual. Version 16*. Odeon A/S.

Reed, P. The Knowledge of Carpenters from the Early Medieval Period to the 18th Century in Setting Out Roofs and Buildings without Geometry and Numerical Measurement https://www.medievalbuildings.co.uk/pdfs/Carpenters-Knowledge.pdf

Reed, P. (2020). The Knowledge of Carpenters from the Early Medieval Period to the Eighteenth Century in Setting Out Roofs and Buildings Without Geometry and Numerical Measurement. *Vernacular Architecture*, *51*(1), 30-49.

Roberts, M. (2008). A Preliminary Roof Typology for the North East of England c. 1200-1700. *Vernacular Architecture*, *39*, 27-49.

Round, J. H. (Ed.). (1913). *Rotuli de dominabus et pueris et puellis de XII comitatibus [1185]* (Vol. 35). St. Catherine Press.

Ryder, P. F. (2017). *St Mary the Virgin: Blanchland. An Archaeological Assessment. March 2017*.

Schilbach, E. (1970). *Byzantinische Metrologie*. C.H. Beck.

Stevenson, J. (Ed.). (1835). *Chronica de Mailros, e codice unico in Bibliotheca Cottoniana servato, nunc iterum in lucem edita. Notulis indiceque aucta*. The Edinburgh Printing Company.

Stevenson, J. (Ed.). (1841). *Liber Vitae Ecclesiae Dunelmensis; nec non obituaria duo ejusdem ecclesiae*. J. B. Nicholas and Son.

The Pipe Roll Society (Ed.). (1887). *The Great Roll of the Pipe for the Eleventh Year of the Reign of King Henry the Second, A.D. 1164-1165*. Wyman & Sons.

The Pipe Roll Society (Ed.). (1889). *The Great Roll of the Pipe for the Thirteenth Year of the Reign of King Henry the Second, A.D. 1166-1167* (Vol. 11). Hansard Publishing Union, Limited.

The Pipe Roll Society (Ed.). (1890). *The Great Roll of the Pipe for the Fourteenth Year of the Reign of King Henry the Second, A.D. 1167-1168*. Hansard Publishing Union, Limited.

Time and Date. Retrieved 2 January 2025 from https://www.timeanddate.com/weather/@2655379/historic?month=1&year=2023

Young, R., Newton, A. C., & Severn Newton, S. (2023). *Historical and Archaeological Research at Blanchland Abbey*.

Appendix I. Documents from the Pipe Rolls and the *Red Book of the Exchequer* [16]

[16] From: Hall, H. (Ed.). (1896). *The Red Book of the Exchequer, Part I*. Eyre and Spottiswoode. , The Pipe Roll Society (Ed.). (1887). *The Great Roll of the Pipe for the Eleventh Year of the Reign of King Henry the Second, A.D. 1164-1165*. Wyman & Sons.

11 Hen. II, 1164-1165 (a):

Abbreviated Latin text: '*Walt̄ de Bolebec redđ Comp̄ de c. m̄. ꝑ Custoď nepotis sui 7 t̄re ipsi*[9]*. In tħ .XXXIII ł̄i. 7 .VIII đ. Et deb̄ .XXXIII. ł̄i. 7 .VI. s̄. 7 .VIII. đ. 7 .II. fugator̄.*'

Latin text: '*Walterus de Bolebec reddit computum de .C. marcis per custodiam nepotis sui et terrae ipsius. In thesauro .XXIII. librae et .VIII. denarii. Et debet .XXIII. libras et .VI. solidos et .VIII. denarios et .II. fugatores.*'

Translation: 'Walter de Bolebec renders account of 100 marks by custody of his nephew and his land. Into the treasury, 23 pounds and 8 pence. And he owes 23 pounds and 6 shillings and 8 pence and 2 *fugatores*.'

11 Hen. II, 1164-1165 (b):

Abbreviated Latin text: '*Walt̄ de Bolebec redđ Comp̄ de .VI. ł̄i.7 .XIII. s̄ 7 . IIII. đ de feodo Hug̃ de Bolebec. In tħ .II. m̄.*'

Latin text: '*Walterus de Bolebec reddit computum de .VI. libris et .XIII. solidis et .IIII. denariis de feodo Hugonis de Bolebec. In thesauro .II. marcas.*'

Translation: 'Walter de Bolebec renders account of 6 pounds and 13 shillings and 4 pence from the fee of Hugh de Bolebec. Into the treasury, 2 marks.'

Red Book of the Exchequer, 1166:

Latin text: '*Haec est agnitio de tenement Walteri de Bolebec quod Rex ei reddidit post mortem Hugonis de Bolebec fratris sui, scilicet vj milites feodatos ex tempore Regis Henrici, et ante mortem ejus, et ij milites quos Abbas de Rameseia tenet vi et warantisia Regis et ejus praesidio sicut propriam ejus elemosinam; ex quibus nullum servitium habuit postquam Rex praedictam terram ei reddidit.*'

Translation: 'This is the recognition concerning the tenement of Walter de Bolebec which the King restored to him after the death of Hugh de Bolebec his brother, namely 6 feudal knights from the time of King Henry, and before his death, and 2 knights whom the Abbot of Ramsey holds by force and warranty of the King and his protection as his own alms; from whom he had no service after the King restored the aforesaid land to him.'

13 Hen. II, 1166-1167:

Abbreviated Latin text: '*Walt̄ de Bolebec redđ Comp̄ de .X. ł̄i. 7 .XIII. s̄. 7 .IIII. đ. 7 . de .II. fugat̄ . ꝑ Custodia t̄re nepotis sui. In tħro .X. ł̄i. 7 .XIII. s̄ 7 .IIII. đ. 7 .XL. s̄ ꝑ .II. fugat̄. Et Quiet*[9] *est.*'

Latin text: '*Walterus de Bolebec reddit computum de .X. libris et .XIII. solidis et .IIII. denariis et de .II. fugatoribus per Custodiam terrae nepotis sui. In thesauro .X. libras et .XIII. solidos et .IIII. denarios et .XL. solidos per .II. fugatores. Et quietus est.*'

Translation: 'Walter de Bolebec renders account of 10 pounds and 13 shillings and 4 pence and of 2 *fugatores* by custody of the land of his nephew. Into the treasury, 10 pounds and 13 shillings and 4 pence, and 40 shillings for the 2 *fugatores*. And he is discharged.'

14 Hen. II, 1167-1168 (a):

Abbreviated Latin text: '*Hildestona Walt̄i de Bolebec redd̄ Comp̄ de .I. m̄. In ꝑdon̄ ꝑ br̄ . R̄ Regin̄ de Curtenai .I. m̄. Et quieta est.*'

Latin text: '*Hildestona Walteri de Bolebec reddit computum de .I. marca. In perdonis per breve Regis Reginaldo de Curtenai .I. marca. Et quieta est.*'

Translation: 'Hildestona of Walter de Bolebec renders account of 1 mark. In pardons by writ of the King to Reginald de Courtenay, 1 mark. And it is quit.'

14 Hen. II, 1167-1168 (b):

Abbreviated Latin text: '*Regin̄ de Curtenai deb̄ .VI. ł̄i 7 .XIII. s̄ 7 .IIII. d̄ de Mił Walt̄i|| de Bolebec q^{i} ē in custodia ei^{9} . de iłł videlic 7 Mił q°s tenet in capite de Rege.*'

Latin text: '*Reginaldo de Curtenai debet .VI. Libras et .XIII. solidos et .IIII. denarios de Militibus Walteri de Bolebec qui est in custodia ejus de illis videlicet et Militibus quos tenet in capite de Rege.*'

Translation: 'Reginald de Courtenay owes 6 pounds and 13 shillings and 4 pence from the knights of Walter de Bolebec who is in his custody from those, namely, and knights whom he holds in chief from the King.'

Appendix II. TLS Registration Report from FARO Scene v. 6.2

Registration Report

Project	BLA23
Cluster	BLA_23
Recording Period	1/1/2002, 12:13:24 AM 1/1/2002, 5:39:51 AM
Location	
Report Date	6/16/2025, 8:54:21 AM

Color Coding

Point Error	< 9 mm	> 20 mm
Overlap	> 25.0 %	< 10.0 %
Distance Error	< 60 mm	> 80 mm
Horizontal Error	< 20 mm	> 40 mm
Vertical Error	< 20 mm	> 40 mm
Angular Error	< 0.5 deg	> 1.0 deg

Overview

Scan Point Statistics

Maximum Point Error	11.6 mm
Mean Point Error	4.7 mm
Minimum Overlap	3.3 %

Target Statistics

Max. Distance Error	18.1 mm
Mean Distance Error	2.9 mm
Max. Horizontal Error	11.6 mm
Mean Horizontal Error	1.7 mm
Max. Vertical Error	17.8 mm
Mean Vertical Error	1.9 mm
Max. Angular Error	
Mean Angular Error	

Scan Errors

Scan Point Statistics

Cluster/Scan	Connections	Max. Point Error [mm]	Mean Point Error [mm]	Min. Overlap
BLA_23_Scan_036	3	5.7	4.1	45.7 %
BLA_23_Scan_037	2	5.4	4.7	72.8 %
BLA_23_Scan_038	3	7.8	6.6	3.3 %
BLA_23_Scan_039	2	9.6	8.1	11.4 %
BLA_23_Scan_045	2	7.4	4.9	9.2 %
BLA_23_Scan_046	2	7.2	4.8	67.2 %
BLA_23_Scan_048	2	3.7	3.1	84.6 %
BLA_23_Scan_049	2	3.3	3.0	80.5 %
BLA_23_Scan_050	1	3.3	3.3	80.5 %
BLA_23_Scan_051	2	7.2	5.4	67.2 %
BLA_23_Scan_052	1	4.8	4.8	91.2 %
BLA_23_Scan_053	2	4.8	4.7	90.0 %
BLA_23_Scan_054	2	5.5	5.1	47.4 %
BLA_23_Scan_055	2	6.9	6.2	47.4 %
BLA_23_Scan_056	2	9.6	8.2	11.4 %
BLA_23_Scan_020	1	2.2	2.2	64.7 %
BLA_23_Scan_024	1	2.2	2.2	65.1 %
BLA_23_Scan_026	2	5.7	4.9	41.0 %
BLA_23_Scan_027	1	6.5	6.5	60.5 %
BLA_23_Scan_029	2	4.0	2.8	46.3 %
BLA_23_Scan_030	3	2.2	1.8	48.3 %
BLA_23_Scan_031	1	1.7	1.7	59.3 %
BLA_23_Scan_032	1	2.2	2.2	48.3 %
BLA_23_Scan_033	2	11.6	6.5	7.7 %
BLA_23_Scan_034	1	1.4	1.4	94.9 %
BLA_23_Scan_035	1	2.7	2.7	62.6 %
Connection_Bell_Tower	3	7.4	4.9	9.2 %
Excavations	1	7.1	7.1	45.6 %
Bell_Tower_Ext	1	1.6	1.6	45.9 %
Chancel	2	7.8	6.8	3.3 %
Day1_plus_connection	7	11.6	5.4	7.7 %

Target Statistics

Cluster/Scan	Connections	Max. Dist. [mm]	Mean Dist. [mm]	Max. Hor. [mm]	Mean Hor. [mm]	Max. Vert. [mm]	Mean Vert. [mm]	Max. Angle [deg]	Mean Angle [deg]
BLA_23_Scan_036	7	6.7	3.2	3.4	1.5	6.6	2.6		
BLA_23_Scan_037	5	7.9	3.2	2.3	1.3	7.8	2.7		
BLA_23_Scan_038	5	18.1	5.6	4.2	1.6	17.8	5.2		
BLA_23_Scan_039	4	7.9	4.7	1.8	1.2	7.8	4.5		

BLA_23_Scan_045	7	11.1	3.1	11.1	2.5	2.9	1.2		
BLA_23_Scan_046	7	11.6	3.4	11.6	3.0	2.9	1.1		
BLA_23_Scan_048	7	11.6	4.4	11.6	4.2	2.2	0.9		
BLA_23_Scan_049	5	9.3	3.8	9.2	3.6	1.6	0.9		
BLA_23_Scan_050	8	7.4	2.7	3.6	1.6	7.3	1.9		
BLA_23_Scan_051	7	9.1	4.1	3.4	1.7	8.9	3.3		
BLA_23_Scan_052	5	7.9	4.4	2.2	1.4	7.6	4.1		
BLA_23_Scan_053	5	9.1	3.9	3.9	1.4	8.9	3.5		
BLA_23_Scan_054	4	4.9	2.7	3.9	1.2	4.8	2.3		
BLA_23_Scan_055	4	3.8	2.4	1.0	0.6	3.7	2.2		
BLA_23_Scan_056	4	18.1	6.1	4.2	1.5	17.8	5.9		
BLA_23_Scan_020	5	11.6	3.6	8.9	2.4	11.1	2.4		
BLA_23_Scan_024	5	10.1	2.8	8.9	2.0	7.8	1.7		
BLA_23_Scan_026	6	2.3	1.5	1.9	1.1	1.4	0.9		
BLA_23_Scan_027	8	2.6	1.3	1.5	0.7	2.2	0.9		
BLA_23_Scan_029	5	3.4	1.6	1.9	0.9	3.2	1.2		
BLA_23_Scan_030	5	2.4	1.5	1.9	0.9	2.2	1.1		
BLA_23_Scan_031	7	2.7	1.6	1.8	0.9	2.2	1.2		
BLA_23_Scan_032	4	2.4	1.3	1.3	0.8	2.2	1.0		
BLA_23_Scan_033	5	1.7	1.1	1.5	0.9	1.0	0.6		
BLA_23_Scan_034	5	1.6	1.1	1.5	0.9	1.1	0.6		
BLA_23_Scan_035	5	5.7	1.9	2.7	1.0	5.5	1.4		
Connection_Bell_Tower	10	6.1	3.2	4.2	1.5	6.0	2.5		
Excavations	5	3.4	1.6	1.3	0.8	3.2	1.3		
Bell_Tower_Ext	5	4.3	1.8	4.3	1.2	1.9	1.0		
Chancel	3	11.6	7.0	8.9	4.7	11.1	4.5		
Day1_plus_connection	5	3.8	1.9	2.2	1.4	3.2	1.1		

Detailed Errors

Scan Point Statistics

Cluster/Scan 1	Cluster/Scan 2	Point Error [mm]	Overlap
BLA_23_Scan_036	Connection_Bell_Tower/BLA_23_Scan_041	5.7	45.7 %
BLA_23_Scan_037	BLA_23_Scan_036	4.0	72.8 %
BLA_23_Scan_038	BLA_23_Scan_037	5.4	75.4 %
BLA_23_Scan_039	BLA_23_Scan_038	6.7	75.9 %
BLA_23_Scan_045	Connection_Bell_Tower/BLA_23_Scan_041	7.4	9.2 %
BLA_23_Scan_046	BLA_23_Scan_045	2.3	88.6 %
BLA_23_Scan_046	BLA_23_Scan_051	7.2	67.2 %
BLA_23_Scan_048	BLA_23_Scan_051	3.7	84.6 %
BLA_23_Scan_048	BLA_23_Scan_049	2.6	87.6 %
BLA_23_Scan_050	BLA_23_Scan_049	3.3	80.5 %
BLA_23_Scan_052	BLA_23_Scan_053	4.8	91.2 %
BLA_23_Scan_053	BLA_23_Scan_054	4.6	90.0 %
BLA_23_Scan_055	BLA_23_Scan_054	5.5	47.4 %
BLA_23_Scan_056	BLA_23_Scan_039	9.6	11.4 %
BLA_23_Scan_056	BLA_23_Scan_055	6.9	87.2 %
BLA_23_Scan_029	BLA_23_Scan_030	1.6	84.9 %
BLA_23_Scan_031	BLA_23_Scan_030	1.7	59.3 %
BLA_23_Scan_032	BLA_23_Scan_030	2.2	48.3 %
BLA_23_Scan_033	BLA_23_Scan_034	1.4	94.9 %
BLA_23_Scan_033	Day1_plus_connection/BLA_23_Scan_001	11.6	7.7 %
BLA_23_Scan_035	BLA_23_Scan_036	2.7	62.6 %
Bell_Tower_Ext/BLA_23_Scan_043	Connection_Bell_Tower/BLA_23_Scan_041	1.6	45.9 %
Chancel/BLA_23_Scan_021	BLA_23_Scan_038	7.8	3.3 %
Chancel/BLA_23_Scan_021	BLA_23_Scan_026	5.7	41.0 %
Day1_plus_connection/BLA_23_Scan_001	BLA_23_Scan_020	2.2	64.7 %
Day1_plus_connection/BLA_23_Scan_001	BLA_23_Scan_024	2.2	65.1 %
Day1_plus_connection/BLA_23_Scan_001	BLA_23_Scan_026	4.2	75.2 %
Day1_plus_connection/BLA_23_Scan_001	BLA_23_Scan_027	6.5	60.5 %
Day1_plus_connection/BLA_23_Scan_001	BLA_23_Scan_029	4.0	46.3 %
Day1_plus_connection/BLA_23_Scan_001	Excavations/BLA_23_Scan_028	7.1	45.6 %

Target Statistics

Cluster/Scan 1	Target 1	Cluster/Scan 2	Target 2	Dist. [mm]	Hor. [mm]	Ver. [mm]	Angle [deg]
BLA_23_Scan_036	Sphere3	Connection_Bell_Tower	Sphere3	4.2	3.4	2.3	
BLA_23_Scan_036	Sphere27	BLA_23_Scan_035	Sphere27	1.2	0.9	0.9	
BLA_23_Scan_036	Sphere15	BLA_23_Scan_034	Sphere15	1.4	1.0	1.0	
BLA_23_Scan_037	Sphere22	Connection_Bell_Tower	Sphere22	1.8	1.6	0.9	
BLA_23_Scan_037	Sphere3	Connection_Bell_Tower	Sphere3	2.5	2.3	0.7	

BLA_23_Scan_037	Sphere3	BLA_23_Scan_036	Sphere3	3.4	1.6	3.0
BLA_23_Scan_037	Sphere22	BLA_23_Scan_036	Sphere22	1.9	1.2	1.4
BLA_23_Scan_037	Sphere3	BLA_23_Scan_035	Sphere3	0.7	0.7	0.1
BLA_23_Scan_037	Sphere33	BLA_23_Scan_038	Sphere33	1.5	1.3	0.8
BLA_23_Scan_037	Sphere34	BLA_23_Scan_038	Sphere34	2.7	0.7	2.7
BLA_23_Scan_037	Sphere22	BLA_23_Scan_038	Sphere22	5.1	0.6	5.1
BLA_23_Scan_037	Sphere33	BLA_23_Scan_039	Sphere33	2.7	1.8	2.1
BLA_23_Scan_037	Sphere34	BLA_23_Scan_039	Sphere34	7.9	1.3	7.8
BLA_23_Scan_038	Sphere22	BLA_23_Scan_036	Sphere22	6.5	1.1	6.5
BLA_23_Scan_038	Point3	BLA_23_Scan_056	Point3	18.1	3.5	17.8
BLA_23_Scan_039	Sphere22	Connection_Bell_Tower	Sphere22	6.1	1.0	6.0
BLA_23_Scan_039	Sphere22	BLA_23_Scan_036	Sphere22	6.7	1.2	6.6
BLA_23_Scan_039	Sphere22	BLA_23_Scan_037	Sphere22	5.3	1.2	5.2
BLA_23_Scan_039	Sphere33	BLA_23_Scan_038	Sphere33	2.9	0.8	2.9
BLA_23_Scan_039	Sphere34	BLA_23_Scan_038	Sphere34	5.4	1.6	5.1
BLA_23_Scan_039	Sphere22	BLA_23_Scan_038	Sphere22	0.6	0.6	0.1
BLA_23_Scan_045	Sphere36	Connection_Bell_Tower	Sphere36	2.7	1.5	2.3
BLA_23_Scan_045	Sphere37	Connection_Bell_Tower	Sphere37	2.7	0.7	2.6
BLA_23_Scan_045	Sphere35	Connection_Bell_Tower	Sphere35	2.9	1.5	2.4
BLA_23_Scan_045	Sphere43	BLA_23_Scan_046	Sphere43	0.6	0.3	0.5
BLA_23_Scan_045	Sphere36	BLA_23_Scan_048	Sphere36	5.6	5.6	0.1
BLA_23_Scan_045	Sphere43	BLA_23_Scan_048	Sphere43	2.8	2.6	0.9
BLA_23_Scan_045	Sphere42	BLA_23_Scan_049	Sphere42	8.6	8.6	0.6
BLA_23_Scan_045	Sphere43	BLA_23_Scan_049	Sphere43	2.5	1.9	1.6
BLA_23_Scan_045	Sphere36	BLA_23_Scan_050	Sphere36	2.2	2.1	0.8
BLA_23_Scan_045	Sphere43	BLA_23_Scan_050	Sphere43	2.6	1.7	2.0
BLA_23_Scan_045	Sphere36	Bell_Tower_Ext	Sphere36	1.6	1.5	0.6
BLA_23_Scan_046	Sphere36	Connection_Bell_Tower	Sphere36	2.4	0.9	2.2
BLA_23_Scan_046	Sphere37	Connection_Bell_Tower	Sphere37	3.0	0.7	2.9
BLA_23_Scan_046	Sphere42	BLA_23_Scan_045	Sphere42	1.0	0.7	0.8
BLA_23_Scan_046	Sphere36	BLA_23_Scan_045	Sphere36	1.2	1.2	0.1
BLA_23_Scan_046	Sphere37	BLA_23_Scan_045	Sphere37	0.3	0.1	0.3
BLA_23_Scan_046	Sphere36	Bell_Tower_Ext	Sphere36	0.8	0.6	0.5
BLA_23_Scan_046	Sphere36	BLA_23_Scan_048	Sphere36	4.9	4.9	0.0
BLA_23_Scan_046	Sphere45	BLA_23_Scan_048	Sphere45	6.1	5.7	1.9
BLA_23_Scan_046	Sphere36	BLA_23_Scan_050	Sphere36	1.7	1.5	0.8
BLA_23_Scan_046	Sphere42	BLA_23_Scan_049	Sphere42	9.3	9.2	1.3
BLA_23_Scan_046	Sphere45	BLA_23_Scan_049	Sphere45	7.2	7.1	1.5
BLA_23_Scan_048	Sphere36	Connection_Bell_Tower	Sphere36	4.8	4.2	2.2
BLA_23_Scan_048	Sphere42	BLA_23_Scan_045	Sphere42	11.1	11.1	0.7
BLA_23_Scan_048	Sphere42	BLA_23_Scan_046	Sphere42	11.6	11.6	0.1
BLA_23_Scan_048	Sphere43	BLA_23_Scan_046	Sphere43	2.8	2.8	0.4
BLA_23_Scan_048	Sphere42	BLA_23_Scan_049	Sphere42	4.0	3.8	1.3
BLA_23_Scan_048	Sphere45	BLA_23_Scan_049	Sphere45	3.2	3.1	0.4
BLA_23_Scan_048	Sphere36	BLA_23_Scan_050	Sphere36	3.7	3.6	0.8
BLA_23_Scan_048	Sphere36	Bell_Tower_Ext	Sphere36	4.3	4.3	0.5
BLA_23_Scan_049	Sphere43	BLA_23_Scan_046	Sphere43	2.3	2.0	1.1
BLA_23_Scan_049	Sphere43	BLA_23_Scan_048	Sphere43	1.3	1.1	0.7
BLA_23_Scan_049	Sphere50	BLA_23_Scan_048	Sphere50	1.3	0.8	1.0

BLA_23_Scan_049	Sphere50	BLA_23_Scan_050	Sphere50	2.2	2.0	0.9	
BLA_23_Scan_049	Sphere50	BLA_23_Scan_051	Sphere50	3.4	3.4	0.0	
BLA_23_Scan_050	Sphere36	Connection_Bell_Tower	Sphere36	3.1	0.6	3.1	
BLA_23_Scan_050	Sphere43	BLA_23_Scan_046	Sphere43	2.1	1.5	1.5	
BLA_23_Scan_050	Sphere43	BLA_23_Scan_048	Sphere43	3.0	2.8	1.1	
BLA_23_Scan_050	Sphere50	BLA_23_Scan_048	Sphere50	2.4	1.5	1.9	
BLA_23_Scan_050	Sphere43	BLA_23_Scan_049	Sphere43	1.7	1.7	0.4	
BLA_23_Scan_050	Sphere54	BLA_23_Scan_051	Sphere54	0.9	0.2	0.9	
BLA_23_Scan_050	Sphere55	BLA_23_Scan_051	Sphere55	7.4	1.6	7.3	
BLA_23_Scan_050	Sphere54	BLA_23_Scan_052	Sphere54	7.0	2.2	6.7	
BLA_23_Scan_050	Sphere55	BLA_23_Scan_052	Sphere55	1.6	0.9	1.3	
BLA_23_Scan_050	Sphere36	Bell_Tower_Ext	Sphere36	1.6	0.8	1.3	
BLA_23_Scan_051	Sphere43	BLA_23_Scan_045	Sphere43	3.4	1.8	2.9	
BLA_23_Scan_051	Sphere43	BLA_23_Scan_046	Sphere43	2.8	1.5	2.3	
BLA_23_Scan_051	Sphere43	BLA_23_Scan_048	Sphere43	3.2	2.6	1.9	
BLA_23_Scan_051	Sphere50	BLA_23_Scan_048	Sphere50	3.5	3.3	0.9	
BLA_23_Scan_051	Sphere43	BLA_23_Scan_049	Sphere43	1.9	1.5	1.2	
BLA_23_Scan_051	Sphere50	BLA_23_Scan_050	Sphere50	2.3	2.1	1.0	
BLA_23_Scan_051	Sphere43	BLA_23_Scan_050	Sphere43	0.9	0.2	0.9	
BLA_23_Scan_051	Sphere56	BLA_23_Scan_052	Sphere56	5.1	1.7	4.9	
BLA_23_Scan_051	Sphere55	BLA_23_Scan_052	Sphere55	6.0	0.7	5.9	
BLA_23_Scan_051	Sphere56	BLA_23_Scan_053	Sphere56	9.1	1.7	8.9	
BLA_23_Scan_052	Sphere54	BLA_23_Scan_051	Sphere54	7.9	2.0	7.6	
BLA_23_Scan_052	Sphere59	BLA_23_Scan_053	Sphere59	1.2	0.7	0.9	
BLA_23_Scan_052	Sphere59	BLA_23_Scan_054	Sphere59	3.5	1.7	3.0	
BLA_23_Scan_052	Sphere59	BLA_23_Scan_055	Sphere59	3.1	0.8	3.0	
BLA_23_Scan_053	Sphere56	BLA_23_Scan_052	Sphere56	4.1	0.7	4.1	
BLA_23_Scan_053	Sphere58	BLA_23_Scan_052	Sphere58	4.1	2.1	3.5	
BLA_23_Scan_053	Sphere60	BLA_23_Scan_054	Sphere60	4.9	3.9	2.9	
BLA_23_Scan_054	Sphere62	BLA_23_Scan_056	Sphere62	4.9	0.4	4.8	
BLA_23_Scan_054	Sphere61	BLA_23_Scan_053	Sphere61	2.5	1.2	2.2	
BLA_23_Scan_054	Sphere59	BLA_23_Scan_053	Sphere59	2.4	1.3	2.1	
BLA_23_Scan_054	Sphere59	BLA_23_Scan_055	Sphere59	1.0	1.0	0.0	
BLA_23_Scan_054	Sphere61	BLA_23_Scan_055	Sphere61	0.7	0.4	0.5	
BLA_23_Scan_055	Sphere62	BLA_23_Scan_056	Sphere62	3.3	0.4	3.3	
BLA_23_Scan_055	Sphere63	BLA_23_Scan_056	Sphere63	3.8	1.0	3.7	
BLA_23_Scan_055	Sphere61	BLA_23_Scan_053	Sphere61	2.8	0.8	2.7	
BLA_23_Scan_055	Sphere59	BLA_23_Scan_053	Sphere59	2.2	0.6	2.1	
BLA_23_Scan_055	Sphere62	BLA_23_Scan_054	Sphere62	1.5	0.2	1.5	
BLA_23_Scan_056	Point3d	BLA_23_Scan_038	Point3d	7.1	4.2	5.7	
BLA_23_Scan_056	Sphere61	BLA_23_Scan_053	Sphere61	5.6	1.2	5.5	
BLA_23_Scan_056	Sphere61	BLA_23_Scan_054	Sphere61	3.3	0.5	3.3	
BLA_23_Scan_056	Sphere61	BLA_23_Scan_055	Sphere61	2.8	0.4	2.8	
BLA_23_Scan_020	Point3d10	Chancel	Point3d10	11.6	3.4	11.1	
BLA_23_Scan_020	Point3d9	Chancel	Point3d9	11.5	8.9	7.3	
BLA_23_Scan_020	Sphere	Chancel	Sphere	3.8	2.9	2.5	
BLA_23_Scan_020	Sphere	Day1_plus_connection	Sphere	1.3	1.1	0.7	
BLA_23_Scan_020	Sphere2	Day1_plus_connection	Sphere2	2.4	2.0	1.3	
BLA_23_Scan_020	Sphere1	BLA_23_Scan_024	Sphere1	1.7	0.7	1.6	

BLA_23_Scan_020	Sphere	BLA_23_Scan_024	Sphere	1.3	0.3	1.2
BLA_23_Scan_020	Sphere1	BLA_23_Scan_026	Sphere1	1.4	1.4	0.2
BLA_23_Scan_024	Sphere	Chancel	Sphere	3.4	3.2	1.2
BLA_23_Scan_024	Sphere6	BLA_23_Scan_020	Sphere6	2.6	1.5	2.1
BLA_23_Scan_024	Sphere2	BLA_23_Scan_020	Sphere2	2.0	1.1	1.6
BLA_23_Scan_024	Sphere	Day1_plus_connection	Sphere	2.4	1.4	1.9
BLA_23_Scan_024	Sphere2	Day1_plus_connection	Sphere2	1.7	1.7	0.3
BLA_23_Scan_026	Sphere6	BLA_23_Scan_020	Sphere6	2.1	1.9	0.9
BLA_23_Scan_026	Sphere2	BLA_23_Scan_020	Sphere2	2.3	1.9	1.3
BLA_23_Scan_026	Sphere8	Excavations	Sphere8	1.3	0.7	1.1
BLA_23_Scan_026	Sphere7	Excavations	Sphere7	0.8	0.7	0.4
BLA_23_Scan_026	Sphere2	Day1_plus_connection	Sphere2	1.9	1.9	0.0
BLA_23_Scan_026	Sphere1	BLA_23_Scan_024	Sphere1	1.6	0.8	1.4
BLA_23_Scan_026	Sphere6	BLA_23_Scan_024	Sphere6	2.0	1.6	1.2
BLA_23_Scan_026	Sphere2	BLA_23_Scan_024	Sphere2	0.9	0.8	0.3
BLA_23_Scan_026	Sphere7	BLA_23_Scan_027	Sphere7	1.3	0.7	1.1
BLA_23_Scan_026	Sphere8	BLA_23_Scan_027	Sphere8	0.5	0.4	0.2
BLA_23_Scan_026	Sphere8	BLA_23_Scan_029	Sphere8	1.8	1.2	1.4
BLA_23_Scan_027	Sphere6	BLA_23_Scan_020	Sphere6	2.6	1.3	2.2
BLA_23_Scan_027	Sphere8	Excavations	Sphere8	1.4	1.1	0.9
BLA_23_Scan_027	Sphere6	BLA_23_Scan_024	Sphere6	0.9	0.9	0.1
BLA_23_Scan_027	Sphere6	BLA_23_Scan_026	Sphere6	1.5	0.8	1.3
BLA_23_Scan_027	Sphere9	BLA_23_Scan_029	Sphere9	0.4	0.4	0.0
BLA_23_Scan_027	Sphere10	BLA_23_Scan_029	Sphere10	0.9	0.8	0.4
BLA_23_Scan_027	Sphere9	BLA_23_Scan_030	Sphere9	1.2	0.8	0.9
BLA_23_Scan_027	Sphere10	BLA_23_Scan_030	Sphere10	1.5	0.6	1.4
BLA_23_Scan_027	Sphere9	BLA_23_Scan_031	Sphere9	1.8	1.2	1.3
BLA_23_Scan_029	Sphere11	Excavations	Sphere11	3.4	1.3	3.2
BLA_23_Scan_029	Sphere8	Excavations	Sphere8	1.3	1.2	0.3
BLA_23_Scan_029	Sphere7	Excavations	Sphere7	1.2	0.5	1.1
BLA_23_Scan_029	Sphere7	BLA_23_Scan_026	Sphere7	1.0	0.6	0.7
BLA_23_Scan_029	Sphere7	BLA_23_Scan_027	Sphere7	0.6	0.5	0.3
BLA_23_Scan_029	Sphere8	BLA_23_Scan_027	Sphere8	1.9	1.5	1.2
BLA_23_Scan_029	Sphere11	BLA_23_Scan_030	Sphere11	2.2	1.9	1.0
BLA_23_Scan_029	Sphere10	BLA_23_Scan_030	Sphere10	1.9	0.4	1.8
BLA_23_Scan_029	Sphere11	BLA_23_Scan_031	Sphere11	2.7	1.8	2.1
BLA_23_Scan_030	Sphere11	Excavations	Sphere11	2.4	0.9	2.2
BLA_23_Scan_030	Sphere9	BLA_23_Scan_029	Sphere9	1.0	0.4	0.9
BLA_23_Scan_030	Sphere12	BLA_23_Scan_031	Sphere12	2.4	1.6	1.8
BLA_23_Scan_030	Sphere11	BLA_23_Scan_031	Sphere11	1.6	1.1	1.1
BLA_23_Scan_030	Sphere12	BLA_23_Scan_032	Sphere12	0.9	0.9	0.3
BLA_23_Scan_030	Sphere5	BLA_23_Scan_032	Sphere5	0.8	0.6	0.6
BLA_23_Scan_031	Sphere9	BLA_23_Scan_029	Sphere9	1.6	0.8	1.3
BLA_23_Scan_031	Sphere9	BLA_23_Scan_030	Sphere9	0.6	0.4	0.4
BLA_23_Scan_031	Sphere5	BLA_23_Scan_030	Sphere5	1.8	0.9	1.6
BLA_23_Scan_031	Sphere5	BLA_23_Scan_032	Sphere5	2.2	0.4	2.2
BLA_23_Scan_031	Sphere12	BLA_23_Scan_032	Sphere12	2.4	1.2	2.1
BLA_23_Scan_031	Sphere13	BLA_23_Scan_033	Sphere13	0.5	0.5	0.2
BLA_23_Scan_031	Sphere13	BLA_23_Scan_034	Sphere13	1.1	1.1	0.3

BLA_23_Scan_032	Sphere13	BLA_23_Scan_031	Sphere13	0.6	0.4	0.5
BLA_23_Scan_032	Sphere13	BLA_23_Scan_033	Sphere13	0.9	0.8	0.3
BLA_23_Scan_032	Sphere14	BLA_23_Scan_033	Sphere14	1.7	1.3	1.0
BLA_23_Scan_032	Sphere13	BLA_23_Scan_034	Sphere13	1.0	0.7	0.7
BLA_23_Scan_033	Sphere15	BLA_23_Scan_036	Sphere15	1.0	0.8	0.6
BLA_23_Scan_033	Sphere13	BLA_23_Scan_034	Sphere13	1.5	1.4	0.5
BLA_23_Scan_033	Sphere16	BLA_23_Scan_034	Sphere16	1.0	0.9	0.5
BLA_23_Scan_033	Sphere15	BLA_23_Scan_034	Sphere15	1.6	1.5	0.4
BLA_23_Scan_033	Sphere16	BLA_23_Scan_035	Sphere16	1.2	0.7	1.0
BLA_23_Scan_033	Sphere15	BLA_23_Scan_035	Sphere15	1.1	0.7	0.8
BLA_23_Scan_034	Sphere18	BLA_23_Scan_033	Sphere18	0.9	0.6	0.7
BLA_23_Scan_034	Sphere19	BLA_23_Scan_035	Sphere19	1.1	0.4	1.1
BLA_23_Scan_035	Sphere3	Connection_Bell_Tower	Sphere3	2.8	2.7	0.6
BLA_23_Scan_035	Sphere3	BLA_23_Scan_036	Sphere3	3.1	1.0	2.9
BLA_23_Scan_035	Sphere15	BLA_23_Scan_036	Sphere15	1.7	1.0	1.3
BLA_23_Scan_035	Sphere16	BLA_23_Scan_034	Sphere16	0.6	0.4	0.5
BLA_23_Scan_035	Sphere15	BLA_23_Scan_034	Sphere15	1.2	1.2	0.3
Connection_Bell_Tower	Sphere22	BLA_23_Scan_036	Sphere22	2.2	2.1	0.5
Connection_Bell_Tower	Sphere27	BLA_23_Scan_036	Sphere27	5.2	2.5	4.6
Connection_Bell_Tower	Sphere22	BLA_23_Scan_038	Sphere22	6.0	1.2	5.9
Connection_Bell_Tower	Sphere27	BLA_23_Scan_035	Sphere27	5.7	1.6	5.5
Excavations	Sphere9	BLA_23_Scan_027	Sphere9	1.9	0.5	1.8
Excavations	Sphere7	BLA_23_Scan_027	Sphere7	1.5	0.1	1.5
Excavations	Sphere9	BLA_23_Scan_029	Sphere9	1.9	0.4	1.8
Excavations	Sphere9	BLA_23_Scan_030	Sphere9	1.2	0.7	0.9
Excavations	Sphere9	BLA_23_Scan_031	Sphere9	1.3	1.2	0.5
Excavations	Sphere11	BLA_23_Scan_031	Sphere11	1.3	0.6	1.1
Bell_Tower_Ext	Sphere36	Connection_Bell_Tower	Sphere36	1.8	0.3	1.8
Bell_Tower_Ext	Sphere29	Connection_Bell_Tower	Sphere29	1.6	1.5	0.6
Bell_Tower_Ext	Sphere37	Connection_Bell_Tower	Sphere37	1.9	0.2	1.9
Bell_Tower_Ext	Sphere35	Connection_Bell_Tower	Sphere35	1.4	0.4	1.4
Bell_Tower_Ext	Sphere35	BLA_23_Scan_045	Sphere35	2.1	1.9	1.0
Bell_Tower_Ext	Sphere37	BLA_23_Scan_045	Sphere37	1.1	0.8	0.8
Bell_Tower_Ext	Sphere37	BLA_23_Scan_046	Sphere37	1.3	0.8	1.0
Chancel	Point3d8	BLA_23_Scan_020	Point3d8	6.5	6.5	0.8
Chancel	Sphere68	BLA_23_Scan_024	Sphere68	4.2	3.7	1.9
Chancel	Point3d12	BLA_23_Scan_024	Point3d12	8.2	2.8	7.8
Chancel	Point3d11	BLA_23_Scan_024	Point3d11	10.1	8.9	4.8
Chancel	Sphere	Day1_plus_connection	Sphere	3.8	2.2	3.2
Day1_plus_connection	Sphere6	BLA_23_Scan_020	Sphere6	2.3	1.3	1.9
Day1_plus_connection	Sphere1	BLA_23_Scan_020	Sphere1	2.4	2.0	1.4
Day1_plus_connection	Sphere6	BLA_23_Scan_024	Sphere6	0.6	0.5	0.2
Day1_plus_connection	Sphere1	BLA_23_Scan_024	Sphere1	1.6	1.6	0.2
Day1_plus_connection	Sphere6	BLA_23_Scan_026	Sphere6	1.5	1.1	1.0
Day1_plus_connection	Sphere1	BLA_23_Scan_026	Sphere1	2.1	1.8	1.2
Day1_plus_connection	Sphere6	BLA_23_Scan_027	Sphere6	0.5	0.3	0.3

Inclinometer Mismatches

Cluster/Scan	Scan	Mismatch [deg]
Connection_Bell_Tower	BLA_23_Scan_040	0.0176
BLA_23_Scan_048	BLA_23_Scan_048	0
Day1_plus_connection	BLA_23_Scan_002	0.0072
Day1_plus_connection	BLA_23_Scan_007	0.0305
Chancel	BLA_23_Scan_022	0.0092
Day1_plus_connection	BLA_23_Scan_003	0.0120
BLA_23_Scan_033	BLA_23_Scan_033	0
Day1_plus_connection	BLA_23_Scan_009	0.0035
Day1_plus_connection	BLA_23_Scan_013	0.0188
Day1_plus_connection	BLA_23_Scan_005	0.0222
BLA_23_Scan_031	BLA_23_Scan_031	0
Day1_plus_connection	BLA_23_Scan_006	0.0219
BLA_23_Scan_056	BLA_23_Scan_056	0
BLA_23_Scan_052	BLA_23_Scan_052	0
Day1_plus_connection	BLA_23_Scan_016	0.0017
BLA_23_Scan_050	BLA_23_Scan_050	0
BLA_23_Scan_035	BLA_23_Scan_035	0
Day1_plus_connection	BLA_23_Scan_018	0.0017
Day1_plus_connection	BLA_23_Scan_014	0.0434
BLA_23_Scan_034	BLA_23_Scan_034	0
BLA_23_Scan_053	BLA_23_Scan_053	0
Day1_plus_connection	BLA_23_Scan_008	0.0328
BLA_23_Scan_039	BLA_23_Scan_039	0
Day1_plus_connection	BLA_23_Scan_017	0.0017
Excavations	BLA_23_Scan_028	0
Excavations	BLA_23_Scan_047	0
Day1_plus_connection	BLA_23_Scan_011	0.0110
BLA_23_Scan_038	BLA_23_Scan_038	0
Day1_plus_connection	BLA_23_Scan_015	0.0466
BLA_23_Scan_046	BLA_23_Scan_046	0
BLA_23_Scan_032	BLA_23_Scan_032	0
Day1_plus_connection	BLA_23_Scan_010	0.0316
BLA_23_Scan_026	BLA_23_Scan_026	0
Day1_plus_connection	BLA_23_Scan_012	0.0141
BLA_23_Scan_027	BLA_23_Scan_027	0
BLA_23_Scan_037	BLA_23_Scan_037	0
BLA_23_Scan_024	BLA_23_Scan_024	0
BLA_23_Scan_045	BLA_23_Scan_045	0
BLA_23_Scan_049	BLA_23_Scan_049	0
BLA_23_Scan_029	BLA_23_Scan_029	0
Bell_Tower_Ext	BLA_23_Scan_043	0
BLA_23_Scan_051	BLA_23_Scan_051	0
BLA_23_Scan_030	BLA_23_Scan_030	0
Chancel	BLA_23_Scan_021	0.0467
BLA_23_Scan_020	BLA_23_Scan_020	0

BLA_23_Scan_055	BLA_23_Scan_055	0
Day1_plus_connection	BLA_23_Scan_001	0.0150
BLA_23_Scan_036	BLA_23_Scan_036	0
Connection_Bell_Tower	BLA_23_Scan_041	0.0160
Chancel	BLA_23_Scan_025	0.0377
Chancel	BLA_23_Scan_023	0.0363
Bell_Tower_Ext	BLA_23_Scan_044	0
BLA_23_Scan_054	BLA_23_Scan_054	0
Day1_plus_connection	BLA_23_Scan_019	0.0293
Connection_Bell_Tower	BLA_23_Scan_042	0.0036

Appendix III. TLS Orthophotos: File Register

Filename	Extension	Size	Description
Area_trnsp.tif	.tif	145.7 MB	Orthophoto
EE_a_ext.tif	.tif	32.4 MB	Orthophoto
EE_a_ext.txt	.txt	389.0 B	File description
EE_a_int.tif	.tif	21.8 MB	Orthophoto
EE_a_int.txt	.txt	385.0 B	File description
EE_a_trnsp.tif	.tif	4.3 MB	Orthophoto
EE_a_trnsp.txt	.txt	387.0 B	File description
EE_b_ext.tif	.tif	19.3 MB	Orthophoto
EE_b_ext.txt	.txt	387.0 B	File description
EE_b_int.tif	.tif	18.4 MB	Orthophoto
EE_b_int.txt	.txt	393.0 B	File description
EE_b_trnsp.tif	.tif	3.8 MB	Orthophoto
EE_b_trnsp.txt	.txt	395.0 B	File description
EE_c_ext.tif	.tif	62.3 MB	Orthophoto
EE_c_ext.txt	.txt	393.0 B	File description
EE_c_int.tif	.tif	53.8 MB	Orthophoto
EE_c_int.txt	.txt	393.0 B	File description
EE_c_trnsp.tif	.tif	10.1 MB	Orthophoto
EE_c_trnsp.txt	.txt	395.0 B	File description
EE_d_ext.tif	.tif	80.4 MB	Orthophoto
EE_d_ext.txt	.txt	393.0 B	File description
EE_d_int.tif	.tif	87.0 MB	Orthophoto
EE_d_int.txt	.txt	391.0 B	File description
EE_d_trnsp.tif	.tif	11.7 MB	Orthophoto
EE_d_trnsp.txt	.txt	395.0 B	File description
NE_ext.tif	.tif	44.5 MB	Orthophoto
NE_ext.txt	.txt	385.0 B	File description
NE_int.tif	.tif	37.0 MB	Orthophoto
NE_int.txt	.txt	385.0 B	File description
NE_trnsp.tif	.tif	5.7 MB	Orthophoto
NE_trnsp.txt	.txt	387.0 B	File description
SE_ext.tif	.tif	42.2 MB	Orthophoto
SE_ext.txt	.txt	387.0 B	File description
SE_ext_a.tif	.tif	56.2 MB	Orthophoto
SE_ext_a.txt	.txt	388.0 B	File description
SE_int.tif	.tif	46.3 MB	Orthophoto
SE_int.txt	.txt	387.0 B	File description
SE_int_a.tif	.tif	61.2 MB	Orthophoto
SE_int_a.txt	.txt	390.0 B	File description
SE_trnsp.tif	.tif	4.5 MB	Orthophoto
SE_trnsp.txt	.txt	389.0 B	File description
SE_trnsp_a.tif	.tif	7.7 MB	Orthophoto
SE_trnsp_a.txt	.txt	390.0 B	File description
TEE_ext.tif	.tif	48.0 MB	Orthophoto

TEE_ext.txt	.txt	390.0 B	File description
TEE_int.tif	.tif	33.6 MB	Orthophoto
TEE_int.txt	.txt	392.0 B	File description
TEE_trnsp.tif	.tif	6.4 MB	Orthophoto
TEE_trnsp.txt	.txt	394.0 B	File description
TNE_ext.tif	.tif	47.5 MB	Orthophoto
TNE_ext.txt	.txt	390.0 B	File description
TNE_int.tif	.tif	19.3 MB	Orthophoto
TNE_int.txt	.txt	392.0 B	File description
TNE_trnsp.tif	.tif	4.9 MB	Orthophoto
TNE_trnsp.txt	.txt	394.0 B	File description
TSE_ext.tif	.tif	33.1 MB	Orthophoto
TSE_ext.txt	.txt	392.0 B	File description
TSE_int.tif	.tif	18.1 MB	Orthophoto
TSE_int.txt	.txt	390.0 B	File description
TSE_trnsp.tif	.tif	5.8 MB	Orthophoto
TSE_trnsp.txt	.txt	390.0 B	File description
TWE_ext.tif	.tif	51.8 MB	Orthophoto
TWE_ext.txt	.txt	392.0 B	File description
TWE_int.tif	.tif	32.2 MB	Orthophoto
TWE_int.txt	.txt	392.0 B	File description
TWE_trnsp.tif	.tif	5.7 MB	Orthophoto
TWE_trnsp.txt	.txt	394.0 B	File description

Appendix IV. Dimensions Measured from TLS Point Cloud

Area	Dimension	Metres	Level above datum (m)
Nave	N wall, W window, external, span, 1st N to S	0.9355	3.2107-3.3670
Nave	N wall, W window, external, span, 2nd N to S	1.3631	3.2107-3.3671
Nave	N wall, W window, external, span, 3rd N to S	1.5036	3.2107-3.3672
Nave	N wall, W window, internal span, 1st S to N	0.8037	3.2107-3.3673
Nave	N wall, W window, internal span, 2nd S to N	1.7173	3.2107-3.3674
Nave	N wall, W window, shorter span	0.6728	3.2107-3.3675
Nave	Nave, E end, width near floor level	8.3790	0.2710-0.4272
Nave	Nave, E wall, thickness near floor level	1.6299	0.2710-0.4272
Nave	Nave, N wall, easternmost pier, E-W width (lower moulding excluded)	1.0967	0.2710-0.4272
Nave	Nave, N wall, easternmost pier, N-S width (lower moulding excluded)	0.5361	0.2710-0.4272
Nave	Nave, N wall, span between piers	4.5389	0.2710-0.4272
Nave	Nave, N wall, thickness near floor level	1.0491	0.2710-0.4272
Nave	Nave, N wall, westernmost pier, E-W width (lower moulding excluded)	0.7597	0.2710-0.4272
Nave	Nave, N wall, westernmost pier, N-S width (lower moulding excluded)	0.5690	0.2710-0.4272
Nave	Nave, N wall, span between piers	4.5311	3.2107-3.3669
Nave	Nave, N wall, thickness	0.9980	3.2107-3.3669
Nave	Nave, width near E end	8.5688	3.2107-3.3669
Nave	Nave, S wall, thickness	1.0249	3.2107-3.3669
Nave	N wall, E pier, N-S width	0.4563	3.2107-3.3669
Nave	N wall, E pier, E-W width	1.0464	3.2107-3.3669
Nave	N wall, E window, external, span, 1st N to S	1.0522	3.2107-3.3669
Nave	N wall, E window, external, span, 2nd N to S	1.3491	3.2107-3.3669
Nave	N wall, E window, external, span, 3rd N to S	1.5036	3.2107-3.3669
Nave	N wall, E window, internal, span, 1st S to N	0.8232	3.2107-3.3669
Nave	N wall, E window, internal, span, 2nd S to N	1.1665	3.2107-3.3669
Nave	N wall, E window, internal, span, 3rd S to N	1.7443	3.2107-3.3669
Nave	N wall, E window, internal, span, 4th S to N	1.8977	3.2107-3.3669
Nave	N wall, E window, shorter span	0.6702	3.2107-3.3669
Nave	S wall, E window, external, span, 1st S to N	1.0379	3.2107-3.3676
Nave	S wall, E window, external, span, 2nd S to N	1.3357	3.2107-3.3677
Nave	S wall, E window, external, span, 3rd S to N	1.4919	3.2107-3.3678
Nave	S wall, E window, internal, span, 1st N to S	0.8152	3.2107-3.3679
Nave	S wall, E window, internal, span, 2nd N to S	1.1904	3.2107-3.3680
Nave	S wall, E window, internal, span, 3rd N to S	1.7217	3.2107-3.3681
Nave	S wall, E window, internal, span, 4th N to S	1.8798	3.2107-3.3682
Nave	S wall, E window, shorter span	0.6577	3.2107-3.3683
Nave	S wall, W window, external, span, 1st S to N	1.0381	3.2107-3.3684
Nave	S wall, W window, external, span, 2nd S to N	1.3185	3.2107-3.3685
Nave	S wall, W window, external, span, 3rd S to N	1.4747	3.2107-3.3686
Nave	N and S walls, geometrical span of windows, divided into 5	1.9260	

Nave	N wall, windows, span defining arches	1.3169	
Nave	N wall, horizontal distance between axes of windows	4.3692	
Nave	S wall, horizontal distance between axes of windows	4.4478	
Nave	N wall, vertical distance between mouldings	4.3645	
Tower	Main entrance, span, jambs included	1.1619	0.9438-1.0999
Tower	Main entrance, span, jambs excluded	1.7099	0.9438-1.0999
Tower	Tower, E side, internal length	5.2731	0.9438-1.0999
Tower	Tower, N side, internal length	4.9082	0.9438-1.0999
Tower	Tower, internal, S side	4.6385	3.2107-3.3691
Tower	Tower, external, E side, central portion	3.7188	3.2107-3.3692
Tower	Tower, external, E side, S recess	0.5149	3.2107-3.3693
Tower	Tower, external, E side, N recess	0.4901	3.2107-3.3694
Tower	Tower, external, E side, N portion	2.7972	3.2107-3.3695
Tower	Tower, external, N side, E portion	2.6961	3.2107-3.3696
Tower	Tower, external, N side, E recess	0.4986	3.2107-3.3697
Tower	Tower, external, N side, central portion	3.7732	3.2107-3.3698
Tower	Tower, external, N side, W recess	0.4998	3.2107-3.3699
Tower	Tower, external, N side, W portion	2.8714	3.2107-3.3700
Tower	Tower, external,W side, N portion	2.8514	3.2107-3.3701
Tower	Tower, external, W side, N recess	0.5218	3.2107-3.3702
Tower	Tower, external, W side, central portion	3.7618	3.2107-3.3703
Tower	Tower, external, W side, S recess	0.5141	3.2107-3.3704
Tower	Tower, E wall, thickness in central portion	1.8025	3.2107-3.3707
Tower	Tower, E wall, thickness in N portion	2.3007	3.2107-3.3708
Tower	Tower, N wall, thickness in E portion	2.2624	3.2107-3.3709
Tower	Tower, N wall, thickness in central portion	1.7627	3.2107-3.3710
Tower	Tower, N wall, thickness in W portion	2.2605	3.2107-3.3711
Tower	Tower, W wall, thickness in N portion	2.2996	3.2107-3.3712
Tower	Tower, W wall, thickness in central portion	1.7779	3.2107-3.3713
Tower	Tower, W wall, thickness in S portion	2.2967	3.2107-3.3714
Tower	Tower, E wall, geometrical door span, divided into 6	1.7292	
Tower	Tower, E wall, innermost door span, divided into 4	1.1528	
Tower	Tower, N wall, geometrical span of the window, divided into 7	2.5075	
Tower	Tower, W wall, geometrical span of door, divided into 10	2.8820	
Tower	Tower, W wall, geometrical span of the window, not divided	1.9453	
Tower	Tower, W wall,widest span of window, 7/11 of geometrical span	1.2379	
Tower	Tower, W wall, narrowest span of window, 4/13 of geometrical span	0.5973	
Tower	Tower, W wall, piscina, width	0.4817	
Transept	Transept, column, diameter	0.8836	0.2710-0.4272

Transept	Transept, W side, internal length	8.2132	0.2710-0.4272
Transept	Transept, S arch, clear span, including moulding	4.8070	3.2107-3.3687
Transept	Transept, S arch, S widest span	5.7792	3.2107-3.3688
Transept	Transept, N arch, clear span	3.9896	3.2107-3.3689
Transept	Transept, N arch, N widest span	4.2758	3.2107-3.3690
Transept	Transept, N arch, S side, 1st span N to S	4.2816	3.2107-3.3691
Transept	Transept, N arch, S side, 2nd span N to S	4.6460	3.2107-3.3692
Transept	Transept, N arch, S side, 3rd span N to S	4.8970	3.2107-3.3693
Transept	Transept, N arch, S side, 4th span N to S	5.2109	3.2107-3.3694
Transept	Transept, N arch, geometric span divided into 5	5.5100	
Transept	Transept, N arch, S side, 5th span N to S	5.4529	3.2107-3.3695
Transept	Transept, S side	7.0507	3.2107-3.3705
Transept	Transept, N side	7.1613	3.2107-3.3706
Transept	Transept, W wall, thickness	1.0516	1.5995-1.7557
Transept	Transept, W wall, N window, external, 1st span E to W	2.1551	3.2107-3.3715
Transept	Transept, W wall, N window, external, 2nd span E to W	2.8265	3.2107-3.3716
Transept	Transept, W wall, N window, external, 3rd span E to W	2.9938	3.2107-3.3717
Transept	Transept, W wall, N window, internal, 1st span W to E	2.3958	3.2107-3.3718
Transept	Transept, W wall, N window, internal, 2nd span W to E	2.5782	3.2107-3.3719
Transept	Transept, W wall, N window, internal, 3rd span W to E	2.9869	3.2107-3.3720
Transept	Transept, W wall, N window, shortest span	1.8070	3.2107-3.3721
Transept	Transept, W wall, S window, external, 1st span E to W	2.1517	3.2107-3.3720
Transept	Transept, W wall, S window, external, 2nd span E to W	2.8221	3.2107-3.3721
Transept	Transept, W wall, S window, external, 3rd span E to W	2.9821	3.2107-3.3722
Transept	Transept, W wall, S window, internal, 1st span W to E	2.4118	3.2107-3.3723
Transept	Transept, W wall, S window, internal, 2nd span W to E	2.5955	3.2107-3.3724
Transept	Transept, W wall, S window, internal, 3rd span W to E	2.9961	3.2107-3.3725
Transept	Transept, W wall, S window, shortest span	1.8200	3.2107-3.3726
Transept	Transept, S arch, geometrical span, divided into 3	6.3330	
Transept	Transept, S arch, clear span divided into 7 parts, conceptual	4.8228	
Transept	Transept, S arch, span divided into 7 parts, innermost intrados actual	4.7843	
Transept	Transept, S arch, span divided into 6 parts, outermost intrados	5.7729	

Transept	Transept, E wall, external, span and side square of windows, divided into 3	1.4137	
Transept	Transept, E wall, external, distance between axe of windows	4.1807	
Transept	Transept, E wall, internal, span of windows, divided into 3	2.0111	
Transept	Transept, E wall, thickness, S portion	1.1267	6.9650-7.1420
Transept	Transept, E wall, thickness, central portion	1.1702	6.9650-7.1420
Transept	Transept, E wall, thickness, N portion	1.0495	6.9650-7.1420
Transept	Transept, E arches, geometrical span, divided into 7	4.3428	
Transept	Transept, E side, internal length	8.1377	
Transept	Transept, W side, geometric span of window, divided into 5 parts	2.9568	

Appendix V. AI Report on Algorithm for Determining Building Unit Module (Claude Opus 4)

Methodology for Determining Building Unit Module

1. Problem Definition

1.1 Overview

This appendix details the computational methodology employed to determine the optimal base unit for a building's modular design system. The building dimensions follow a pattern based on a fundamental unit subdivided into twelfths (1/12), where all major dimensions must be expressible as whole numbers of these subdivisions that satisfy specific divisibility constraints.

1.2 Mathematical Constraints

Given:

- A base unit u (in meters) within the range [0.25, 0.35]
- Each unit is subdivided into 12 equal parts (twelfths)
- A set of 14 metric dimensions with associated divisibility requirements

The objective is to find the value of u such that each metric dimension d can be expressed as:

- $d \approx n \times (u/12)$, where n is a positive integer
- n must be exactly divisible by a specified divisor k

1.3 Error Tolerance

All metric dimensions are subject to a maximum error tolerance of 1%, accounting for construction tolerances and measurement uncertainties.

2. Computational Approach

2.1 Algorithm Design

The solution employs an exhaustive search algorithm with the following structure:

FOR each candidate unit u FROM 0.250 TO 0.350 STEP 0.001:

  FOR each dimension d with divisor k:

1. Convert d to twelfths: t = d / (u/12)
2. Find nearest divisible value: t' = round(t/k) × k
3. Calculate adjusted dimension: d' = t' × (u/12)
4. Calculate error: e = d' - d

5. Accumulate absolute error

ENDFOR

Store total error for candidate u

ENDFOR

Sort candidates by total error and select optimal

2.2 Key Calculations

2.2.1 Conversion to Twelfths

For a dimension *d* and unit *u*, the number of twelfths is:

total_twelfths = d / (u/12) = 12d/u

2.2.2 Finding Nearest Divisible Value

To ensure exact divisibility by *k*:

nearest_divisible_twelfths = round(total_twelfths/k) × k

This guarantees that the result is the closest integer multiple of *k* to the original value.

2.2.3 Error Calculation

The error for each dimension is:

error = (nearest_divisible_twelfths × u/12) - d

The total fitness metric is the sum of absolute errors:

total_error = Σ|error_i|

2.3 Numerical Precision Considerations

- All calculations use double-precision floating-point arithmetic
- Unit values are rounded to 3 decimal places (0.001 m precision)
- Twelfth counts are rounded to the nearest integer
- Final results are presented with appropriate significant figures

3. Implementation Details

3.1 Data Structure

Each candidate solution stores:

- Base unit value (m)

- Total absolute error (m)
- For each dimension:
    - Original metric value
    - Divisibility requirement
    - Total twelfths (adjusted)
    - Units and twelfths breakdown
    - Target value (adjusted metric)
    - Result after division
    - Individual error

3.2 Verification Procedure

For each solution, the following verifications are performed:

1. **Exact divisibility**: Confirm that (total_twelfths ÷ divisor) yields an integer
2. **Error bounds**: Verify that |error| < 0.01 × original_dimension
3. **Reconstruction**: Confirm that (result × divisor) = total_twelfths

4. Example Calculation

To illustrate the methodology, consider the dimension 4.369 m with divisor 2:

Step 1: Select candidate unit

- Let u = 0.265 m

Step 2: Convert to twelfths

- total_twelfths = 4.369 / (0.265/12) = 4.369 / 0.0220833... = 197.817...

Step 3: Find nearest divisible value

- nearest = round(197.817.../2) × 2 = 99 × 2 = 198

Step 4: Convert to units and twelfths

- 198 twelfths = 16 units + 6 twelfths (since 198 = 16×12 + 6)

Step 5: Calculate target dimension

- target = 198 × (0.265/12) = 4.3725 m

Step 6: Calculate result after division

- result = 198 / 2 = 99 twelfths = 8 units + 3 twelfths

Step 7: Calculate error

- error = 4.3725 - 4.369 = +0.0035 m (0.08% of original)

5. Computational Resources

The analysis was performed using:

- Search space: 101 candidate values (0.250 to 0.350 m in 0.001 m steps)
- Evaluations per candidate: 14 dimension checks
- Total calculations: 1,414 dimension evaluations
- Computation time: < 1 second on modern hardware

The algorithm's linear time complexity O(n×m) where n = number of candidates and m = number of constraints, makes it suitable for similar architectural optimization problems.

Formal Mathematical Specification

Optimization Problem Definition

Given

- Set of constraints **C** = $\{(d_1, k_1), (d_2, k_2), \ldots, (d_n, k_n)\}$
  - where $d_i \in \mathbb{R}^+$ is a dimension in meters
  - where $k_i \in \mathbb{Z}^+$ is a divisibility requirement
- Search domain: $u \in [0.25, 0.35]$ meters
- Tolerance: $\varepsilon = 0.01$ (1%)

Find:

The optimal unit u* that minimizes the total absolute error:

u* = argmin_{u} $\sum_i |e_i(u)|$

Subject to:

1. For each constraint (d_i, k_i):
   - $t_i = 12d_i/u$ (total twelfths)
   - $t'_i = k_i \times \text{round}(t_i/k_i)$ (adjusted to be divisible by k_i)
   - $t'_i \bmod k_i = 0$ (exact divisibility)
   - $|e_i(u)| / d_i \leq \varepsilon$ (error tolerance)

where $e_i(u) = (t'_i \times u/12) - d_i$

Algorithm Specification

Step 1: Discretize Search Space

U = $\{u : u = 0.250 + 0.001j, j \in \{0, 1, \ldots, 100\}\}$

Step 2: For each u ∈ U, compute:

2.1 For each constraint (d_i, k_i):

$t_i = 12d_i/u$ # Exact twelfths

$t'_i = k_i \times \lfloor t_i/k_i + 0.5 \rfloor$ # Nearest divisible value

$d'_i = t'_i u/12$ # Adjusted dimension

$e_i = d'_i - d_i$ # Error

2.2 Total error:

$E(u) = \sum_i |e_i|$

Step 3: Select optimal unit:

$u^* = \min\{u \in U : E(u)\}$

Mathematical Functions

Twelfth Conversion Function:

$f(d, u) = 12d/u$

Divisibility Adjustment Function:

$g(t, k) = k \times \lfloor t/k + 0.5 \rfloor$

Error Function:

$e(d, u, k) = g(f(d, u), k) \times u/12 - d$

Objective Function:

$E(u) = \sum_{i=1}^{n} |e(d_i, u, k_i)|$

Implementation in Mathematical Software

MATLAB/Octave:

```
matlab
function [u_opt, results] = findOptimalUnit(constraints)
  U = 0.250:0.001:0.350;
  n_constraints = size(constraints, 1);
  errors = zeros(length(U), 1);

  for i = 1:length(U)
    u = U(i);
    total_error = 0;

    for j = 1:n_constraints
      d = constraints(j, 1);
      k = constraints(j, 2);

      t = 12 * d / u;
      t_adj = k * round(t / k);
      d_adj = t_adj * u / 12;

      total_error = total_error + abs(d_adj - d);
```

```
    end

    errors(i) = total_error;
  end

  [~, idx] = min(errors);
  u_opt = U(idx);
end
```

R:

```
r
findOptimalUnit <- function(constraints) {
  U <- seq(0.250, 0.350, by = 0.001)

  errors <- sapply(U, function(u) {
    sum(apply(constraints, 1, function(row) {
      d <- row[1]
      k <- row[2]
      t <- 12 * d / u
      t_adj <- k * round(t / k)
      d_adj <- t_adj * u / 12
      abs(d_adj - d)
    }))
  })

  u_opt <- U[which.min(errors)]
  return(u_opt)
}
```

Mathematica:

```
mathematica
findOptimalUnit[constraints_] := Module[
  {U, errors, errorFunc},

  U = Range[0.250, 0.350, 0.001];

  errorFunc[u_, {d_, k_}] := Module[
    {t, tAdj, dAdj},
    t = 12 d / u;
    tAdj = k Round[t / k];
    dAdj = tAdj u / 12;
    Abs[dAdj - d]
```

```
  ];

  errors = Table[
    Total[errorFunc[u, #] & /@ constraints],
    {u, U}
  ];

  U[[Position[errors, Min[errors]][[1, 1]]]]
]
```

Verification Conditions

For the optimal solution u*, verify:

1. **Exact Divisibility**: $\forall i : t'_i \bmod k_i = 0$
2. **Error Tolerance**: $\forall i : |e_i(u^*)| / d_i \leq 0.01$
3. **Global Optimality**: $E(u^*) \leq E(u) \; \forall u \in U$

Appendix VI. Algorithm for Determining Building Unit Module: Results.

Candidate 1: 0.265 m

Total Error: 0.280 m

Maximum Error: 0.055 m

Metric Dimension (m)	Original as Units + 12ths	Total 12ths	Divisible by	Exact Division?	Target Value (m)	Result as Units + 12ths	Calculated Value (m)	Error (m)	Unit Used (m)
4.369	16 + 6/12	198	2	✓ (99)	4.3725	8 + 3/12	2.186	0.003	0.265
3.961	15 + 0/12	180	6	✓ (30)	3.9750	2 + 6/12	0.662	0.014	0.265
1.926	7 + 1/12	85	5	✓ (17)	1.8771	1 + 5/12	0.375	-0.049	0.265
5.510	20 + 10/12	250	5	✓ (50)	5.5208	4 + 2/12	1.104	0.011	0.265
6.333	24 + 0/12	288	3	✓ (96)	6.3600	8 + 0/12	2.120	0.027	0.265
4.343	16 + 4/12	196	7	✓ (28)	4.3283	2 + 4/12	0.618	-0.015	0.265
2.957	11 + 3/12	135	5	✓ (27)	2.9813	2 + 3/12	0.596	0.024	0.265
1.729	6 + 6/12	78	6	✓ (13)	1.7225	1 + 1/12	0.287	-0.007	0.265
1.945	7 + 4/12	88	11	✓ (8)	1.9433	0 + 8/12	0.177	-0.002	0.265
1.238	4 + 8/12	56	7	✓ (8)	1.2367	0 + 8/12	0.177	-0.001	0.265
0.597	2 + 4/12	28	4	✓ (7)	0.6183	0 + 7/12	0.155	0.021	0.265
0.648	2 + 4/12	28	4	✓ (7)	0.6183	0 + 7/12	0.155	-0.030	0.265
0.508	2 + 0/12	24	3	✓ (8)	0.5300	0 + 8/12	0.177	0.022	0.265
6.901	25 + 10/12	310	10	✓ (31)	6.8458	2 + 7/12	0.685	-0.055	0.265

Candidate 2: 0.266 m

Total Error: 0.288 m

Maximum Error: 0.042 m

Metric Dimension (m)	Original as Units + 12ths	Total 12ths	Divisible by	Exact Division?	Target Value (m)	Result as Units + 12ths	Calculated Value (m)	Error (m)	Unit Used (m)
4.369	16 + 6/12	198	2	✓ (99)	4.389	8 + 3/12	2.195	0.020	0.266
3.961	15 + 0/12	180	6	✓ (30)	3.990	2 + 6/12	0.665	0.029	0.266
1.926	7 + 1/12	85	5	✓ (17)	1.884	1 + 5/12	0.377	-0.042	0.266
5.510	20 + 10/12	250	5	✓ (50)	5.542	4 + 2/12	1.108	0.032	0.266
6.333	23 + 9/12	285	3	✓ (95)	6.318	7 + 11/12	2.106	-0.015	0.266
4.343	16 + 4/12	196	7	✓ (28)	4.345	2 + 4/12	0.621	0.002	0.266
2.957	11 + 3/12	135	5	✓ (27)	2.993	2 + 3/12	0.599	0.036	0.266
1.729	6 + 6/12	78	6	✓ (13)	1.729	1 + 1/12	0.288	0.000	0.266
1.945	7 + 4/12	88	11	✓ (8)	1.951	0 + 8/12	0.177	0.006	0.266
1.238	4 + 8/12	56	7	✓ (8)	1.241	0 + 8/12	0.177	0.003	0.266
0.597	2 + 4/12	28	4	✓ (7)	0.621	0 + 7/12	0.155	0.024	0.266
0.648	2 + 4/12	28	4	✓ (7)	0.621	0 + 7/12	0.155	-0.027	0.266
0.508	2 + 0/12	24	3	✓ (8)	0.532	0 + 8/12	0.177	0.024	0.266
6.901	25 + 10/12	310	10	✓ (31)	6.872	2 + 7/12	0.687	-0.029	0.266

Candidate 3: 0.264 m

Total Error: 0.305 m

Maximum Error: 0.081 m

Metric Dimension (m)	Original as Units + 12ths	Total 12ths	Divisible by	Exact Division?	Target Value (m)	Result as Units + 12ths	Calculated Value (m)	Error (m)	Unit Used (m)
4.369	16 + 6/12	198	2	✓ (99)	4.356	8 + 3/12	2.178	-0.013	0.264
3.961	15 + 0/12	180	6	✓ (30)	3.960	2 + 6/12	0.660	-0.001	0.264
1.926	7 + 6/12	90	5	✓ (18)	1.980	1 + 6/12	0.396	0.054	0.264
5.510	20 + 10/12	250	5	✓ (50)	5.500	4 + 2/12	1.100	-0.010	0.264
6.333	24 + 0/12	288	3	✓ (96)	6.336	8 + 0/12	2.112	0.003	0.264
4.343	16 + 4/12	196	7	✓ (28)	4.312	2 + 4/12	0.616	-0.031	0.264
2.957	11 + 3/12	135	5	✓ (27)	2.970	2 + 3/12	0.594	0.013	0.264
1.729	6 + 6/12	78	6	✓ (13)	1.716	1 + 1/12	0.286	-0.013	0.264
1.945	7 + 4/12	88	11	✓ (8)	1.936	0 + 8/12	0.176	-0.009	0.264
1.238	4 + 8/12	56	7	✓ (8)	1.232	0 + 8/12	0.176	-0.006	0.264
0.597	2 + 4/12	28	4	✓ (7)	0.616	0 + 7/12	0.154	0.019	0.264
0.648	2 + 4/12	28	4	✓ (7)	0.616	0 + 7/12	0.154	-0.032	0.264
0.508	2 + 0/12	24	3	✓ (8)	0.528	0 + 8/12	0.176	0.020	0.264
6.901	25 + 10/12	310	10	✓ (31)	6.820	2 + 7/12	0.682	-0.081	0.264

Candidate 4: 0.308 m

Total Error: 0.310 m

Maximum Error: 0.043 m

Metric Dimension (m)	Original as Units + 12ths	Total 12ths	Divisible by	Exact Division?	Target Value (m)	Result as Units + 12ths	Calculated Value (m)	Error (m)	Unit Used (m)
4.369	14 + 2/12	170	2	✓ (85)	4.3633	7 + 1/12	2.182	-0.006	0.308
3.961	13 + 0/12	156	6	✓ (26)	4.0040	2 + 2/12	0.667	0.043	0.308
1.926	6 + 3/12	75	5	✓ (15)	1.9250	1 + 3/12	0.385	-0.001	0.308
5.510	17 + 11/12	215	5	✓ (43)	5.5183	3 + 7/12	1.104	0.008	0.308
6.333	20 + 6/12	246	3	✓ (82)	6.3140	6 + 10/12	2.105	-0.019	0.308
4.343	14 + 0/12	168	7	✓ (24)	4.3120	2 + 0/12	0.616	-0.031	0.308
2.957	9 + 7/12	115	5	✓ (23)	2.9517	1 + 11/12	0.590	-0.005	0.308
1.729	5 + 6/12	66	6	✓ (11)	1.6940	0 + 11/12	0.282	-0.035	0.308
1.945	6 + 5/12	77	11	✓ (7)	1.9763	0 + 7/12	0.180	0.031	0.308
1.238	4 + 1/12	49	7	✓ (7)	1.2577	0 + 7/12	0.180	0.020	0.308
0.597	2 + 0/12	24	4	✓ (6)	0.6160	0 + 6/12	0.154	0.019	0.308
0.648	2 + 0/12	24	4	✓ (6)	0.6160	0 + 6/12	0.154	-0.032	0.308
0.508	1 + 9/12	21	3	✓ (7)	0.5390	0 + 7/12	0.180	0.031	0.308
6.901	22 + 6/12	270	10	✓ (27)	6.9300	2 + 3/12	0.693	0.029	0.308

Candidate 5: 0.267 m

Total Error: 0.320 m

Maximum Error: 0.053 m

Metric Dimension (m)	Original as Units + 12ths	Total 12ths	Divisible by	Exact Division?	Target Value (m)	Result as Units + 12ths	Calculated Value (m)	Error (m)	Unit Used (m)
4.369	16 + 4/12	196	2	✓ (98)	4.361	8 + 2/12	2.181	-0.008	0.267
3.961	15 + 0/12	180	6	✓ (30)	4.005	2 + 6/12	0.668	0.044	0.267
1.926	7 + 1/12	85	5	✓ (17)	1.891	1 + 5/12	0.378	-0.035	0.267
5.510	20 + 10/12	250	5	✓ (50)	5.563	4 + 2/12	1.113	0.053	0.267
6.333	23 + 9/12	285	3	✓ (95)	6.341	7 + 11/12	2.114	0.008	0.267
4.343	16 + 4/12	196	7	✓ (28)	4.361	2 + 4/12	0.623	0.018	0.267
2.957	11 + 3/12	135	5	✓ (27)	3.004	2 + 3/12	0.601	0.047	0.267
1.729	6 + 6/12	78	6	✓ (13)	1.736	1 + 1/12	0.289	0.007	0.267
1.945	7 + 4/12	88	11	✓ (8)	1.958	0 + 8/12	0.178	0.013	0.267
1.238	4 + 8/12	56	7	✓ (8)	1.246	0 + 8/12	0.178	0.008	0.267
0.597	2 + 4/12	28	4	✓ (7)	0.623	0 + 7/12	0.156	0.026	0.267
0.648	2 + 4/12	28	4	✓ (7)	0.623	0 + 7/12	0.156	-0.025	0.267
0.508	2 + 0/12	24	3	✓ (8)	0.534	0 + 8/12	0.178	0.026	0.267
6.901	25 + 10/12	310	10	✓ (31)	6.898	2 + 7/12	0.690	-0.003	0.267

Appendix VII. Impulse Response Audio Files Register

Filename	Extension	Size	Description
BLA_23_Sourc01Mic01_3m.wav	.wav	263.5 KB	Calibration measurement
BLA_23_Sourc01Mic01_3m_repetaed_calibrated.wav	.wav	263.5 KB	Source A - Receiver 1
BLA_23_Sourc01Mic02.wav	.wav	263.5 KB	Source A - Receiver 2
BLA_23_Sourc01Mic03.wav	.wav	263.5 KB	Source A - Receiver 3
BLA_23_Sourc01Mic04.wav	.wav	263.5 KB	Source A - Receiver 4
BLA_23_Sourc01Mic05.wav	.wav	263.5 KB	Source A - Receiver 5
BLA_23_Sourc01Mic06.wav	.wav	263.5 KB	Source A - Receiver 6
BLA_23_Sourc01Mic07.wav	.wav	263.5 KB	Source A - Receiver 7
BLA_23_Sourc01Mic08.wav	.wav	263.5 KB	Source A - Receiver 8
BLA_23_Sourc01Mic09.wav	.wav	263.5 KB	Source A - Receiver 9
BLA_23_Sourc01Mic10.wav	.wav	263.5 KB	Source A - Receiver 10
BLA_23_Sourc01Mic11.wav	.wav	263.5 KB	Source A - Receiver 11
BLA_23_Sourc01Mic12.wav	.wav	263.5 KB	Source A - Receiver 12
BLA_23_Sourc02Mic01.wav	.wav	263.5 KB	Source B - Receiver 1
BLA_23_Sourc02Mic02.wav	.wav	263.5 KB	Source B - Receiver 2
BLA_23_Sourc02Mic03.wav	.wav	263.5 KB	Source B - Receiver 3
BLA_23_Sourc02Mic04.wav	.wav	263.5 KB	Source B - Receiver 4
BLA_23_Sourc02Mic05.wav	.wav	263.5 KB	Source B - Receiver 5
BLA_23_Sourc02Mic06.wav	.wav	263.5 KB	Source B - Receiver 6
BLA_23_Sourc02Mic07.wav	.wav	263.5 KB	Source B - Receiver 7
BLA_23_Sourc02Mic08.wav	.wav	263.5 KB	Source B - Receiver 8
BLA_23_Sourc02Mic09.wav	.wav	263.5 KB	Source B - Receiver 9
BLA_23_Sourc02Mic10.wav	.wav	263.5 KB	Source B - Receiver 10
BLA_23_Sourc02Mic11.wav	.wav	263.5 KB	Source B - Receiver 11
BLA_23_Sourc02Mic12.wav	.wav	263.5 KB	Source B - Receiver 12

Appendix VIII. Materials for Acoustic Simulations in ODEON

Layer	Material	Scatter	Transp	Type	63 Hz	125 Hz	250 Hz	500 Hz	1000 Hz	2000 Hz	4000 Hz	8000 Hz	Total Surfaces	Total Area
DIBOND	Steel door	0.01	0	Normal	0.036	0.09	0.055	0.05	0.146	0.097	0.007	0.054	1	0.24
FABRIC_ALTAR_TABLECLOTH_HANGING	Curtains	0.2	0	Normal	0.059	0.048	0.068	0.12	0.675	0.743	0.736	0.794	3	3.74
FABRIC_ALTAR_TABLECLOTH_ON_WOOD	Curtains	0.2	0	Normal	0.059	0.048	0.068	0.12	0.675	0.743	0.736	0.794	4	2.11
FABRIC_CARPETS	Carpet heavy, on concrete (Harris, 1991)	0.1	0	Normal	0.028	0.032	0.074	0.14	0.192	0.801	0.833	0.75	26	54.04
FABRIC_CHAIRS_CUSHIONS	Pillow / Quilt	0.05	0	Normal	0.241	0.176	0.192	0.37	0.541	0.873	0.963	0.99	260	9.1
FABRIC_CURTAINS	Curtains	0.2	0	Fractional	0.059	0.048	0.068	0.12	0.675	0.743	0.736	0.794	89	4.8
FABRIC_CUSHIONS	Pillow / Quilt	0.05	0	Normal	0.241	0.176	0.192	0.37	0.541	0.873	0.963	0.99	739	23.98
FABRIC_KNEELER	Pillow / Quilt	0.05	0	Normal	0.241	0.176	0.192	0.37	0.541	0.873	0.963	0.99	4	1.04
FABRIC_PULPIT	Curtains	0.2	0	Normal	0.059	0.048	0.068	0.12	0.675	0.743	0.736	0.794	1	0.31
FLOWERS	Flowers	0.6	0.8	Normal	0.047	0.129	0.131	0.186	0.308	0.274	0.477	0.755	82	1.4
FOAMEX	Steel door	0.01	0	Normal	0.036	0.09	0.055	0.05	0.146	0.097	0.007	0.054	6	0.9
GLASS_FRAMES	Single pane of glass (Ref. Multiconsult, Norway)	0.01	0	Normal	0.199	0.153	0.043	0.049	0.046	0.015	0.015	0.047	1	0.3
GLASS_FURNITURE	Single pane of glass (Ref. Multiconsult, Norway)	0.01	0	Normal	0.199	0.153	0.043	0.049	0.046	0.015	0.015	0.047	1	0.45
GLASS_STAINED	Glass, ordinary window glass (Harris, 1991)	0.1	0	Normal	0.106	0.497	0.426	0.26	0.129	0.077	0.03	0.019	54	72.25
MARBLE_EPIGRAPH	Marble or glazed tile (Harris, 1991)	0.05	0	Normal	0.023	0.044	0.049	0.021	0.021	0.039	0.031	0.054	6	1.08
MARBLE_GRAVESTONES	Marble or glazed tile (Harris, 1991)	0.05	0	Normal	0.023	0.044	0.049	0.021	0.021	0.039	0.031	0.054	41	14.48
MARBLE_VASE	Marble or glazed tile (Harris, 1991)	0.05	0	Normal	0.023	0.044	0.049	0.021	0.021	0.039	0.031	0.054	623	1.37
METAL_ALTAR_FURNITURE	Metal, organ pipes and furniture	0.01	0	Normal	0.279	0.321	0.389	0.363	0.276	0.41	0.189	0.291	1108	0.31
METAL_FRAMES	Steel door	0.01	0	Normal	0.036	0.09	0.055	0.05	0.146	0.097	0.007	0.054	1	0.18
METAL_ORGAN	Metal, organ pipes and furniture	0.01	0	Normal	0.279	0.321	0.389	0.363	0.276	0.41	0.189	0.291	675	19.71
METAL_POSTERS	Metal, organ pipes and furniture	0.01	0	Normal	0.279	0.321	0.389	0.363	0.276	0.41	0.189	0.291	26	0.34
PAINT_FRAMES	Solid wooden door (Bobran, 1973)	0.05	0	Normal	0.299	0.079	0.029	0.078	0.119	0.132	0.209	0.089	4	4.51
PAPER_BOOK	Plaster with wallpaper on backing paper (Bobran, 1973)	0.05	0	Normal	0.035	0.024	0.059	0.052	0.109	0.076	0.072	0.106	6	0.1
PLASTERBOARD_CEILING	Plasterboard (12mm(1/2") in suspended ceiling grid)	0.01	0	Normal	0.112	0.107	0.074	0.056	0.095	0.068	0.115	0.066	416	65.36
PLASTIC_POSTERS	Linoleum or vinyl stuck to concrete (Petersen, 1983)	0.01	0	Normal	0.026	0.041	0.018	0.041	0.057	0.101	0.06	0.043	2	3.26
PLATFORMS	Hollow wooden podium (Ref. Dalenbck, CATT)	0.05	0	Normal	0.435	0.285	0.432	0.246	0.203	0.193	0.068	0.055	6	63.93
STONE_CURVE	Sandstone	0.05	0	Fractional	0.045	0.074	0.073	0.093	0.104	0.089	0.053	0.035	6295	103.75
STONE_FLAT	Sandstone	0.05	0	Normal	0.045	0.074	0.073	0.093	0.104	0.089	0.053	0.035	6297	780
STONE_FLOOR	Sandstone	0.05	0	Normal	0.045	0.074	0.073	0.093	0.104	0.089	0.053	0.035	77	275.42
STONE_FONT	Sandstone	0.05	0	Normal	0.045	0.074	0.073	0.093	0.104	0.089	0.053	0.035	67	3.83
TRANSPARENT_SOUND_SOURCES	Transparent	0.01	0	Normal	0	0	0	0	0	0	0	0	144	0.48
WAX_ALTAR_FURNITURE	Linoleum or vinyl stuck to concrete (Petersen, 1983)	0.01	0	Normal	0.026	0.041	0.018	0.041	0.057	0.101	0.06	0.043	20	0
WOOD_BEAMS_CEILING	Coffered ceiling	0.05	0	Normal	0.712	0.289	0.282	0.223	0.183	0.152	0.227	0.184	1008	27.47
WOOD_CHAIRS	Solid wooden door (Bobran, 1973)	0.05	0	Normal	0.299	0.079	0.029	0.078	0.119	0.132	0.209	0.089	3326	30.38
WOOD_CHANCEL_CURVE	Solid wooden door (Bobran, 1973)	0.05	0	Fractional	0.299	0.079	0.029	0.078	0.119	0.132	0.209	0.089	54	2
WOOD_CHANCEL_FLAT	Solid wooden door (Bobran, 1973)	0.05	0	Normal	0.299	0.079	0.029	0.078	0.119	0.132	0.209	0.089	22368	52.57
WOOD_CHOIR	Solid wooden door (Bobran, 1973)	0.05	0	Normal	0.299	0.079	0.029	0.078	0.119	0.132	0.209	0.089	2068	39.65
WOOD_CHOIR_PANELS_CURVE	Plywood paneling, 1 cm thick (Harris, 1991)	0.05	0	Fractional	0.423	0.233	0.118	0.088	0.084	0.128	0.166	0.164	15	0.84
WOOD_CHOIR_PANELS_FLAT	Plywood paneling, 1 cm thick (Harris, 1991)	0.05	0	Normal	0.423	0.233	0.118	0.088	0.084	0.128	0.166	0.164	9124	100.12
WOOD_COFFERED_CEILING	Coffered ceiling	0.05	0	Normal	0.712	0.289	0.282	0.223	0.183	0.152	0.227	0.184	20860	212.04
WOOD_DOORS	Solid wooden door (Bobran, 1973)	0.05	0	Normal	0.299	0.079	0.029	0.078	0.119	0.132	0.209	0.089	134	13.6
WOOD_FONT	Solid wooden door (Bobran, 1973)	0.05	0	Normal	0.299	0.079	0.029	0.078	0.119	0.132	0.209	0.089	45	1.22
WOOD_FRAMES	Solid wooden door (Bobran, 1973)	0.05	0	Normal	0.299	0.079	0.029	0.078	0.119	0.132	0.209	0.089	441	12.27
WOOD_FRAMEWORK_CURVE	Solid wooden door (Bobran, 1973)	0.05	0	Fractional	0.299	0.079	0.029	0.078	0.119	0.132	0.209	0.089	71	0.81
WOOD_FRAMEWORK_FLAT	Solid wooden door (Bobran, 1973)	0.05	0	Normal	0.299	0.079	0.029	0.078	0.119	0.132	0.209	0.089	3540	34.73
WOOD_FURNITURE	Solid wooden door (Bobran, 1973)	0.05	0	Normal	0.299	0.079	0.029	0.078	0.119	0.132	0.209	0.089	535	9.95
WOOD_KNEELERS	Solid wooden door (Bobran, 1973)	0.05	0	Normal	0.299	0.079	0.029	0.078	0.119	0.132	0.209	0.089	856	7.03
WOOD_ORGAN	Solid wooden door (Bobran, 1973)	0.05	0	Normal	0.299	0.079	0.029	0.078	0.119	0.132	0.209	0.089	225	58.79
WOOD_ORGAN_ACCESS	Solid wooden door (Bobran, 1973)	0.05	0	Normal	0.299	0.079	0.029	0.078	0.119	0.132	0.209	0.089	40	4.51
WOOD_PANEL_CEILING	Coffered ceiling	0.05	0	Normal	0.712	0.289	0.282	0.223	0.183	0.152	0.227	0.184	52	28.57
WOOD_PEWS	Solid wooden door (Bobran, 1973)	0.05	0	Normal	0.299	0.079	0.029	0.078	0.119	0.132	0.209	0.089	2216	150.19
WOOD_PLATFORMS	Hollow wooden podium (Ref. Dalenbck, CATT)	0.05	0	Normal	0.435	0.285	0.432	0.246	0.203	0.193	0.068	0.055	71	93.32
WOOD_PULPIT_STAND	Solid wooden door (Bobran, 1973)	0.05	0	Normal	0.299	0.079	0.029	0.078	0.119	0.132	0.209	0.089	82	0.1
WOOD_TABLES	Solid wooden door (Bobran, 1973)	0.05	0	Normal	0.299	0.079	0.029	0.078	0.119	0.132	0.209	0.089	2504	22.38
WOOD_TRUSSES_CEILING	Solid wooden door (Bobran, 1973)	0.05	0	Normal	0.299	0.079	0.029	0.078	0.119	0.132	0.209	0.089	163	66.18

Appendix IX. Register of Acoustic Data from ODEON

Filename	Extension	Size	Description
BLA23_Materials_Tests_01-02.txt	.txt	5.9 MB	List of materials for tests 1 and 2
BLA23_Materials_Tests_03-04.txt	.txt	5.7 MB	List of materials for tests 3 and 4
BLA23_Materials_Tests_05-06.txt	.txt	5.7 MB	List of materials for tests 5 and 6
BLA23_Materials_Tests_07-08.txt	.txt	5.7 MB	List of materials for tests 7 and 8
BLA23_Materials_Tests_09_to_11.txt	.txt	5.9 MB	List of materials for tests 9 to 11
Test_01_Data.txt	.txt	195.4 KB	Data for test 1
Test_01_Setting.pdf	.pdf	312.3 KB	Sources and receivers for test 1
Test_02_Data.txt	.txt	195.4 KB	Data for test 2
Test_02_Setting.pdf	.pdf	312.5 KB	Sources and receivers for test 2
Test_03_Data.txt	.txt	196.8 KB	Data for test 3
Test_03_Setting.pdf	.pdf	313.1 KB	Sources and receivers for test 3
Test_04_Data.txt	.txt	196.8 KB	Data for test 4
Test_04_Setting.pdf	.pdf	313.1 KB	Sources and receivers for test 4
Test_05_Data.txt	.txt	197.0 KB	Data for test 5
Test_05_Setting.pdf	.pdf	312.7 KB	Sources and receivers for test 5
Test_06_Data.txt	.txt	196.9 KB	Data for test 6
Test_06_Setting.pdf	.pdf	312.8 KB	Sources and receivers for test 6
Test_07_Data.txt	.txt	197.9 KB	Data for test 7
Test_07_Setting.pdf	.pdf	313.4 KB	Sources and receivers for test 7
Test_08_Data.txt	.txt	197.8 KB	Data for test 8
Test_08_Setting.pdf	.pdf	313.8 KB	Sources and receivers for test 8
Test_09_Data.txt	.txt	155.3 KB	Data for test 9
Test_09_Setting.pdf	.pdf	316.2 KB	Sources and receivers for test 9
Test_10_Data.txt	.txt	156.2 KB	Data for test 10
Test_10_Setting.pdf	.pdf	316.8 KB	Sources and receivers for test 10
Test_11_Data.txt	.txt	110.1 KB	Data for test 11
Test_11_Setting.pdf	.pdf	316.2 KB	Sources and receivers for test 11